12-2014

Robust Geotechnical Design - Methodology and Applications

Lei Wang
Clemson University, lwang6@g.clemson.edu

ROBUST GEOTECHNICAL DESIGN – METHODOLOGY AND APPLICATIONS

A Dissertation
Presented to
the Graduate School of
Clemson University

In Partial Fulfillment
of the Requirements for the Degree
Doctor of Philosophy
Civil Engineering

---

by
Lei Wang
December 2013

Accepted by:
Dr. C. Hsein Juang, Committee Chair
Dr. Sez Atamturktur, Co-Chair
Dr. Ronald Andrus
Dr. Yongxi Huang

ABSTRACT

This dissertation is aimed at developing a novel robust geotechnical design methodology and demonstrating this methodology for the design of geotechnical systems. The goal of a robust design is to make the response of a system insensitive to, or robust against, the variation of uncertain geotechnical parameters (termed *noise factors* in the context of robust design) by carefully adjusting *design parameters* (those that can be controlled by the designer such as geometry of the design). Through an extensive investigation, a robust geotechnical design methodology that considers explicitly safety, robustness, and cost is developed. Various robustness measures are considered in this study, and the developed methodology is implemented with a multi-objective optimization scheme, in which safety is considered as a constraint and cost and robustness are treated as the objectives. Because the cost and the robustness are conflicting objectives, the robust design optimization does not yield a single best solution. Rather, a Pareto front is obtained, which is a collection of non-dominated optimal designs. The Pareto front reveals a trade-off relationship between cost and robustness, which enables the engineer to make an informed design decision according to a target level of cost or robustness. The significance and versatility of the new design methodology are illustrated with multiple geotechnical applications, including the design of drilled shafts, shallow foundations, and braced excavations.

DEDICATION

I dedicate this dissertation to my parents for their love and support all these years.

ACKNOWLEDGMENTS

I would first like to express my sincere gratitude to my advisors, Dr. C. Hsein Juang and Dr. Sez Atamturktur, for their invaluable advices, supports and encouragements. Without their guidance and persistent advices, this dissertation would not have been possible. I would also like to thank my committee members, Dr. Ronald Andrus and Dr. Yongxi Huang for their advices and support during the course of this dissertation study. I would like to express my sincere appreciation to Dr. Nadarajah Ravichandran and Dr. Weichiang Pang for their assistance and support during my PhD study at Clemson.

I am grateful to my fellow co-workers and graduate students at Clemson, Zhe Luo, Jason Zhang, Zhifeng Liu, Wenping Gong, Sara Khoshnevisan, Bin Pei, Akhter Hossain, Shimelies Aboye for engaging discussion and friendship. I am also grateful to Biao Li, Jinying Zhu, Mengxin Song, Hao Hao for their support.

I would like to thank my parents. They always understand and support me with a lot of patience. They are the power of my study.

This study has been supported in part by the National Science Foundation through Grant CMMI-1200117 and the Glenn Department of Civil Engineering, Clemson University. The results and opinions expressed in this dissertation do not necessarily reflect the views and policies of the National Science Foundation. Finally, I would like to thank the Shrikhande family and the Glenn Department of Civil Engineering for awarding me the Aniket Shrikhande Memorial Annual Graduate Fellowship.

TABLE OF CONTENTS

Table of Contents (Continued)

Page

LIST OF TABLES

List of Tables (Continued)

Table Page

LIST OF FIGURES

List of Figures (Continued)

List of Figures (Continued)

Figure Page

CHAPTER ONE

INTRODUCTION

Motivation and Background

It is well recognized that uncertainty of soil parameters is generally unavoidable in the geotechnical design (Whitman 2000). The uncertainty in the soil parameters, as well as the uncertainty in the adopted analysis model, can lead to the uncertainty in the solution (e.g., predicted response or performance of a system). In a deterministic approach, the engineer uses factors of safety that have been "calibrated" by experience to cope with the uncertainties in the entire solution process. Of course, the factor of safety adopted in a particular design depends not only on the degree of uncertainties but also on the consequence of failure; in other words, it depends on the "calculated risk" (Casagrande 1965; Whitman 1984). To consider the uncertainties in a more rational way, the probability- or reliability-based approaches that consider explicitly the uncertainties in the soil parameters and analysis model have been proposed (e.g., Harr 1987; Wu et al. 1989; Tang and Gilbert 1993; Christian et al. 1994; Lacasse and Nadim 1996; Duncan 2000; Griffiths et al. 2002; Phoon et al. 2003a&b; Chalermyanont and Benson 2004; Fenton et al. 2005; Fenton and Griffiths 2008; Schuster et al. 2008; Juang et al. 2009; Najjar and Gilbert 2009; Juang et al. 2011; Wang et al. 2011; Zhang et al. 2011; Lee et al. 2012).

In a traditional geotechnical design, multiple candidate designs are first checked against code-specified safety (including strength and serviceability) requirements, and the

acceptable designs are then optimized for cost (by means of a mathematical optimization procedure considering all possible designs or simply by selecting the least-cost design from a few possible alternatives) to produce a final design. In this design process, the safety requirements are analyzed by either deterministic methods or probabilistic methods. The deterministic methods use factor of safety (F_S) as a measure of safety, while probabilistic methods use reliability index or probability of failure as the measure of safety. With the F_S-based approach, the uncertainties in the soil parameters and the associated analysis model are not considered explicitly in the analysis but their effect is considered in the design by adopting a threshold F_S value. With the probabilistic (or reliability-based) approach, these uncertainties are included explicitly in the analysis, and the design is considered acceptable if the reliability index or failure probability requirement is satisfied. Finally, cost optimization among the acceptable designs is performed to yield the final design.

Regardless of whether the F_S-based approach or the reliability-based approach is employed, the traditional design focuses mainly on safety and cost; design "robustness" is not *explicitly* considered. Robust Design, which originated in the field of Industrial Engineering (Taguchi 1986; Tsui 1992; Phadke 1989; Chen et al. 1996; Chen and Lewis 1999) aims to make the product of a design insensitive to (or robust against) "hard-to-control" input parameters (termed "noise factors") by adjusting "easy-to-control" input parameters (termed "design parameters"). The early applications of robust design are closely related to the product design to avoid the effect of the uncertainty from environmental and operating conditions. More recent applications are found in various

fields such as mechanical design, structural design, and aeronautical design (e.g., Lee and Park 2001; Sandgren and Cameron 2002; Kang 2005; Zhang et al. 2005; Doltsinis and Kang 2005; Doltsinis and Kang 2006; Lagaros and Fragiadakis 2007; Lagaros and Papadrakakis 2007; Marano et al. 2008; Lagaros et al. 2010; Jamali et al. 2010; Lee et al. 2010; Paiva 2010). The essence of this design approach is to consider robustness explicitly in the design process along with safety and economic requirements. The focus of this dissertation study is to turn this robust design concept into a Robust Geotechnical Design (RGD) methodology.

The traditional design approach that does not consider robustness against noise factors (such as soil parameters variability and/or construction variation) may have two drawbacks. First, the lowest-cost design may no longer satisfy the safety requirements if the actual variations of the noise factors are underestimated. Here, the design requirements may be violated because of the high variation of the system response due to the underestimated variation of noise factors. Second, facing high variability of the system response, the designer may choose an overly conservative design that guarantees safety; as a result, the design may become inefficient and costly. This dilemma between the over-design for safety and the under-design for cost-savings is, of course, not a new problem in geotechnical engineering. By reducing the variation of the system response to ensure the design robustness against noise factors, the RGD approach can ease such dilemma in the decision making process. Of course, the variation of the system response may also be reduced by reducing the variation in soil parameters. However, in many geotechnical projects the ability to reduce soil variability is restricted by the nature of soil

deposit (i.e., inherent soil variability) and/or the number of soil test data that is available. In this regard, it is important to note that the RGD methodology seeks the reduction in the variation of system responses by adjusting only the "easy-to-control" design parameters, and not the "hard-to-control" noise factors.

In this dissertation, the proposed RGD methodology is used to achieve design robustness against uncertainties in sample statistics of soil parameters, geotechnical spatial variability, as well as uncertainties in the adopted analysis models. The RGD methodology is further refined to integrate with finite element method, advanced probabilistic method, random field theory and bootstrapping technique in various geotechnical applications. In the following chapters, the RGD methodology is demonstrated with design of drilled shafts, shallow foundations, and braced excavations. The significance and versatility of the RGD methodology is presented.

Objectives and Dissertation Organization

The objectives of this research are to (1) explore and develop a Robust Geotechnical Design methodology for use in geotechnical engineering to achieve robustness against uncertainty in noise factors while satisfying safety and cost requirements, (2) integrate the new methodology with finite element method, advanced probabilistic method, random field theory and bootstrapping technique, (3) demonstrate the applicability of this new methodology in the various geotechnical problems including drilled shafts, shallow foundations, and braced excavations.

This dissertation consists of five chapters. The introduction is presented in current chapter, Chapter I, to set the stage and organize the entire dissertation. The next three chapters, Chapter II through Chapter IV, present major contents of the dissertation work. In Chapter II, a robust geotechnical design methodology is presented and applied for the design of drilled shaft in sand. The variation in the estimated sample statistics of soil parameters is estimated based on the typical ranges published in the literature and the non-dominated sorting technique is used to identify the Pareto Front. In Chapter III, the robust geotechnical design methodology is applied in the design of shallow foundations, in which, the robustness against uncertainty in the adopted geotechnical model is also incorporated, in addition to uncertainty in the soil parameters. The bootstrapping technique is employed to estimate the uncertainty in the sample statistics based on limited test data for shallow foundation design. In Chapter IV, the robust geotechnical design methodology is further refined and applied for the design of braced excavations in clays, in which, the maximum wall deflection is used as the system response in a braced excavation and a finite element code is employed as the deterministic model for system response analysis. Finally, in Chapter V, the last chapter, the main conclusions of this dissertation are presented.

CHAPTER TWO

ROBUST GEOTECHNICAL DESIGN OF DRILLED SHAFTS IN SAND[*]

Introduction

In a traditional geotechnical design, regardless of whether the deterministic approach or the probabilistic approach is adopted, the design is often based on a trail-and-error process considering safety and cost. Safety is usually checked first to ensure the candidate design satisfying the prescribed "safety" requirements (in terms of factor of safety or probability of failure). Then the design with the least cost is selected from the pool of all acceptable designs that have been screened based on safety requirements (Wang and Kulhawy 2008; Wang et al. 2009; Wang et al. 2011; Zhang et al. 2011). Thus, the reliability-based design is quite straightforward if the results of the reliability analysis are accurate and precise so that there will be no question whether a given design satisfies the safety requirement. The accuracy and precision of a reliability analysis, however, depends on how well the random soil parameters are characterized (Phoon et al. 2003a; Chalermyanont and Benson 2004). If the knowledge of the statistical distribution of soil parameters is "perfect," the results of reliability analysis will be accurate and precise and the reliability-based design can be easily implemented with least cost objective constrained with a minimum reliability index requirement.

---

[*] A similar form of this chapter has been published at the time of writing: Juang CH, Wang L, Liu Z, Ravichandran N, Huang H, Zhang J. (2013). Robust Geotechnical Design of drilled shafts in sand – new design perspective. Journal of Geotechnical and Geoenvironmental Engineering, 139(12): 2007-2019.

In a real-world geotechnical project, the distribution of a soil parameter is quite uncertain due to lack of data, measurement error, and/or error caused by use of empirical correlations. The variation range of geotechnical parameters is usually quite large (Harr 1987; Phoon and Kuhalwy 1999a&b) and thus the variation can be either overestimated or underestimated. Such overestimation or underestimation of the variation of soil parameters can lead to over-design or under-design. While reduction of the uncertainty in soil parameters is important, which should be pursued whenever it is deemed cost-effective, here, we focus on a different approach by achieving robustness in the design without eliminating the sources of uncertainty. Here, a design is considered *robust* if the variation in the system response is insensitive to (or robust against) the variation of uncertain soil parameters (called noise factors). The essence of a robust design is to select a design (through the adoption of a set of design parameters) that yields a minimal variation in the system response without eliminating the sources of uncertainty or reducing the level of uncertainty.

In this chapter, a robust geotechnical design (RGD) methodology is proposed to fulfill the goal of minimizing the effects of the uncertainty of soil parameters. One widely accepted definition of robust design (Taguchi 1986; Chen et al. 1996) is manipulating design parameters (i.e., the so-called "easy to control" factors) so that the system response of the design is insensitive to, or robust against, the variation of noise factors (i.e., the so-called "hard to control" factors). In a geotechnical design, the noise factors are the uncertain soil parameters and other factors such as those related to construction. Thus, in a robust design, regions in the design space that yield low variation in the system

response should be sought. The robust design will have an acceptable performance even with unexpected variation in soil parameters.

It should be noted that adjusting the design parameters through the concept of robust design is just one option to meet the design requirements. It may be feasible to achieve similar goal by improving soil parameter characterization. A balanced approach is to adopt a suitable site characterization and testing program, followed by a robust design with the estimated parameter uncertainty.

RGD is not a design methodology to compete with the traditional F_S-based approach or the reliability-based approach; rather, it is a design strategy to complement the traditional design methods. With the RGD approach, the focus is to satisfy three design objectives, namely safety, cost, and robustness (against the variation in system response caused by noise factors). As with many multi-objective engineering problems, it is possible that no single best solution exists that satisfies all three objectives. In such situations, a detailed study of the trade-offs among these design objectives can lead to a more informed design decision.

In this chapter, robustness is considered within the framework of a reliability-based design. The computed failure probability of drilled shaft is modeled as the response of the system. The variation in the computed failure probability caused by the uncertainty in the estimated variation of soil parameters is evaluated using statistical methods. The robustness for reliability-based design is achieved if the variation of the failure probability can be minimized by manipulating design parameters of the rock slope. In the sections that follow, a brief review of a reliability-based model for axial capacity of

drilled shaft (Phoon et al.1995; Wang et al. 2011a) is first provided. Then, the reliability-based RGD methodology is presented, followed by an illustrative example to demonstrate the significance of design robustness and the effectiveness of this methodology for selection of the "best" design based on multiple objectives.

Reliability-Based Design of Drilled Shafts

A summary of a reliability-based design of drilled shafts in sand presented by Phoon et al. (1995) is provided herein. The schematic diagram of a drilled shaft in loose sand subjected to an axial load under drained condition is shown in Figure 2.1. In this example, the water table is set at the ground surface. The diameter and depth (length) of the shaft are denoted as B and D, respectively. Other design parameters regarding soil and structure properties are listed in Table 2.1. In the reliability-based design framework, B and D are selected to meet the target reliability index through a trial-and-error process.

Table 2.1: Sample statistics of soil parameters

Soil Parameter	Type of Distribution	Mean	Coefficient of Variation (COV)
Effective friction angle, ϕ'	Lognormal	32°	7%
Coefficient of earth pressure at rest, K_0	Lognormal	1.0	50%

Note: The correlation coefficient between ϕ' and K_0 is -0.75.

The requirements of both ultimate limit state (ULS) and serviceability limit state (SLS) have to be satisfied in a reliability-based design. For either ULS or SLS

requirement, the drilled shaft is considered failed if the compression load exceeds the shaft compression capacities. In this study, the axial compression load F is set as the 50-year return period load F_{50} for both ULS and SLS design (F_{50} = 800 kN in this example). The ULS compression capacity (denoted as Q_{ULS}) is determined with the following equation (Kulhawy 1991):

$$Q_{ULS} = Q_{side} + Q_{tip} - W \tag{2.1}$$

where Q_{side}, Q_{tip}, and W are side resistance, tip resistance, and effective shaft weight, respectively. Considering that the cohesion term is neglected in the design of drilled shafts in sand, the Q_{side}, and Q_{tip} can be computed as (Kulhawy 1991):

$$Q_{side} = \pi B D \left(K / K_0\right)_n K_0 \sigma'_{vm} \tan\phi' \tag{2.2}$$

$$Q_{tip} = 0.25\pi B^2 \left[0.5B\left(\gamma - \gamma_w\right) N_\gamma \zeta_{\gamma s} \zeta_{\gamma d} \zeta_{\gamma r} + \left(\gamma - \gamma_w\right) D N_q \zeta_{qs} \zeta_{qd} \zeta_{qr}\right] \tag{2.3}$$

where $(K/K_0)_n$ = nominal operative in-situ horizontal stress coefficient ratio; σ'_{vm} = mean vertical effective stress along the shaft depth; ϕ' = soil effective stress friction angle; and N_γ, N_q = bearing capacity factors defined as (Vesić 1975):

$$N_q = \tan^2\left(45° + \phi'/2\right)\exp\left(\pi\tan\phi'\right) \tag{2.4}$$

$$N_\gamma = 2\left(N_q + 1\right)\tan\phi' \tag{2.5}$$

And $\zeta_{\gamma s}$ and ζ_{qs} = shape correction factors; $\zeta_{\gamma d}$ and ζ_{qd} = depth correction factors; and $\zeta_{\gamma r}$ and ζ_{qr} = rigidity correction factors for respective bearing capacity factors. Detailed methods for computing the bearing capacity factors and correction factors are documented in Kulhawy (1991).

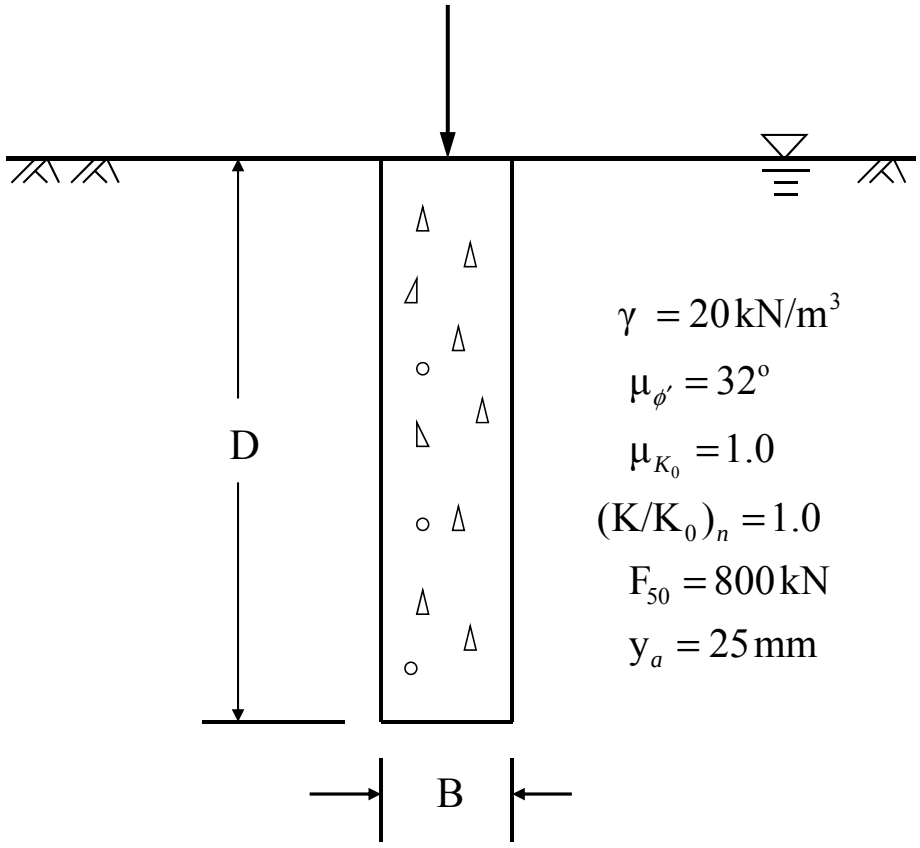

Figure 2.1: An example drilled shaft under drained compression
(adapted after Phoon et al. 1995)

Then, the SLS compression capacity (denoted as Q_{SLS}) is determined with the following equation (Phoon et al. 1995; Wang et al. 2011a):

$$Q_{SLS} = 0.625a\left(\frac{y_a}{B}\right)^b Q_{ULS} \tag{2.6}$$

where a = 4.0 and b = 0.4 are the curve-fitted parameters for the load-displacement model, and y_a = allowable displacement, which is 25mm for this problem.

The probability of ULS failure (p_f^{ULS}) and the probability of SLS failure (p_f^{SLS}) are defined as $P_r\left(Q_{ULS} < F_{50}\right)$ and $P_r\left(Q_{SLS} < F_{50}\right)$, respectively. The reliability-based design can be realized by meeting the target failure probability requirements, namely, $p_f^{SLS} < p_T^{SLS}$ and $p_f^{ULS} < p_T^{ULS}$, where p_T^{SLS} and p_T^{ULS} are the target failure probabilities based on the serviceability limit state and the ultimate limit state, respectively.

Methodology for Reliability-Based Robust Geotechnical Design

In a reliability-based RGD, the design robustness is considered explicitly in the reliability-based design framework. Although the robustness may be interpreted differently (e.g., Taguchi 1986; Chen et al. 1996; Doltsinis and Kang 2005; Park et al. 2006; Ait Brik et al. 2007; Papadopoulos and Lagaros 2009), here a geotechnical design is considered *robust* if the performance measure (i.e., failure probability p_f^{ULS} or p_f^{SLS}) is insensitive to the variation of noise factors (i.e., uncertain soil parameters). Note that the probability of failure is usually determined using Monte Carlo simulation (MCS) or reliability-based methods that require knowledge of the variation of soil parameters. If the actual variations of soil parameters are greater than the estimated variations that are

used in the reliability-based analysis, the probability of failure may be underestimated. Thus, the generally accepted reliability-based designs that do not consider robustness in the analysis could violate the safety requirements ($p_f^{ULS} < p_T^{ULS}$ and $p_f^{SLS} < p_T^{SLS}$) if the variations of soil parameters are underestimated. The chance for this violation may be greatly reduced if the variation of the failure probability, which is considered as the system response, can be minimized by adjusting design parameters.

Thus, in a reliability-based RGD, the goal is to achieve design robustness by adjusting design parameters (such as *B* and *D* in the drilled shaft design) to minimize the variation of the probability of failure. In many cases, however, greater robustness can only be achieved at a high cost and thus, a trade-off exists, which can best be investigated through multi-objective optimization.

Estimation of the coefficients of variation of soil parameters

As pointed out by Phoon et al. (1995), drained friction angle ϕ' and coefficient of earth pressure at rest K_0 are the two random variables that should be considered for the reliability-based design of drilled shaft in loose sand.

In geotechnical practice, soil parameters are often determined from a limited number of test data, thus, the statistical parameters derived from a small sample may be subjected to error. In general, the "population" mean can be adequately estimated from the "sample" mean even with a small sample (Wu et al. 1989). However, the estimation of standard deviation of the population based on a sample is often not as accurate, especially with a smaller sample. Of course, the measurement error and the model with

which soil parameters are derived (e.g., estimation of ϕ' based on SPT or other means) could also contribute to the variation of the derived parameters.

Duncan (2000) suggested that the standard deviation of a random variable might be obtained by (1) direct calculation from data, (2) use of published coefficient of variation (COV), or (3) estimate based on the "three-sigma rule." The evaluation of parameter uncertainty for a specific problem is the duty of the engineer in charge. In this chapter, the published COVs are adopted for illustration of robustness concept in a geotechnical design. The COV of ϕ' of loose sand, denoted as $COV[\phi']$, typically ranges from 0.05 to 0.10 (Amundaray 1994), and the COV of K_0, denoted as $COV[K_0]$, typically ranges from 0.20 to 0.90 (Phoon et al. 1995). For a typical reliability-based design, it is reasonable to take the mean value of the range of COV of a given parameter as its coefficient of variation. Thus, $COV[\phi'] \approx 0.07$ and $COV[K_0] \approx 0.50$ may be used in a reliability-based design of drilled shafts in sand if there is no additional data.

The outcome of a reliability-based design is affected by the accuracy of the estimated COVs of soil parameters. Because of the uncertainty of the estimated COVs, there will be uncertainty regarding the outcome of the design (e.g., we are not sure whether the design really meets the target reliability index requirement if the COVs are underestimated). In this chapter, the concept of robustness is incorporated to ensure that the design will meet the target reliability index requirement in the face of uncertainty on the estimated COVs.

The uncertainty of the COV of a given soil parameter may be characterized with a range. In fact, when COV is expressed as a range, the uncertainty is readily characterized.

For example, if we consider $COV[\phi']$ to vary from 0.05 to 0.10 based on Amundaray (1994), then the uncertainty about the value of $COV[\phi']$ to be used in the reliability design is readily characterized, as the mean and standard deviation of $COV[\phi']$, denoted as $\mu_{COV[\phi']}$ and $\sigma_{COV[\phi']}$, respectively, can be readily determined based on the three-sigma rule. Thus, for the COV of loose sand varying in the range of 0.05 and 0.10, $\mu_{COV[\phi']} \approx$ 0.07 and $\sigma_{COV[\phi']} \approx$ (0.10-0.05)/4 = 0.0125. It should be noted that when applying the so-called three-sigma rule to geotechnical problems, Duncan (2001) recommended use of a divisor of 4. For all practical purposes, the uncertainty of the estimated $COV[\phi']$ is mainly reflected in the standard deviation, $\sigma_{COV[\phi']}$.

The above discussion indicates that the uncertainty of the estimated COV of a given parameter may be estimated from a range of COV published in the literature. According to Duncan (2001), the range can also be defined with the highest and the lowest conceivable values based on site condition and engineering judgment. Furthermore, when limited test data are available, the bootstrapping method (Amundaray 1994; Luo et al. 2013) may be used to compute the mean and standard deviation of COV in a statistically rigorous manner. Thus, characterization of the uncertainty of the estimated $COV[\phi']$ is within the means of a geotechnical engineer.

Similarly, the mean and standard deviation of $COV[K_0]$, denoted as $\mu_{COV[K_0]}$ and $\sigma_{COV[K_0]}$, respectively, can be determined based on the typical range (0.20 to 0.90)

reported in the literature (Phoon et al. 1995). Following the three-sigma rule, $\mu_{COV[K_0]} \approx$ 0.50 and $\sigma_{COV[K_0]} \approx$ (0.9-0.2)/4 = 0.175.

Finally, ϕ' and K_0 of loose, normally consolidated sands are negatively correlated. According to Mayne and Kulhawy (1982), and personal communications with Mayne (2012) and Phoon (2012), the correlation coefficient ρ_{ϕ',K_0} is estimated to be in the range of −0.6 to −0.9. Following the three-sigma rule, the mean and standard deviation of ρ_{ϕ',K_0}, denoted as $\mu_{\rho_{\phi',K_0}}$ and $\sigma_{\rho_{\phi',K_0}}$, are estimated to be −0.75 and 0.075, respectively. Furthermore, for illustration purpose, both ϕ' and K_0 are assumed to follow lognormal distribution.

As is shown later, the robustness of a reliability-based design is achieved if the system response (in terms of the probability of failure) is insensitive to the variation of the estimated COVs of ϕ' and K_0 and their correlation.

Reliability-based robust geotechnical design approach

A framework for reliability-based robust geotechnical design is presented below using design of drilled shaft in loose sand as an example. In reference to Figure 2.2, the RGD approach is summarized in the following steps (presented with rationale):

Step 1: *Select design parameters and noise factors and identify the design space*. For the design of drilled shaft in sand, the diameter (*B*) and depth (*D*) of the drilled shaft are considered as the design parameters, and the soil parameters ϕ' and K_0 are considered

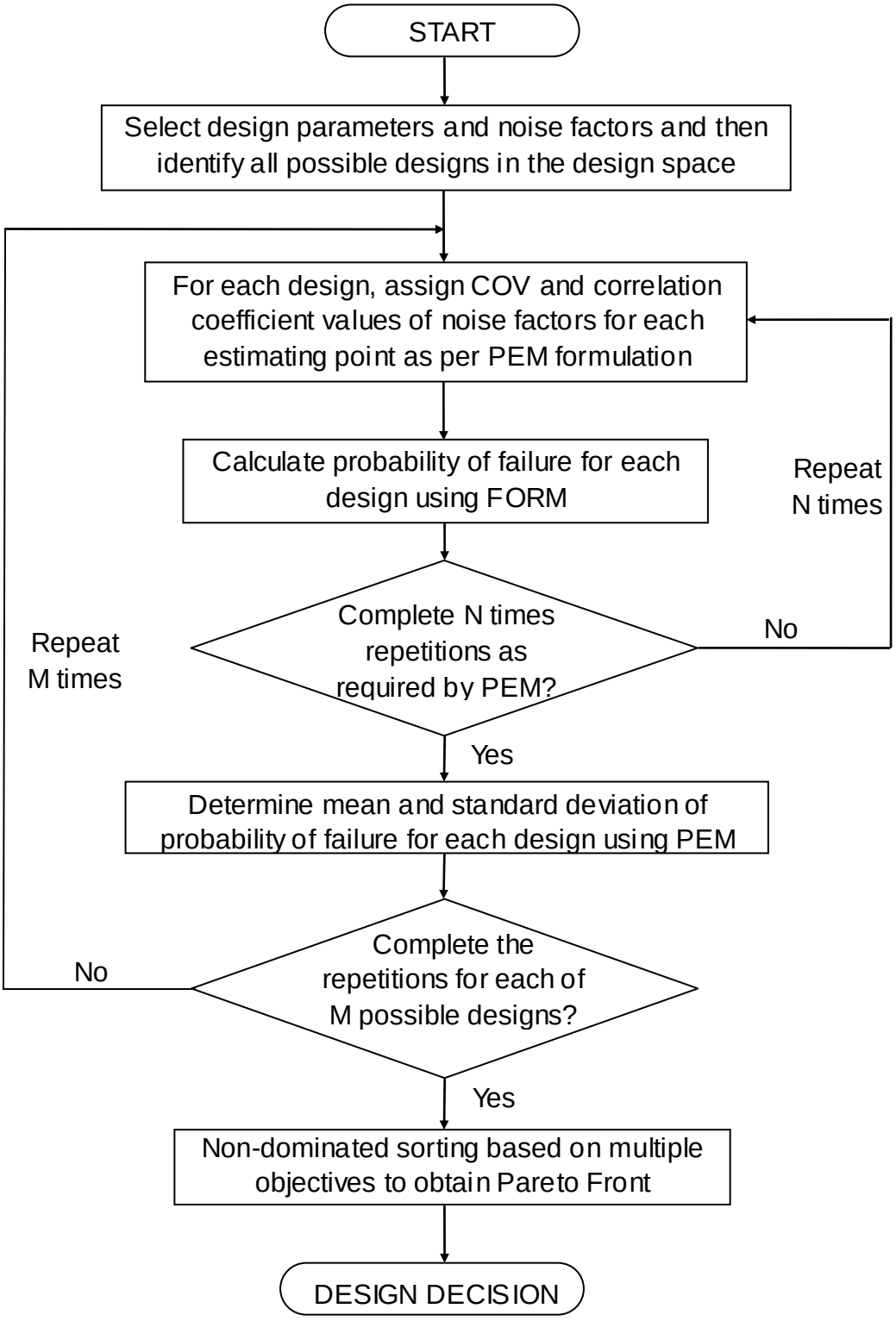

Figure 2.2: Flowchart illustrating robust geotechnical design of drilled shaft

as the noise factors. The statistics of the noise factors are estimated based on available data and guided by experience, as discussed previously. The choice of diameter B is usually limited to equipment and local practice (Wang et al. 2011a), and for illustration purpose in this chapter, only three discrete values (B = 0.9 m, 1.2 m, and 1.5 m) are considered here. The depth D is often computed for a given B that satisfies ULS or SLS requirements, and is typically rounded to the nearest 0.2 m (Wang et al. 2011b). Thus, design parameters B and D can be conveniently modeled in the discrete domain and the design space will consist of finite number of designs (say, M designs). For example, M will be equal to 93 if D is selected from the likely range of 2 m to 8 m (for the drilled shaft shown in Figure 2.1 subjected to an axial compression load F_{50} = 800 kN) for each of the three discrete B values.

Step 2: *Evaluate the variation of the system response as a measure of robustness of a given design*. For each possible design in the design space, the probability of failure can be computed based on either ultimate limit state (ULS) or serviceability limit state (SLS). Here, the probability of failure is treated as a system response (or more precisely, an effect of the system response), and the variation of the system response as a result of the variation of the sample statistics of the noise factors is adopted as a measure of robustness. In this chapter, the modified point estimate method (PEM) by Zhao and Ono (2000) is used for evaluating the mean and standard deviation of the failure probability. The PEM approach requires evaluation of the failure probability at each of a set of N "estimating" points (or sampling points) of the input noise factors, as reflected by the inner loop shown in Figure 2.2. In each repetition, statistics of each of the noise factors at

each PEM estimating point must be assigned, and then the failure probability is computed using the First Order Reliability Method (FORM; see Ang and Tang 1984; Phoon 2004). The resulting N failure probabilities are then used to compute the mean and standard deviation of the failure probability.

Step 3: *Repeat Step 2 for each of the M designs in the design space*. For each design, the mean and standard deviation of the failure probability are determined. This step is represented by the outer loop shown in Figure 2.2.

Step 4: *Perform a fast elitist non-dominated sorting to establish a Pareto Front*. For multi-objective optimization, Non-dominated Sorting Genetic Algorithm version II (NSGA-II) by Deb et al. (2002) is widely used. The sorting technique of NSGA-II is adopted herein.

Note that in single-objective optimization, one tries to get a design that is superior to all other designs. For example, in a reliability-based optimization, one may seek to find the least-cost design using reliability as a constraint. Such a scheme tends to result in a design with the least cost but barely meet the reliability requirement. However, this design may not be the "best" solution for stakeholders who are willing to pay more for less risk. When multiple objectives are enforced, it is likely that no single best design exits that is superior to all other designs in all objectives. However, a set of designs may exist that are superior to all other designs in all objectives; but within the set, none of them is superior or inferior to each other in all objectives. These designs constitute a Pareto Front. Pareto Front is named after Vilfredo Pareto, an economist who first used this concept in economic studies (Amoroso 1938; Mathur 1991). Figure 2.3 shows a

conceptual illustration of a Pareto Front in a bi-objective setting (Gencturk and Elnashai 2011). Each point on the Pareto Front is optimal in the sense that no improvement can be achieved in one objective without worsening in at least one other objective. When the optimization process yields a Pareto Front, a trade-off situation is implied. For example, if the cost and the robustness are two objectives in the trade-off relationship, the designer can approach it in two ways. If an acceptable cost range of the design is pre-defined, the most robust design within the cost range will be the best design. On the other hand, if certain level of robustness is required and specified, the least cost design that meets the robustness requirement will be the best design.

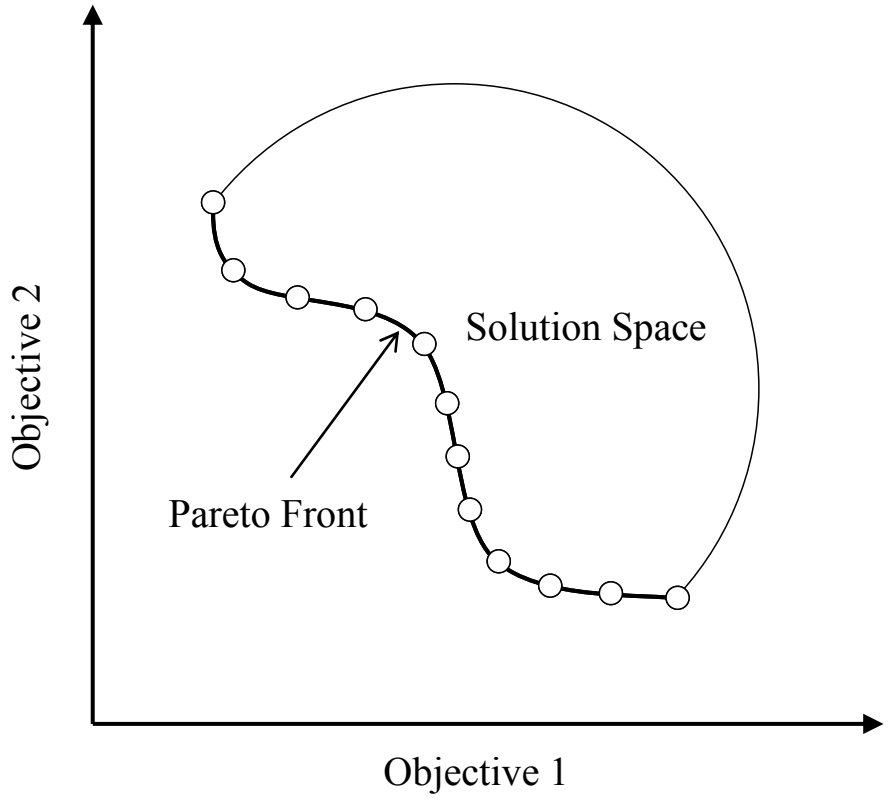

Figure 2.3: Conceptual illustration of a Pareto Front in a bi-objective space (modified after Gencturk and Elnashai 2011)

Finally, it should be noted that the procedure described above (in reference to Figure 2.2) is only one possible implementation of the RGD methodology. Other implementations may be equally effective. For example, FORM as a means to compute the failure probability for a given design with a set of known statistics of each of the noise factors may be replaced by MCS. Similarly, PEM as a means to compute the variation of the system response (i.e., the failure probability) may also be replaced by MCS or other means. Since only finite, and relatively small, number of designs are considered in this illustrative example (M = 93), only the sorting part of the NSGA-II algorithm is employed for selecting "points" (or designs) for the Pareto Front. However, if M becomes much larger, the full algorithm of NSGA-II may be employed for the multi-objective optimization.

Reliability-Based Design without Robustness Consideration

To provide a reference for reliability-based RGD, reliability-based design of a drilled shaft without considering robustness is first presented. For a drilled shaft shown in Figure 2.1 with soil parameters described in Table 2.1 (in particular, $COV[\phi']$ = 0.07, $COV[K_0]$ = 0.50, and ρ_{ϕ',K_0} = −0.75), the probability of SLS and ULS failure for various designs for a given axial load of F_{50} = 800 kN is analyzed using FORM. The results are shown in Figure 2.4. The results indicate that the SLS requirement controls the design of drilled shaft under axial compression load, which is consistent with those reported by other investigators (e.g., Wang et al. 2011a).

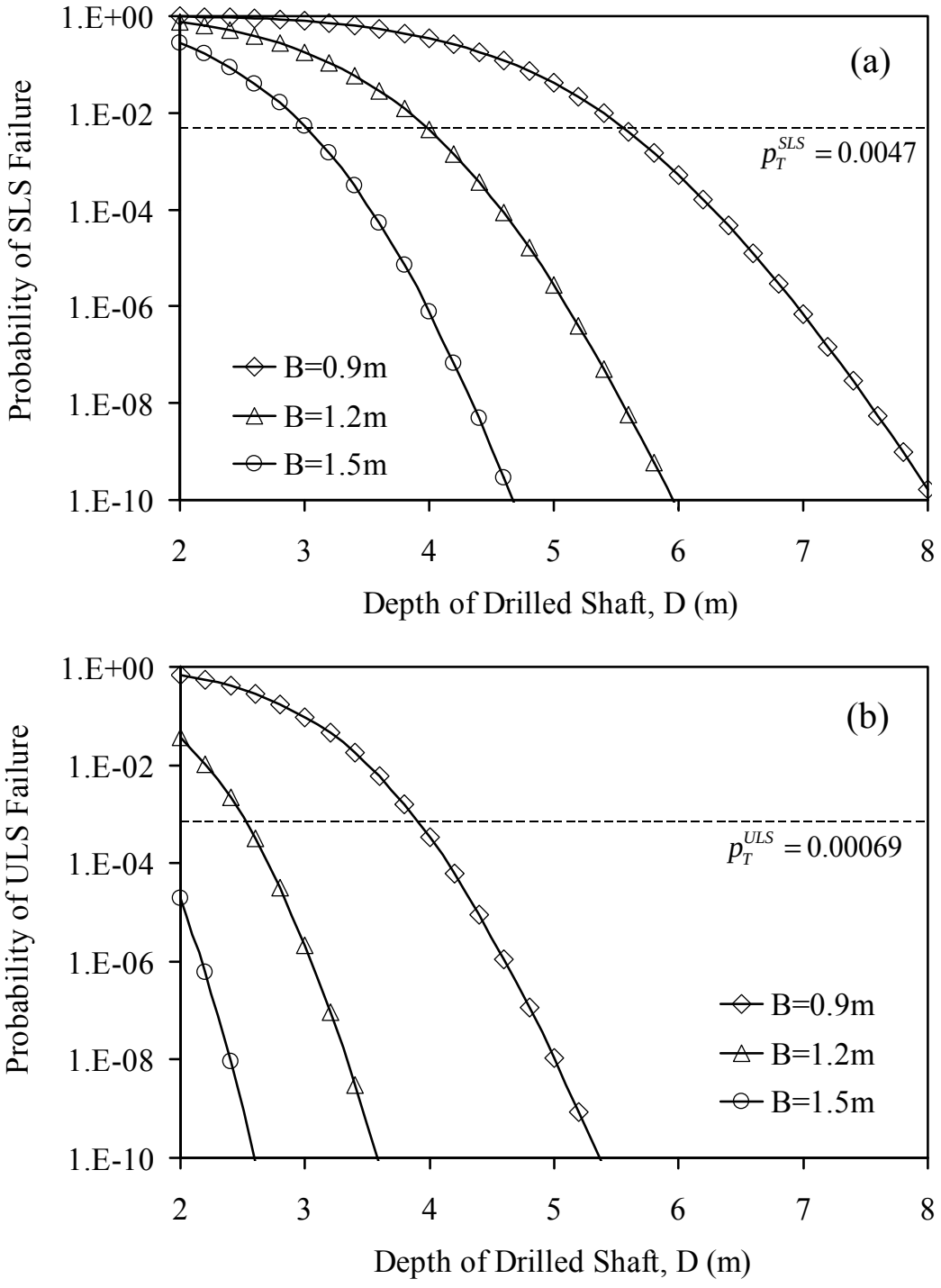

Figure 2.4: Probability of failure obtained using FORM with $COV[\phi']$= 7% $COV[K_0]$= 50% ρ_{ϕ',K_0} = −0.75 : (a) SLS failure; (b) ULS failure

In fact, in all analyses performed in this study, the SLS requirement always controls the design of drilled shafts in sand for axial compression. Thus, in the subsequent analysis only the SLS failure probability is considered.

Table 2.2: Summary of drilled shaft unit construction cost
(data from R.S. Means Co. 2007)

Drilled shaft diameters, B (m)	National average unit construction cost (USD) for shaft depth D = 0.3m
0.9	77.5
1.2	116.0
1.5	157.0

In a reliability-based design, the reliability requirement is generally used as a constraint (i.e., the actual reliability index must be greater than the target value or the corresponding failure probability must be less than the target value) to screen for the acceptable designs, and then the optimal design is obtained by minimizing the cost (Zhang et al. 2011). For a comprehensive design, the total life-cycle cost of the structure may be considered (Frangopol and Maute 2003). For simplicity, only the initial cost of a drilled shaft is considered in this chapter so that we can focus on the subject of design robustness. The initial cost generally refers to the cost for completing a drilled shaft construction, including both material and labor cost, which can be estimated from published, annually updated literature, such as Means Building Construction Cost Data (R.S. Means Co. 2007). The U.S. national average unit costs for constructing drilled shafts with respective diameters of 0.9 m, 1.2 m and 1.5 m are summarized in Table 2.2. The costs for constructing a unit depth (0.3 m) are USD 77.5, 116 and 157, respectively for the three diameters (Wang et al. 2011a). If the "best" design is to be chosen based on

least cost subjected to the constraint that the SLS failure probability is less than a target value (say, 0.0047), the design with B = 0.9 m and D = 5.6 m will be selected.

Table 2.3: Least-cost designs under various COV and correlation assumptions for soil parameters

$COV[\phi']$	$COV[K_0]$	ρ_{ϕ',K_0}	B (m)	D (m)	Cost (USD)	SLS failure probability p_f^{SLS}
0.05	0.2	-0.6	0.9	5.4	1395	0.00188
0.05	0.5	-0.6	0.9	5.2	1343	0.00356
0.05	0.9	-0.6	1.2	3.6	1392	0.00395
0.07	0.2	-0.6	0.9	6.0	1550	0.00362
0.07	0.5	-0.6	0.9	6.0	1550	0.00230
0.07	0.9	-0.6	0.9	6.0	1550	0.00343
0.1	0.2	-0.6	0.9	7.0	1808	0.00458
0.1	0.5	-0.6	0.9	7.0	1808	0.00297
0.1	0.9	-0.6	0.9	7.0	1808	0.00431
0.05	0.2	-0.75	0.9	5.2	1343	0.00350
0.05	0.5	-0.75	0.9	5.0	1292	0.00373
0.05	0.9	-0.75	0.9	5.0	1292	0.00428
0.07	0.2	-0.75	0.9	6.0	1550	0.00232
0.07	0.5	-0.75	0.9	5.6	1447	0.00402
0.07	0.9	-0.75	0.9	5.6	1447	0.00416
0.1	0.2	-0.75	0.9	7.0	1808	0.00304
0.1	0.5	-0.75	0.9	6.6	1705	0.00316
0.1	0.9	-0.75	0.9	6.6	1705	0.00326
0.05	0.2	-0.9	0.9	5.2	1343	0.00185
0.05	0.5	-0.9	0.9	4.8	1240	0.00207
0.05	0.9	-0.9	0.9	4.8	1240	0.00089
0.07	0.2	-0.9	0.9	5.8	1498	0.00317
0.07	0.5	-0.9	0.9	5.4	1395	0.00151
0.07	0.9	-0.9	0.9	5.2	1343	0.00256
0.1	0.2	-0.9	0.9	6.8	1757	0.00328
0.1	0.5	-0.9	0.9	6.2	1602	0.00207
0.1	0.9	-0.9	0.9	6.0	1550	0.00207

To demonstrate the effect of the variation in the estimated statistics of soil parameters, two series of the analysis are performed. One is to determine the least cost designs for various assumed COV and correlation coefficient values (see Table 2.3), and the other seeks to determine the failure probability of a given design under various levels of COV and correlation coefficient (see Table 2.4).

Table 2.3 shows that the least cost designs are different for different assumed COV and correlation coefficient values. The implication is that the determination of least cost design in a reliability-based design is meaningful only if the statistics of soil parameters ($COV[\phi']$, $COV[K_0]$, and ρ_{ϕ',K_0}) are fixed values. Thus, if the COV and correlation coefficient values are underestimated or overestimated by a certain margin, then there is a chance (significant probability) that an acceptable design (a design that satisfies ULS and SLS constraints based on fixed statistics values) will no longer satisfactory. This inference is demonstrated with results shown in Table 2.4, where the performance of an acceptable design (B = 0.9 m and D = 5.6 m based on an assumption of fixed statistics values, $COV[\phi']$= 0.07, $COV[K_0]$= 0.50, ρ_{ϕ',K_0} = −0.75, and a target failure probability of $p_T^{SLS} = 0.0047$) is reanalyzed with various levels of variation in soil parameters. As can be seen from Table 2.4, if this design is implemented in a sand site with $COV[\phi']$= 0.10, the SLS failure requirement will no longer be satisfied, as the failure probability will be greater than the target probability of failure of $p_T^{SLS} = 0.0047$.

Table 2.4: SLS failure probability of a given design (B= 0.9m, D= 5.6m) under various COV and correlation assumptions

$COV[\phi']$	$COV[K_0]$	ρ_{ϕ',K_0}	B (m)	D (m)	Cost (USD)	SLS failure probability p_f^{SLS}
0.05	0.2	-0.6	0.9	5.6	1447	5.95E-04
0.05	0.5	-0.6	0.9	5.6	1447	3.54E-04
0.05	0.9	-0.6	0.9	5.6	1447	7.12E-04
0.07	0.2	-0.6	0.9	5.6	1447	1.35E-02
0.07	0.5	-0.6	0.9	5.6	1447	9.75E-03
0.07	0.9	-0.6	0.9	5.6	1447	1.25E-02
0.1	0.2	-0.6	0.9	5.6	1447	6.99E-02
0.1	0.5	-0.6	0.9	5.6	1447	6.19E-02
0.1	0.9	-0.6	0.9	5.6	1447	6.76E-02
0.05	0.2	-0.75	0.9	5.6	1447	2.55E-04
0.05	0.5	-0.75	0.9	5.6	1447	3.23E-05
0.05	0.9	-0.75	0.9	5.6	1447	5.98E-05
0.07	0.2	-0.75	0.9	5.6	1447	1.06E-02
0.07	0.5	-0.75	0.9	5.6	1447	4.02E-03
0.07	0.9	-0.75	0.9	5.6	1447	4.16E-03
0.1	0.2	-0.75	0.9	5.6	1447	6.51E-02
0.1	0.5	-0.75	0.9	5.6	1447	4.79E-02
0.1	0.9	-0.75	0.9	5.6	1447	4.60E-02
0.05	0.2	-0.9	0.9	5.6	1447	5.17E-05
0.05	0.5	-0.9	0.9	5.6	1447	5.13E-09
0.05	0.9	-0.9	0.9	5.6	1447	4.67E-09
0.07	0.2	-0.9	0.9	5.6	1447	7.53E-03
0.07	0.5	-0.9	0.9	5.6	1447	2.59E-04
0.07	0.9	-0.9	0.9	5.6	1447	8.12E-05
0.1	0.2	-0.9	0.9	5.6	1447	5.98E-02
0.1	0.5	-0.9	0.9	5.6	1447	2.82E-02
0.1	0.9	-0.9	0.9	5.6	1447	1.46E-02

Table 2.5: Comparison of SLS failure probability for three designs under various COV and correlation assumptions for soil parameters

$COV[\phi']$	$COV[K_0]$	ρ_{ϕ',K_0}	SLS failure probability, p_f^{SLS}		
			Design 1 (B=0.9m, D=6.0m) 1550USD	Design 2 (B=0.9m, D=6.4m) 1653USD	Design 3 (B=0.9m, D=7.0m) 1808USD
0.05	0.2	-0.6	4.05E-05	1.62E-06	4.81E-09
0.05	0.5	-0.6	2.42E-05	1.20E-06	7.81E-09
0.05	0.9	-0.6	7.17E-05	5.70E-06	8.83E-08
0.07	0.2	-0.6	3.62E-03	7.57E-04	4.36E-05
0.07	0.5	-0.6	2.30E-03	4.40E-04	2.62E-05
0.07	0.9	-0.6	3.43E-03	8.20E-04	7.64E-05
0.1	0.2	-0.6	3.67E-02	1.74E-02	4.58E-03
0.1	0.5	-0.6	2.99E-02	1.29E-02	2.97E-03
0.1	0.9	-0.6	3.41E-02	1.58E-02	4.31E-03
0.05	0.2	-0.75	8.34E-06	1.10E-07	2.78E-11
0.05	0.5	-0.75	6.01E-07	6.40E-09	2.93E-12
0.05	0.9	-0.75	1.94E-06	4.28E-08	7.62E-11
0.07	0.2	-0.75	2.32E-03	3.52E-04	9.07E-06
0.07	0.5	-0.75	5.18E-04	4.63E-05	6.74E-07
0.07	0.9	-0.75	6.36E-04	7.62E-05	2.14E-06
0.1	0.2	-0.75	3.25E-02	1.42E-02	3.04E-03
0.1	0.5	-0.75	1.88E-02	6.03E-03	7.46E-04
0.1	0.9	-0.75	1.79E-02	5.95E-03	8.89E-04
0.05	0.2	-0.9	2.12E-07	6.17E-11	1.16E-18
0.05	0.5	-0.9	4.99E-13	1.09E-17	1.11E-25
0.05	0.9	-0.9	1.61E-12	2.03E-16	6.01E-23
0.07	0.2	-0.9	1.15E-03	8.65E-05	2.34E-07
0.07	0.5	-0.9	3.12E-06	1.29E-08	6.36E-13
0.07	0.9	-0.9	1.18E-06	8.86E-09	2.04E-12
0.1	0.2	-0.9	2.78E-02	1.08E-02	1.62E-03
0.1	0.5	-0.9	5.79E-03	6.27E-04	6.76E-06
0.1	0.9	-0.9	2.07E-03	1.88E-04	2.51E-06
Std. dev. of probability of SLS failure based on PEM			5.84E-03	2.17E-03	4.27E-04

Reliability-Based Design Considering Robustness

To investigate the issue of design robustness, the same drilled shaft problem (see Figure 2.1 and Table 2.1) is analyzed with additional knowledge of the variation of $COV[\phi']$, $COV[K_0]$ and ρ_{ϕ',K_0}. Specially, the reliability-based design is based on the following additional data: $\mu_{COV[\phi']} = 0.07$, $\sigma_{COV[\phi']} = 0.125$, $\mu_{COV[K_0]} = 0.50$, $\sigma_{COV[K_0]} = 0.175$, $\mu_{\rho_{\phi',K_0}} = -0.75$, and $\sigma_{\rho_{\phi',K_0}} = 0.075$. It should be noted that these values are just used as an example to illustrate the concept of robustness in the design, although they are deemed appropriate based on an assessment of these parameters presented previously.

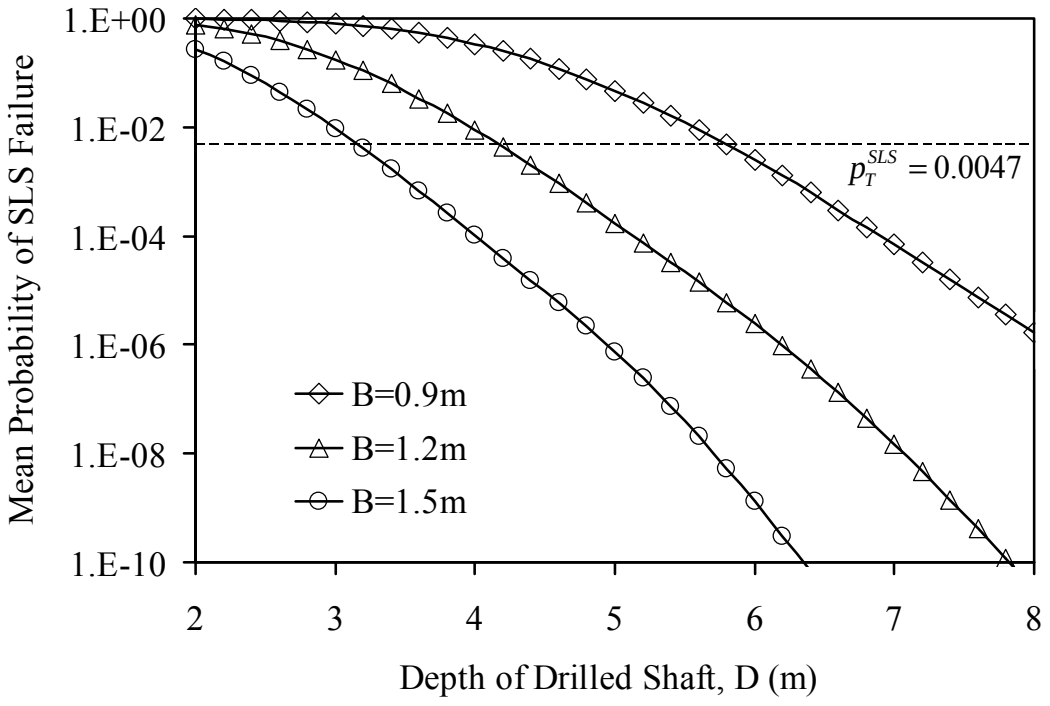

Figure 2.5: Mean of the SLS failure probability using the PEM procedure

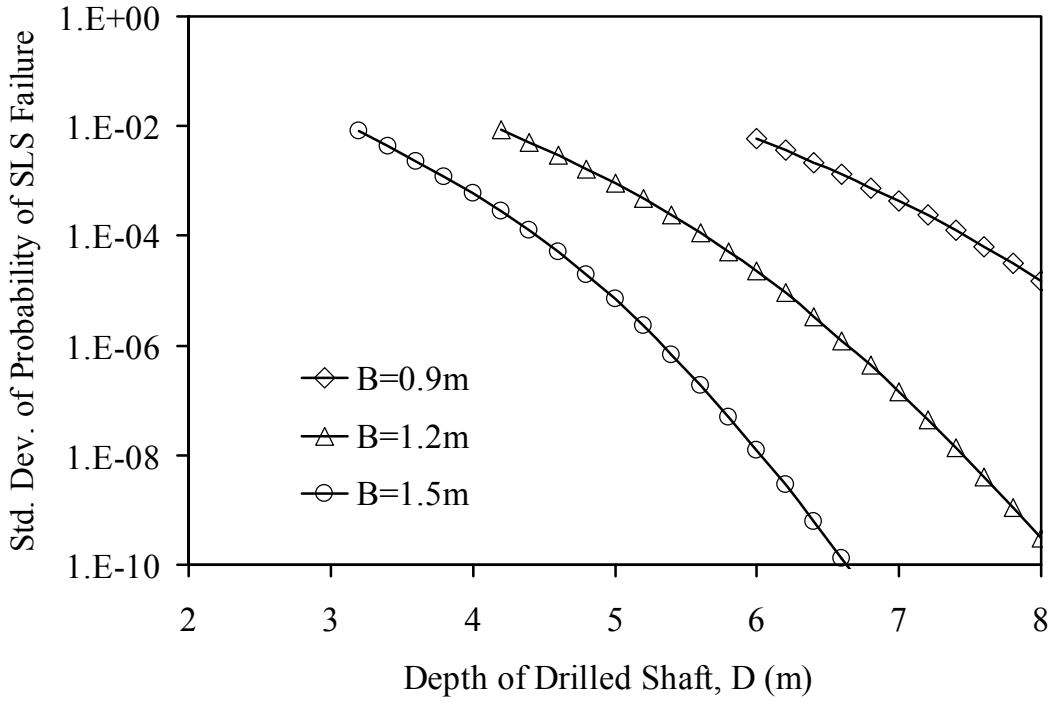

Figure 2.6: Standard deviation of the SLS failure probability using the PEM procedure

Following the procedure described previously (in reference to Figure 2.2), the mean and standard deviation of the probability of SLS failure p_f^{SLS}, namely μ_p and σ_p, can be obtained for various designs (i.e., various pairs of *B* and *D*). Figure 2.5 shows the mean SLS failure probability (μ_p) for various designs. As can be seen, many designs have a mean failure probability greater than the target failure probability ($p_T^{SLS} = 0.0047$). Figure 2.6 shows the standard deviation of the SLS failure probability (σ_p). Note that in this figure, only acceptable designs (those that have a μ_p less than the target failure probability) are plotted.

It is noted that the robustness of a reliability-based design, in which acceptance of the design is based on the requirement that $p_f^{SLS} < p_T^{SLS}$, may be measured in terms of the standard deviation of the SLS failure probability (σ_p). Thus, a design is said to have a greater robustness if σ_p caused by the uncertainty of $COV[\phi']$, $COV[K_0]$ and ρ_{ϕ',K_0} is smaller. In Figure 2.6, all designs are acceptable based on the traditional reliability-based design concept. If the cost is the only design objective after satisfying the SLS failure requirement, then the design of B = 0.9 m and D = 6.0 m will be selected, which has the least cost of 1550USD. However, this design has the greatest standard deviation of the SLS failure probability, indicating that the design has the lowest level of robustness or is most sensitive to the uncertainty in the estimated statistics of soil parameters. The implication is that such design, albeit most economical from the traditional reliability-based design viewpoint, is likely to fail the SLS failure requirement if the uncertainty of soil parameters statistics is ignored. On the other hand, if a design with a smaller σ_p is chosen, it will be more robust, albeit at a higher cost.

To further illustrate the trade-off between cost and robustness, all acceptable designs ($\mu_p < p_T^{SLS} = 0.0047$) are computed for their costs, and these costs are plotted against robustness (in terms of standard deviation of the SLS failure probability, σ_p). The results are shown in Figure 2.7. Three designs, as indicated in Figure 2.7, are used as an example for further discussion of the trade-off between cost and robustness. Design 1 (B = 0.9 m, D = 6.0 m) has the least cost among all acceptable designs, while Design 2 (B = 0.9 m, D = 6.4 m) and Design 3 (B = 0.9 m, D = 7.0 m) cost more but have a smaller

σ_p value (meaning that the designs are more robust). For each of these three designs, the probability of SLS failure is reanalyzed for various COV and correlation levels for the two soil parameters, ϕ' and K_0. The results of these additional analyses are shown in Table 2.5. It is noted that the uncertainty levels of 27 cases for loose sand shown in Table 2.5 can be roughly divided into three categories, Low variation ($COV[\phi']$= 0.05 and $COV[K_0]$ = 0.2), Medium variation ($COV[\phi']$= 0.07 and $COV[K_0]$ = 0.5), and High variation ($COV[\phi']$= 0.10 and $COV[K_0]$ = 0.9).

Based on the results shown in Table 2.5, Design 1 will perform satisfactory (in terms of meeting the requirement that $p_f^{SLS} < p_T^{SLS} = 0.0047$) if the variation of soil parameters for this sand is Low or Medium. However, Design 1 does not meet the SLS failure probability requirement if it is implemented in a site with high variation in ϕ' and K_0. Thus, for this design, the SLS failure probability is sensitive to the level of uncertainty of soil parameters.

On the contrary, with Design 3, the SLS failure probabilities under all uncertainty scenarios meet the requirement. Thus, for this design, the SLS failure probability is insensitive to the uncertainty in the COV levels of soil parameters. However, the cost is 1808USD for Design 3, compared to the cost of 1550USD for Design 1. Finally, Design 2 is a compromise between Design 1 and Design 3, in which the increase in cost is not as prohibitive (only 1653USD) but it still has some chance of violating the SLS failure probability requirement.

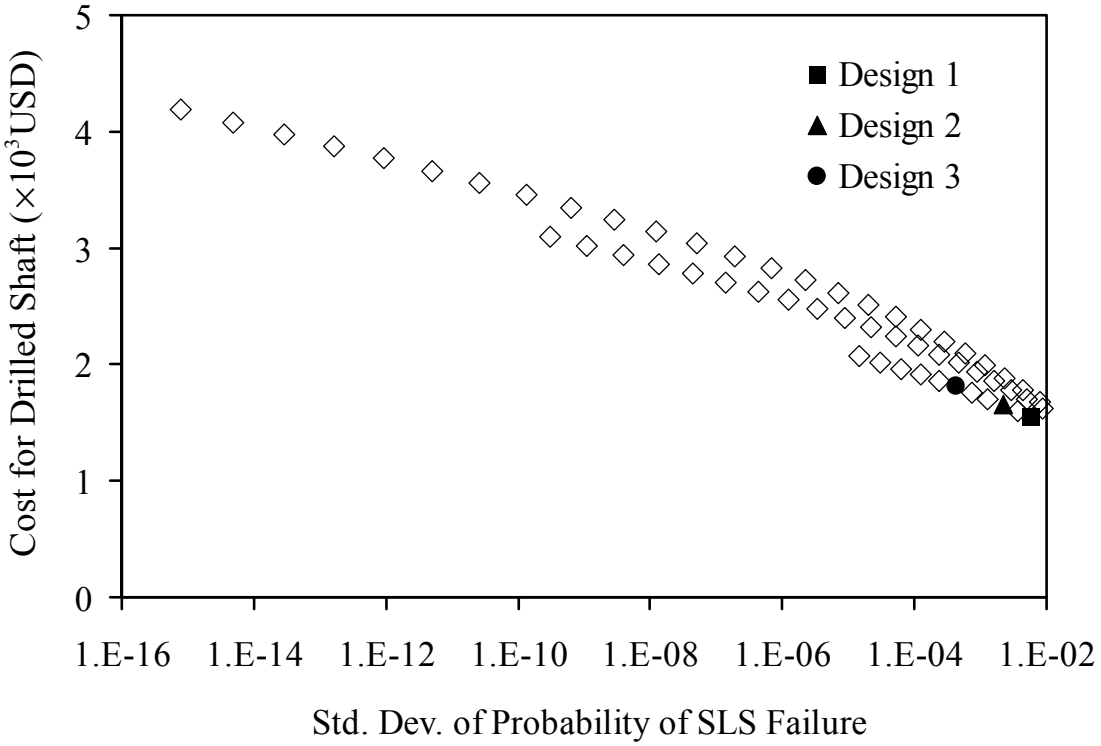

Figure 2.7: Relationship between cost and standard deviation of the SLS failure probability (all acceptable designs are shown, including three arbitrarily selected designs)

The results presented above suggest that design aids are needed for making more informed engineering decisions. In the sections that follow, the concept of Pareto Front is presented to explain the trade-off relationship between cost and robustness, followed by a procedure for selecting better designs.

Two-Objective Non-dominated Sorting for Pareto Front

Pareto-Front consists of designs that are not dominated by other designs with respect to all design objectives. Design A is ***dominated*** by Design B if A is inferior or equal to B in ***every*** objective measure, except one scenario that the performance of A is

equal to the performance of B in all objectives (Cheng and Li 1997). If a design is not dominated by any other designs, it belongs to the Pareto Front.

A non-dominant sorting technique of the Non-dominated Sorting Genetic Algorithm II (NSGA-II), developed by Deb et al. (2002), is used in this chapter to select the non-dominated designs with multiple objectives, which are points on the Pareto Front. For the geotechnical design of drilled shaft in sand, this multi-objective optimization may be set up as follows:

Find $\mathbf{d} = [B, D]$

Subject to: $B \in$ {0.9m, 1.2m, 1.5m} and $D \in$ {2m, 2.2m, 2.4m, … , 8m}

$$\mu_p^{ULS} < p_T^{ULS} = 0.00069$$

$$\mu_p^{SLS} < p_T^{SLS} = 0.0047$$

Objectives: Minimizing the standard deviation SLS failure probability (σ_p)

Minimizing the cost for drilled shaft.

As reflected in the optimization set-up stated above, the design is to be selected from a finite set of *B* and *D* pairs. The target probabilities of failure based on SLS and ULS requirements can both be specified but generally, the design of drilled shafts in sand is controlled by the SLS failure probability requirement. It should be noted that the ULS requirement $\mu_p^{ULS} < p_T^{ULS} = 0.00069$ is based on a reliability index of 3.2, and the SLS requirement $\mu_p^{SLS} < p_T^{SLS} = 0.0047$ is based on a reliability index of 2.6 (Wang et al. 2011a).

Although the multi-objective optimization as prescribed above can easily be carried out using NSGA-II, the number of possible designs in the design space in this drilled shaft example is finite and relatively small (M = 93). Thus, only the non-dominated sorting technique of NSGA-II is applied herein. Among the 93 designs, 56 are found acceptable based on the SLS and ULS failure probability requirements. With the non-dominated sorting, 27 of the 56 acceptable designs are selected into the Pareto Front (with two objectives, cost and robustness in terms of σ_p), as shown in Figure 2.8. It should be noted that the non-dominated sorting is generally more efficient if a larger number of acceptable designs is to be sorted for Pareto Front, especially when more design parameters are involved and/or the interactions between the design parameters and noise factors are much more complex.

While the traditional reliability-based design approach often selects the best design based solely on cost, after satisfying the failure probability requirements, the reliability-based robust design considers robustness in addition to cost. In the case of drilled shaft design, optimization of both cost and robustness yields a Pareto Front, which enables the engineer to make informed decision based on a well-defined trade-off relationship between cost and robustness against the possible soil parameters variability. If a certain maximum cost is desired (i.e., the cost must be less than some desired amount), then the design with greatest robustness will be the best choice. If a certain minimum level of robustness is desired, then the design with least cost will be the best choice.

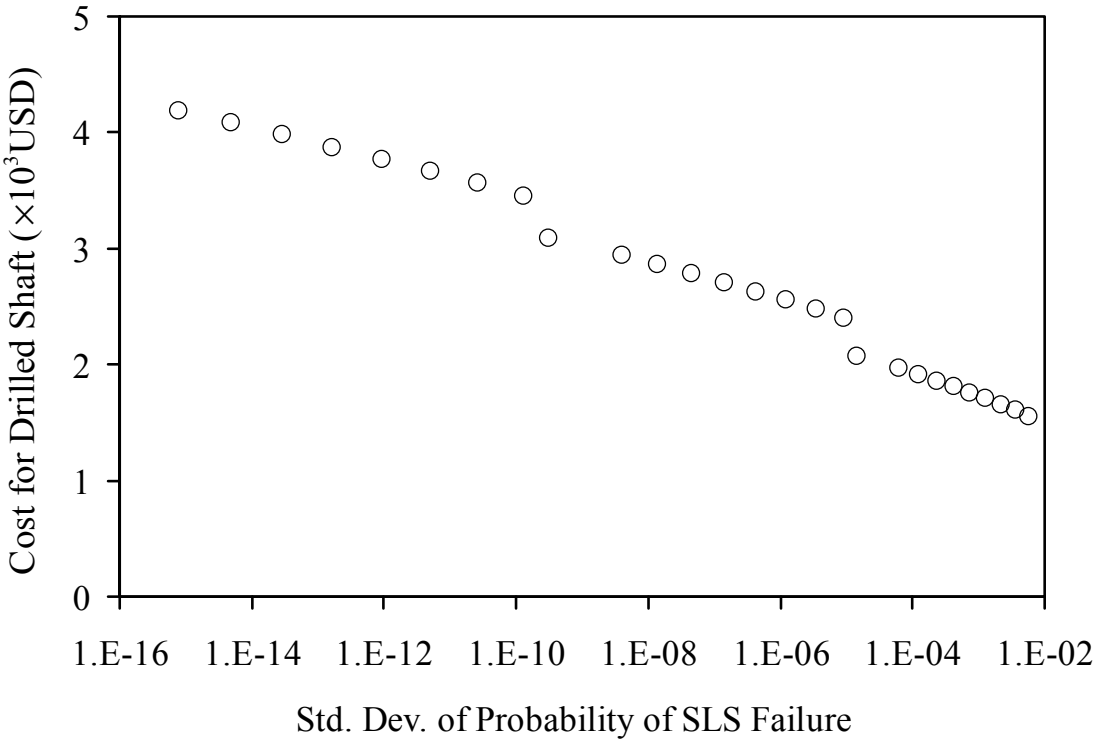

Figure 2.8: Pareto Front based on two-objective non-dominated sorting

Selection of the best design based on feasibility robustness

Although the Pareto Front provides a well-defined trade-off relationship between cost and robustness, it is desirable to take the process further to ease decision making. Here, the concept of "feasibility robustness" (Parkinson et al. 1993) is further adopted. The design with feasibility robustness is the design that can remain "feasible" (i.e., acceptable in terms of satisfying the safety and serviceability requirements) in a pre-defined constraint for certain probability even when it undergoes variations. In this chapter, the feasibility robustness is the robustness against the SLS failure requirement, $p_f^{SLS} < p_T^{SLS} = 0.0047$. Because of the uncertainty in the estimated sample statistics,

$COV[\phi']$, $COV[K_0]$ and ρ_{ϕ',K_0}, the SLS failure probability p_f^{SLS} may be treated as a random variable. Parkinson et al. (1993) suggest that feasibility robustness can be expressed with the following constraint:

$$\Pr[(p_f^{SLS} - 0.0047) < 0] \geq P_0 \tag{2.7}$$

where $\Pr[(p_f^{SLS} - 0.0047) < 0]$ is the probability that the SLS failure requirement can be satisfied (and thus, the system is still feasible), and P_0 is an acceptable level of this probability selected by the designer. The probability $\Pr[(p_f^{SLS} - 0.0047) < 0]$ is referred to herein as the feasibility probability.

Determination of the probability $\Pr[(p_f^{SLS} - 0.0047) < 0]$ requires the knowledge of distribution type of p_f^{SLS}, which is generally difficult to ascertain. Simulations of a given design (for example, B = 0.9 m, D = 6.8 m) show that the resulting histogram of β^{SLS} can be approximated well with a lognormal distribution, as depicted in Figure 2.9. Thus, an equivalent counterpart in terms of $\Pr[(\beta^{SLS} - \beta_T^{SLS}) > 0]$, where $\beta_T^{SLS} = 2.6$ (corresponding to $p_T^{SLS} = 0.0047$), may be used to assess the feasibility robustness.

The mean and standard deviation of β^{SLS}, denoted as μ_β and σ_β, respectively, can be determined using FORM within the framework of PEM. When β^{SLS} is assumed to follow lognormal distribution, the feasibility probability can be computed using simplified procedure such as first order second moment (FOSM) method as follows:

$$\Pr[(\beta^{ULS} - 2.6) > 0] = \Phi(\beta_\beta) \tag{2.8}$$

where Φ is the cumulative standard normal distribution function, and β_β is defined as:

$$\beta_\beta = \frac{\ln\left[\mu_\beta \Big/ \sqrt{1+\left(\frac{\sigma_\beta}{\mu_\beta}\right)^2}\right] - \ln(2.6)}{\sqrt{\ln\left[1+\left(\frac{\sigma_\beta}{\mu_\beta}\right)^2\right]}} \tag{2.9}$$

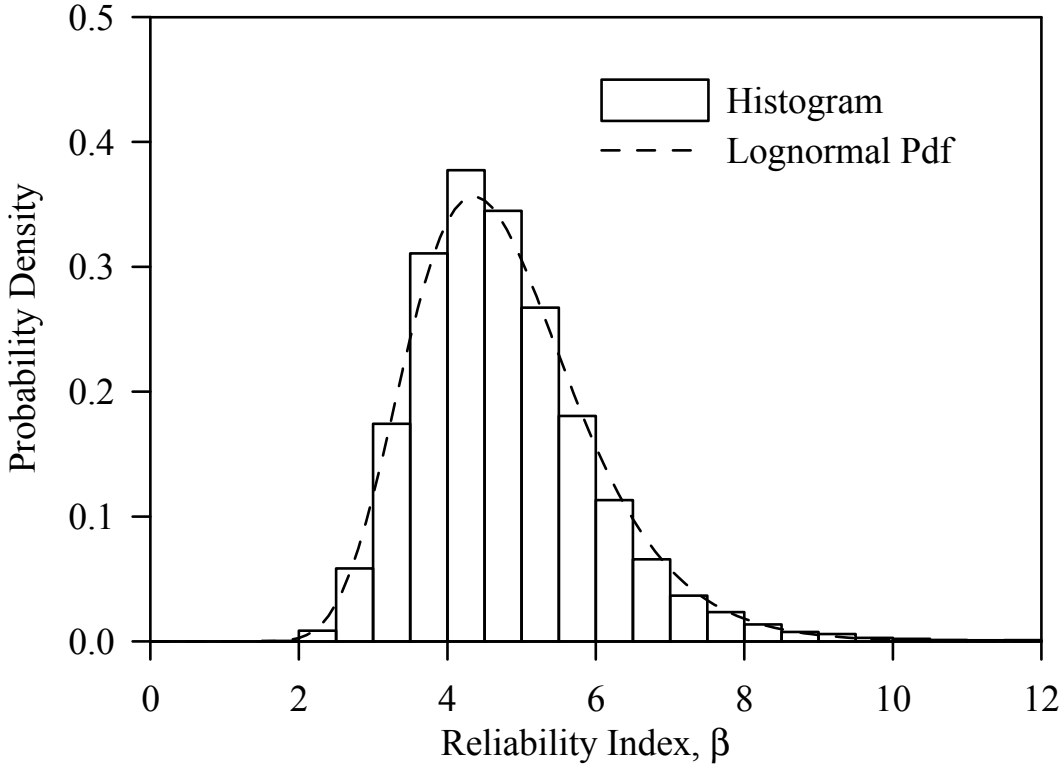

Figure 2.9: Distribution of reliability index for a given design (B = 0.9 m, D = 6.8 m)

If the acceptable level of the feasibility probability is specified as P_0 = 97.72%, then the required β_β value will be 2. In other words, if the β_β computed based on μ_β

and σ_β is equal to 2, then there is a feasibility probability of 97.72% that the SLS failure requirement ($p_f^{SLS} < p_T^{SLS} = 0.0047$ or equivalently $\beta^{SLS} > \beta_T^{SLS} = 2.6$) is satisfied.

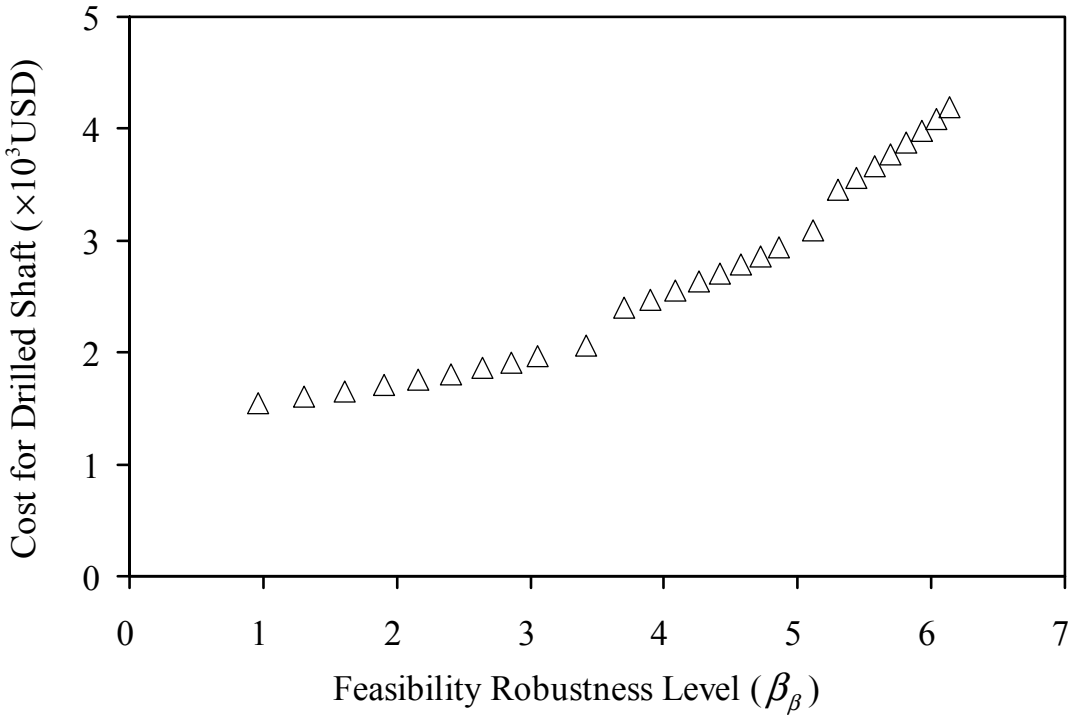

Figure 2.10: Cost versus feasibility robustness for all designs on Pareto Front

Thus, the β_β value may be used as an index for feasibility robustness. Figure 2.10 shows the β_β values computed for all 27 points on the Pareto Front versus the corresponding costs. As expected, the results show that a design with higher feasibility robustness costs more. By selecting a desired feasibility robustness level (in terms of β_β), the least-cost design among those on the Pareto Front can readily be determined. Table

2.6 shows final designs selected from the Pareto Front for various specified feasibility robustness levels.

As a reference, it is observed that the final design obtained for the feasibility robustness level of $\beta_\beta = 2$, namely B = 0.9 m and D = 6.8 m, is approximately the same as the threshold acceptable design that was obtained by the traditional reliability-based design under the higher-end level of soil variability that was examined in Table 2.3. The developed Pareto Front, especially with the computed feasibility robustness, makes it easier to select the best design to meet the designer's objectives.

Table 2.6: Selected reliability-based RGD designs at various feasibility robustness levels

β_β	P_0	B (m)	D (m)	Cost (USD)
1	84.13%	0.9	6.2	1602
2	97.72%	0.9	6.8	1757
3	99.87%	0.9	7.6	1963
4	99.997%	1.2	6.6	2552

Further Discussions

The results presented previously clearly illustrated the need for, and the significance and solution of, robust design to handle the uncertainty in the noise factors. Although the robust geotechnical design (RGD) methodology presented is far from perfect, and indeed several outstanding issues are still being examined in an ongoing study, this chapter is considered a first step, and an important step, in developing the

RGD methodology. A brief description of the issues that are being investigated is provided below.

First, the advantages of Pareto Front for identifying the best designs of drilled shaft as presented in this chapter are not fully realized, as the number of possible designs in the design space is finite and relatively small in the example presented. In this case, the robustness and cost of each possible design can be calculated, as there are only a limited number of combinations of B and D. The advantages of using Pareto Front will become more obvious when more design parameters are involved, more selections of discrete design parameters are implemented (so that the discrete variables are getting closer to being continuous random variables), and/or the interactions between the design parameters and noise factors are more complex. For example, in an ongoing study of robust design of a braced excavation system, the advantages of Pareto Front for identifying the best designs through multi-objectives optimization become more obvious.

Second, robust design concept can be implemented to a deterministic approach or a probabilistic approach. Robustness concept may be implemented in different ways to adapt to the domain problem and/or the solution approach (deterministic or probabilistic approach). In either approach, the presented RGD methodology can be adjusted slightly to adapt to the domain problem.

Third, although the robustness concept has been demonstrated in this chapter, further studies to consider robustness against other sources of uncertainty are warranted. In particular, design robustness against the following uncertainties may also be considered: (1) the distribution type of the input random variables (noise factors), (2) the

effect of spatial correlation distance, (3) the loading complexity, and (4) the effect of construction noise.

Summary

This chapter presents a reliability-based Robust Geotechnical Design (RGD) approach and demonstrates that approach using a drilled shaft design example. Rather than seeking to reduce the variation of noise factors, the RGD approach focuses on achieving an optimal design that is robust against variations in these noise factors. The results of the example show that without considering design robustness, traditional reliability-based design methods may produce a least-cost design that was initially shown as adequate by meeting the failure probability requirement but later found inadequate because of an underestimation of the variation of noise factors. Since an underestimation of the variation of noise factors is not uncommon and the safety requirement cannot be comprised, it is desirable to have a design aid to assist in making a decision between the trade-offs of cost and robustness. By considering robustness as one additional design objective, the proposed RGD approach can be efficiently implemented as a multi-objective optimization problem. The results of the example show that the RGD approach can produce a Pareto Front, a set of non-dominated optimal designs that satisfy the safety requirement. The results also show that a trade-off relationship between cost and feasibility robustness can be established from the Pareto Front for the design of drilled shaft, which can then be used as a design aid in selecting the most suitable design.

CHAPTER THREE

ROBUST GEOTECHNICAL DESIGN OF SHALLOW FOUNDATIONS*

Introduction

Uncertainties in geotechnical models and parameters and their effect have long been recognized (Lacasse and Nadim 1994; Gilbert and Tang 1995; Phoon and Kulhawy 1999; Whitman 2000; Juang et al. 2004; Schuster et al. 2008; Zhang et al. 2009; Juang et al. 2009; Zhang et al. 2012). To perform a geotechnical design using deterministic approach, "conservative" values of the uncertain soil parameters are often adopted along with an experience-calibrated factor of safety. While the deterministic approach has been successfully used for many decades, it lacks the capability to render a consistent measure of safety of the geotechnical system in the face of uncertainties. To obtain a more rational design, many investigators (e.g., Wu et al. 1989; Christian et al. 1994; Whitman 2000; Phoon et al. 2003a,b; Fenton et al. 2005; Najjar and Gilbert 2009; Wang 2011; Zhang et al. 2011) have turned to a probabilistic approach.

Quantification of the uncertainties in soil parameters and geotechnical models is a prerequisite for probability or reliability-based design. If there is abundant amount of quality data that can characterize the statistics of the adopted geotechnical model and its parameters, the result of reliability analysis will be a certain value (a fixed reliability

---

*A similar form of this chapter has been published at the time of writing: Juang CH, Wang L, Atamturktur S, Luo Z. (2012). Reliability-based robust and optimal design of shallow foundations in cohesionless soil in the face of uncertainty. Journal of GeoEngineering, 7(3): 75-87.

index or failure probability). Thus, the design meeting the target reliability (i.e., safety) requirements with least cost would be the "best" choice, and the reliability-based design would be a straightforward process. However, the statistics of soil parameters and model factor (which quantifies the accuracy and precision of the adopted geotechnical model) are quite difficult to ascertain due to lack of data and/or incomplete knowledge. If the statistics of model factor and input parameters cannot be characterized with certainty, the computed failure probability will not be a fixed value. The design decision will not be straightforward with a variable failure probability. In such a scenario, a difficult trade-off decision may be required.

One way to reduce the effect of the uncertainties of statistical characterization of soil parameters and model factors is considering robustness of the system response (e.g., failure probability of the designed geotechnical system) against these uncertainties. A design is deemed "robust" if the predicted system response is "insensitive" to the uncertainties of the statistical characterization of soil parameters and model factors. By considering robustness *explicitly* in the reliability-based design optimization, as is shown later, a more informed design decision may be made.

Robust design concept, originally proposed by Taguchi (1986) for product quality control in manufacturing engineering, has been applied to many design fields including mechanical design, aeronautical design and structural design (e.g., Chen et al. 1996; Tsui 1999; Lagaros and Fragiadakis 2007; Marano et al. 2008; Lee et al. 2010; Paiva 2010). From the perspective of a designer aiming to achieve a robust design, the input parameters for the design can be divided into two groups: easy-to-control and hard-to-

control parameters. In the context of robust design, the easy-to-control parameters such as dimension of a foundation are called *design parameters*, while the hard-to-control factors such as uncertain soil parameters and model factors are called *noise factors*. Assuming that the uncertainty of these noise factors cannot be eliminated (or further reduced because of inherent variability or lack of data), the aim is then to reduce the effects of the uncertainty of these noise factors on the response of the system. Thus, Robust Design aims to find a design (represented by a set of design parameters) that is robust against the uncertainty of these noise factors, thereby reducing the variability of the system response.

In this chapter, a reliability-based robust geotechnical design (RGD) methodology is introduced. Here, the objective of RGD is to ensure the robustness of reliability-based design even if the statistics of noise factors are not precisely defined (meaning that uncertainty exists in the estimated statistical moments of these noise factors). When robustness is included in the design decision along with safety (reliability) and cost, the search for the "best" design becomes a multi-objective optimization problem. One possible approach is to treat the safety requirement as a constraint (for example, by requiring the failure probability of the design to be less than the acceptable target failure probability) in an optimization with respect to cost and robustness. Recall that in a traditional reliability-based design, the safety requirement is used as a constraint and the design is optimized with respect to one objective, cost. Thus, the new RGD approach is seen as an extension of the traditional reliability-based design.

To illustrate the RGD framework, the design of a shallow foundation in cohesionless soil is used as an example herein. The normalized load-settlement curve

approach (Akbas and Kulhawy 2009a; Akbas and Kulhawy 2011), which ensures uniformity in the reliability analysis across both ultimate limit state (ULS) and serviceability limit state (SLS), is adopted for the design of shallow foundation. Through the examples presented, the effectiveness of the reliability-based RGD approach and the significance of considering robustness in the design process are clearly demonstrated.

Deterministic Models for Shallow Foundation

The procedure for calculating the ULS capacity of shallow foundation in cohesionless soil under compressive loads proposed by Vesić (1975), with minor improvements by Kulhawy et al. (1983) is adopted in this chapter. Based on the extensive database of field testing, Akbas and Kulhawy (2009b) demonstrated that the ULS capacity estimated by Vesić model as updated by Kulhawy et al. (1983) agreed well with the field testing results when the foundation width $B \geq 1$ m. The ULS capacity (R_{ULS}) of a shallow foundation with width B, length L, and embedment depth D is calculated as follows (Vesić 1975; Akbas and Kulhawy 2009b):

$$R_{ULS} = [(1/2)B\gamma' N_\gamma \xi_{\gamma s}\xi_{\gamma d}\zeta_{\gamma r} + q' N_q \xi_{qs}\xi_{qd}\zeta_{qr}](BL) \tag{3.1}$$

where γ' = effective unit weight of soil below foundation; q' = effective overburden stress at foundation level; and N_γ and N_γ are bearing capacity factors defined as (Vesić 1975):

$$N_\gamma \approx 2(N_q + 1)\tan\phi' \tag{3.2}$$

$$N_q = e^{\pi \tan \phi'} \tan^2(45 + \phi'/2) \tag{3.3}$$

And $\zeta_{\gamma s}$ and ζ_{qs} = shape correction factors; $\zeta_{\gamma d}$ and ζ_{qd} = depth correction factors; and $\zeta_{\gamma r}$ and ζ_{qr} = rigidity correction factors. Detailed formulations for these correction factors are documented in Kulhawy et al. (1983).

The ULS failure is checked by comparing the bearing capacity (R_{ULS} , as "resistance") with the applied loading *G*+*Q*, where *G* is the permanent load and *Q* is the transient load. The condition $R_{ULS} < G + Q$ denotes the ULS failure of shallow foundation.

For the SLS capacity (R_{SLS}) of shallow foundation, Akbas and Kulhawy (2011) derived the following equation based on the normalized load-settlement behavior of shallow foundation:

$$R_{SLS} = \frac{R_{ULS}(s_t / B)}{a(s_t / B) + b} \tag{3.4}$$

where s_t is the allowable settlement limit (in this chapter, 25 mm), *B* is the width of the foundation, and the coefficients *a* and *b* are parameters of a hyperbolic model that fit the normalized load-settlement curve defined below (Akbas and Kulhawy 2009a):

$$\frac{G+Q}{R_{ULS}} = \frac{s/B}{a(s/B) + b} \tag{3.5}$$

where $(G+Q)/R_{ULS}$ is the normalized loading, and *s* is the corresponding settlement. Based on data from 167 full-scale tests, the mean and coefficient of variation (COV) of *a* and *b* are $\mu_a = 0.70$ and $\delta_a = 22\%$, and $\mu_b = 1.77$ and $\delta_b = 54\%$, respectively.

It is noted that the normalized load-settlement curve approach (Eqs. 4 and 5) provides a framework to correlate the ULS capacity with the SLS capacity, and thus, the two limit states can be treated uniformly. For a given design (with known B, L and D), if the ULS bearing capacity (R_{ULS}) is less than the applied load G+Q, the ULS failure is said to occur. The SLS failure is said to occur if the bearing capacity at the allowable settlement limit (R_{SLS}) is less than the applied load G+Q.

Estimation of Cost for Shallow Foundations

The total cost for a shallow foundation is determined using the cost summation of five individual tasks in foundation construction (Wang and Kulhawy 2008):

$$Z = Q_e c_e + Q_f c_f + Q_c c_c + Q_r c_r + Q_b c_b \tag{3.6}$$

where Q_e, Q_f, Q_c, Q_r, Q_b = quantities for excavation, formwork, concrete, reinforcement, and compacted backfill, respectively; c_e, c_f, c_c, c_r, c_b = unit prices for excavation, formwork, concrete, reinforcement, and compacted backfill, respectively.

Table 3.1: Unit price for shallow foundation (data from Wang and Kulhawy 2008)

Work item	Unit	National average unit price in U.S. (USD)
Excavation	m^3	25.16
Formwork	m^3	51.97
Reinforcement	kg	2.16
Concrete	m^3	173.96
Compacted backfill	m^3	3.97

Table 3.1 gives the U.S. average unit price for construction of shallow foundation compiled by Wang and Kulhawy (2008). The five quantities Q_e, Q_f, Q_c, Q_r, Q_b depend on the design parameters, foundation width B, length L, and embedment depth D. The reader is referred to Wang and Kulhawy (2008) for details.

Design Example of Shallow Foundation

An example of shallow foundation is used to illustrate the proposed reliability-based robust geotechnical design (RGD) approach. A square foundation ($B = L$), as shown in Figure 3.1, is to be designed to support the vertical compressive loads.

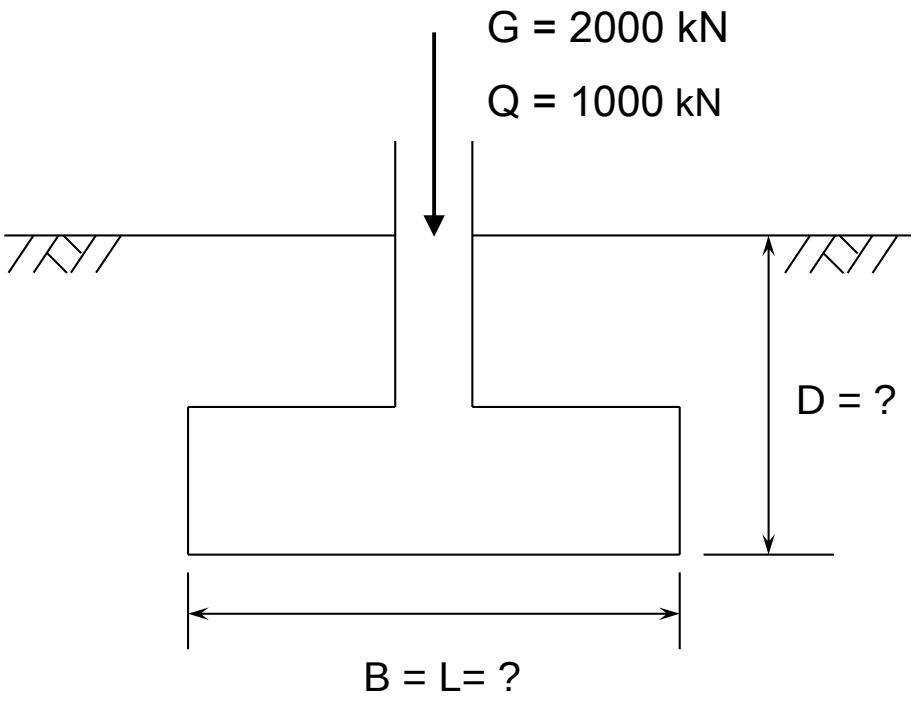

Figure 3.1: A square shallow foundation design example

The vertical compressive loads have a permanent load component of G = 2000 kN and a transient load component of Q =1000 kN. G and Q are assumed to follow lognormal distribution with a COV of G of 10% and a COV of Q of 18% (Zhang et al. 2011). The soil profile at the site is assumed to follow the example presented by Orr and Farrel (1999), which consists of a homogeneous dry sand with a deterministic unit weight of $\gamma = 18.5$ kN/m^3. Ten effective friction angles ϕ' (for dry sand, $c' = 0$) are obtained from triaxial tests conducted on samples of this homogeneous sand and the results are listed in Table 3.2. The ground water is assumed to be well below any topsoil and disturbed ground such that it has negligible effects on the shallow foundation design. The maximum allowable settlement is set at 25 mm for this foundation design.

Table 3.2: Triaxial test results of effective friction angle (data from Orr and Farrell 1999)

Test No.	$\phi'(^o)$
1	33.0
2	35.0
3	33.5
4	32.5
5	37.5
6	34.5
7	36.0
8	31.5
9	37.0
10	33.5

Statistical Characterization of Uncertainty in Noise Factors

Bootstrapping for characterizing uncertainty in sample statistics

In geotechnical engineering practice, soil parameters are usually derived with a small sample, thus the derived sample statistics (such as mean and standard deviation) are often subjected to error. These derived sample statistics, which are required in reliability analysis and design, are often uncertain and should be modeled as random variables. To characterize the uncertainty in these sample statistics, non-parametric bootstrap method may be used (Luo et al. 2013). Bootstrapping is a re-sampling technique that yields an estimate of the mean and standard deviation of the sample statistics.

In reference to Figure 3.2, the procedure for bootstrapping is summarized below (Bourdeau and Amundaray 2005; Luo et al. 2013):

(1) Based on the original sample *A* (with *k* elements or data points), a large number (*N*) of re-samples, $A_j^*, j = 1, N$, are formed by "random sampling with replacement," which means that each element (for example, $a_{j,1}^*$) of A_j^* can assume the value of any of the elements of *A*.

(2) For each re-sample, A_j^*, the statistics of interested X_i (e.g., mean and standard deviation) are computed.

(3) The mean (μ_{X_i}) and standard deviation (σ_{X_i}) of statistics X_i can be computed once Steps 2 has been repeated *N* times.

With only 10 data of ϕ' listed in Table 3.2, there is uncertainty concerning the mean and standard deviation derived from this sample. Thus, bootstrapping method is applied to evaluate the uncertainty of the sample mean and standard deviation.

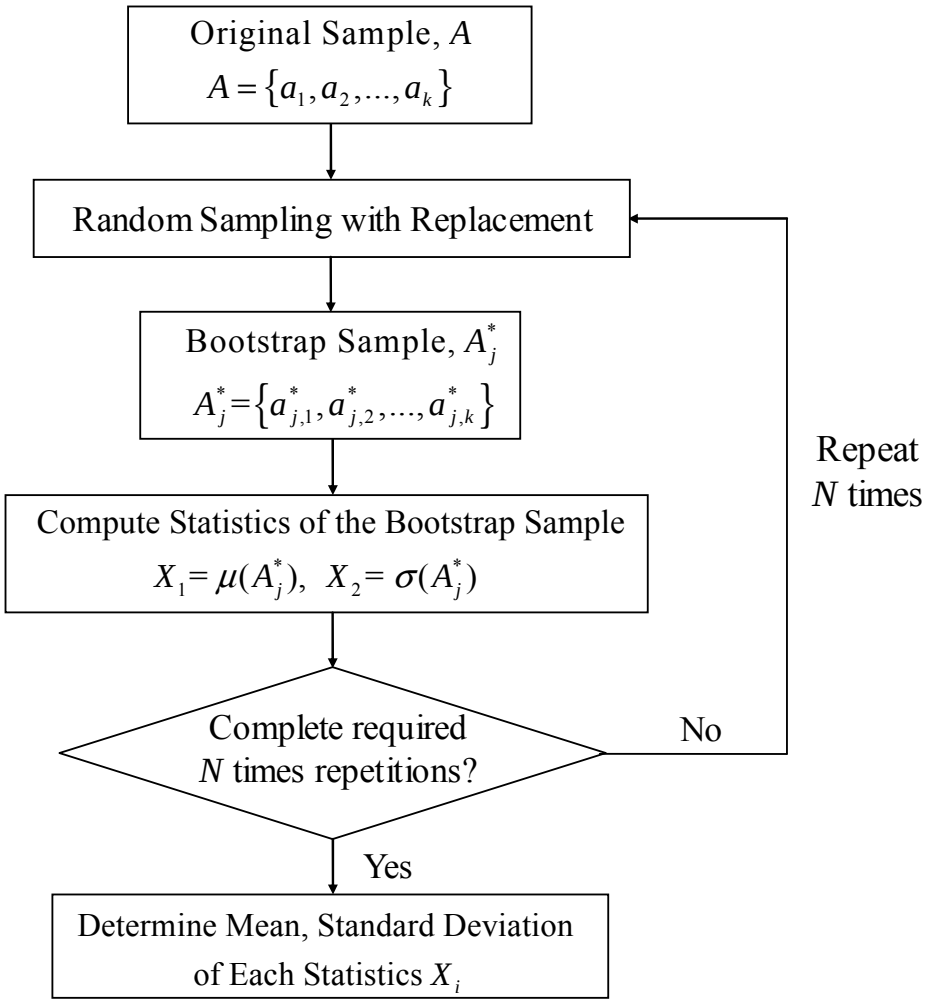

Figure 3.2: Illustration of bootstrap procedure for characterizing uncertainty in sample statistics

While not shown here, it took less than 10,000 bootstrap samples to obtain converged results in this study. With N = 10,000, the histograms of the mean (μ_S) and standard deviation (σ_S) of ϕ' is obtained as shown in Figure 3.3. Both μ_S and σ_S can be approximated well with a normal distribution in this example. Table 3.3 shows the mean and standard deviation of both μ_S and σ_S.

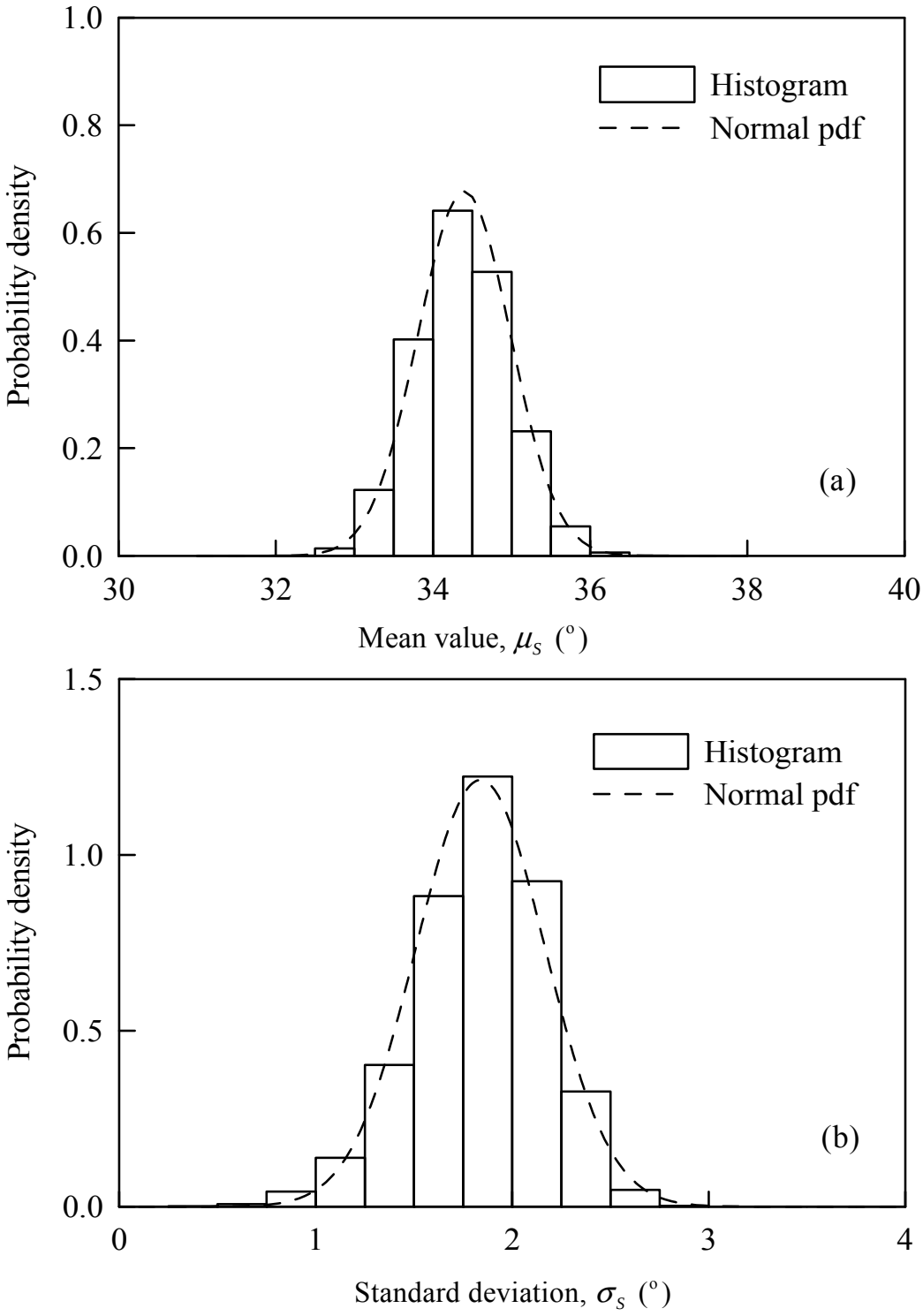

Figure 3.3: Probability distribution of sample statistics of ϕ': (a) mean; (b) standard deviation

Table 3.3: Sample statistics of effective friction angle ϕ' by bootstrapping method

Uncertain variables	μ_S (°)	σ_S (°)
Mean	34.40	1.84
Std. dev.	0.59	0.33

It can be found that the variation of sample mean μ_S is quite negligible (COV of $\mu_S \approx 1.7\%$), while the variation of sample standard deviation σ_S is large (COV of $\sigma_S \approx 17.9\%$). This suggests that the standard deviation of soil parameters estimated from a small sample is usually not precise (i.e., having a large variation), while the sample mean is generally quite precise, which is consistent with the statistical theory.

Statistical characterization of model uncertainty

Model uncertainty is often significant in a geotechnical analysis. In fact, Zhang et al. (2009) has demonstrated that a geotechnical design that did not include model uncertainty in the analysis could be un-conservative even if parametric uncertainty was fully characterized. The model uncertainty is usually calibrated using statistical methods (Phoon and Kulhawy 2005; Dithinde et al. 2011) if data is available. For example, a multiplicative model is often employed to describe the model uncertainty using a model bias factor (or model factor):

$$BF_Q = \frac{\text{observed value}}{\text{predicted value}} = \frac{Q_o}{Q_P} \tag{3.7}$$

For the ULS capacity of shallow foundation, the predicted capacity is the calculated R_{ULS}, while the observed capacity is the "interpreted failure load" obtained from full-scale field load test. In this chapter, the database of field load tests compiled by Akbas and Kulhawy (2009b) is used to compute the mean (μ_{BF}) and standard deviation (σ_{BF}) of bias factor BF_Q. Then, the bootstrapping method is used to characterize the uncertainty in μ_{BF} and σ_{BF}. A summary of the statistical characterization of μ_{BF} and σ_{BF} is provided in Table 3.4.

Table 3.4: Sample statistics of model bias factor BF_Q by bootstrapping method

Uncertain variables	μ_{BF}	σ_{BF}
Mean	1.010	0.203
Std. dev.	0.033	0.034

Table 3.5: Results from bootstrapping method for estimating uncertainty in statistics of *a* and *b*

Uncertain variables	μ_a	μ_b	σ_a	σ_b	ρ_{ab}
Mean	0.6992	1.7675	0.1549	0.9416	-0.7177
Std. dev	0.0139	0.0845	0.0125	0.0794	0.0472

For the SLS failure, the model uncertainty parameters are reflected in parameters *a* and *b*, in addition to the bias factor BF_Q. In this chapter, the mean (μ_a) and standard deviation (σ_a) of parameter *a*, the mean (μ_b) and standard deviation (σ_b) of parameter *b*, and the correlation coefficient (ρ_{ab}) between *a* and *b* are calculated using the database compiled by Akbas and Kulhawy (2009a). To evaluate the possible variation in these

statistical parameters, the bootstrapping method is employed, and the results are shown in Table 3.5.

Reliability-Based Robust Geotechnical Design

An outline for reliability-based robust geotechnical design (RGD) is presented below, using shallow foundation design in cohesionless soil as an example. In reference to Figure 3.4, the RGD approach is summarized in the following steps (with commentaries):

Step 1: *Characterize the uncertainty in the sample statistics of noise factors (including both key soil parameters and model factors) and identify the design domain*. This step is shown as the first two blocks in the left side of the flowchart shown in Figure 3.4. For the design of shallow foundation in cohesionless soils, soil parameter ϕ', the ULS model factor BF_Q and the two curve fitting parameters *a* and *b* of the SLS model are identified as noise factors. The uncertainty in the statistics (mean and standard deviation) of each of the noise factors may be estimated with bootstrapping method.

In the geotechnical design of a square shallow foundation, the design parameters are the foundation width *B* and the embedment depth *D*. The design range for footing width *B* typically varies from a minimum of 1 m to a maximum value of 5 m (Akbas 2007; Akbas and Kulhawy 2011). The minimum foundation embedment depth *D* is set at 1 m based on the load level in this example (Coduto 2000), and the maximum depth is set at 2 m to minimize the disturbance to adjacent structures (Wang and Kulhawy 2008). For

a shallow foundation, the ratio of embedment depth to foundation width (D/B) is generally kept below 4. Of course, the engineer may have to consider local design concerns such as expansive soils, collapsing soils, frost heave, or construction issues. Thus, different constraints may be adopted to identify the domain of design parameters.

For convenience of construction, the foundation dimensions are typically rounded to the nearest 0.1 m (Wang 2011). Thus, within the constraints of three geometric requirements, namely, $1 \le B \le 5$; $1 \le D \le 2$; (D/B) < 4, a finite number of designs (each represented by a pair of B and D) can be identified. For example, for the shallow foundation (Figure 3.1) considered in this chapter, the number of possible designs in the design domain is M ≈ 450.

Step 2: *For each design, determine the mean failure probability of the design and the standard deviation of the failure probability*. This step is shown as the inner loop (Figure 3.4) that ends in the bottom block in the left side of the flowchart. In this chapter, the failure probability based on either ultimate limit state (ULS) or serviceability limit state (SLS) is used as a measure of system response. Recall that a design is considered *robust* if the variation of its system response caused by the uncertainty of noise factors is small. The variation of the failure probability is mainly caused by the variation of the derived statistics of the noise factors. Thus, in this step the mean and standard deviation (as a measure of robustness) of the failure probability are evaluated based on a modified point estimate method (PEM; Zhao and Ono 2000).

When mean (μ_S) and standard deviation (σ_S) of ϕ', as well as mean (μ_{BF}) and standard deviation (σ_{BF}) of model factor BF_Q are fixed values, the traditional reliability

analysis using, for example, first order reliability method (FORM; see Ang and Tang 1984) will yield a fixed value for ULS failure probability. Of course, the resulting ULS failure probability will no longer be a fixed value if uncertainties exist in μ_S, σ_S, μ_{BF} and σ_{BF}, and they have to be treated as random variables. In such a scenario, the variation of the ULS failure probability can be obtained using PEM with 4 input random variables, μ_S, σ_S, μ_{BF} and σ_{BF}. Detailed formulation for PEM with multiple input variables can be found in Zhao and Ono (2000). Similarly, the variation of the SLS failure probability is caused by uncertainty in the statistical moments of noise factors, and thus can be evaluated with 9 input random variables, including μ_S, σ_S, μ_{BF}, σ_{BF}, μ_a, σ_a, μ_b, σ_b and ρ_{ab}. Again, the PEM procedure by Zhao and Ono (2000) can be used to evaluate the variation of the SLS failure probability.

The PEM approach requires an evaluation of the failure probability at each of a set of "estimating" points (or sampling points) of the input random variables. Thus, the computation of the failure probability needs to be repeated for a total of $N = 7 \times k$ times, where k is the number of input random variables and the multiplier "7" represents the seven sampling points that are required in the seven-point PEM formulation by Zhao and Ono (2000). In each repetition, statistics of input random variables at each PEM estimating point must be assigned, and then the failure probability is evaluated using FORM. The resulting N failure probabilities (at the completion of the inner loop shown in Figure 3.4) are then used to compute the mean and standard deviation of the failure probability.

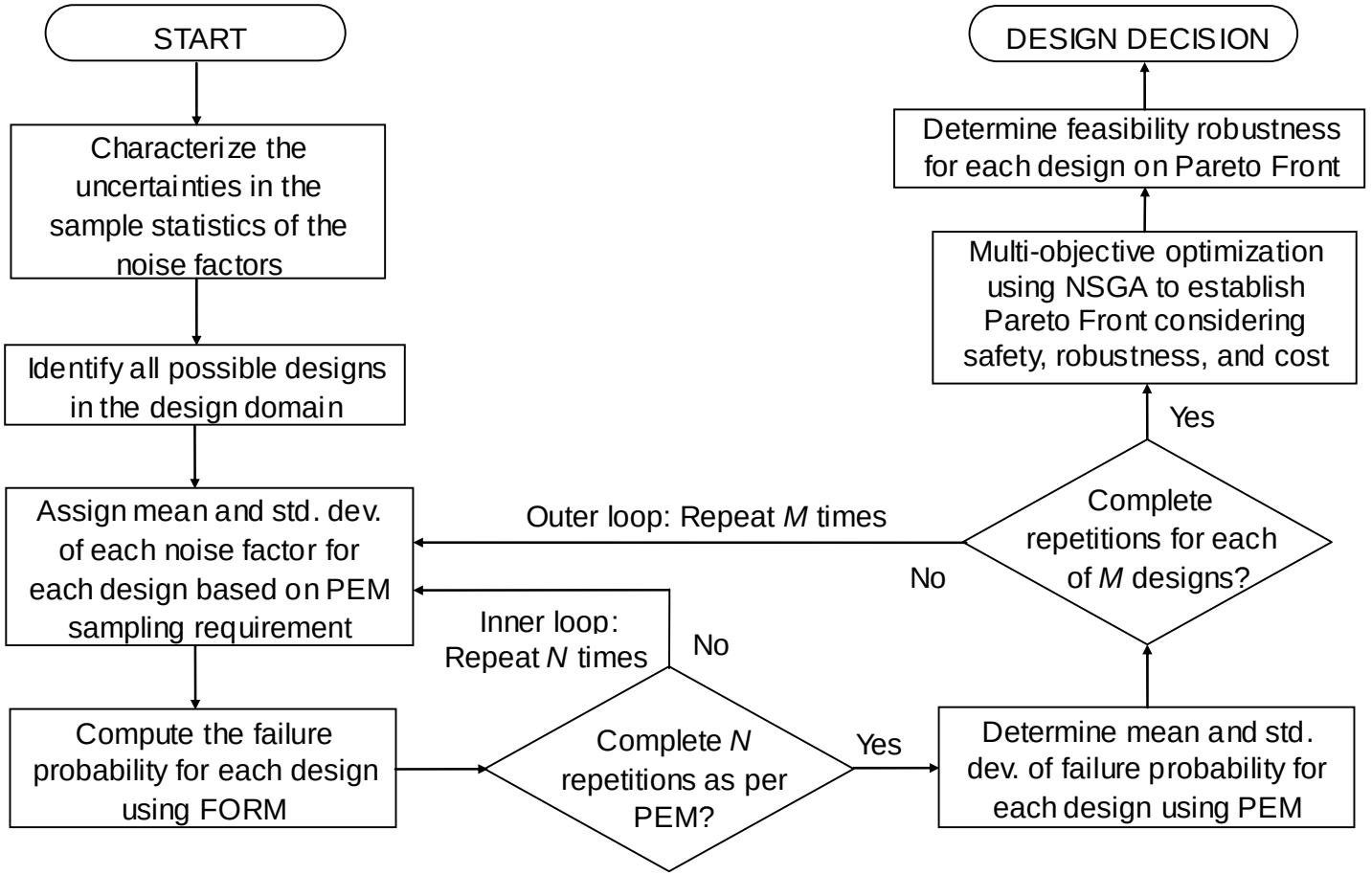

Figure 3.4: Flowchart illustrating robust geotechnical design of shallow foundation

Step 3: *Repeat Step 2 for each of the M designs in the design domain*. For each design, the mean and standard deviation of the failure probability are determined. This step is represented by the outer loop shown in Figure 3.4.

Step 4: *Perform a multi-objective optimization using non-dominated sorting genetic algorithm to establish a Pareto Front, followed by determination of feasibility robustness for choosing best design.* This step is represents by the last two blocks (in the right side) of the flowchart shown in Figure 3.4.

In the proposed RGD methodology, multi-objective optimization is required. In the illustrative example presented later, cost and design robustness are set as the objectives and safety (reliability) is achieved by means of a set of constraints. This is quite similar to the traditional reliability-based design except that the design robustness is explicitly considered as an additional objective. It is noted that the robustness in terms of standard deviation of the failure probability for each design is obtained in Step 3.

The concept of Pareto Front is briefly introduced here. When multiple objectives (in this case, two objectives) are enforced, it is likely that no single best design exists that is superior to all other designs in all objectives. However, a set of designs may exist that are superior to all other designs in all objectives; but within the set, none of them is superior or inferior to others in all objectives. This set of optimal designs constitutes a Pareto Front (Ghosh and Dehuri 2004).

Selection of a set of optimal designs that constitute Pareto Front is a multi-objective optimization problem. In this chapter, the Non-dominated Sorting Genetic Algorithm version II (NSGA-II), developed by Deb et al. (2002), is used to establish the

Pareto Front, in which, the optimal designs are searched in the discrete design domain (Lin and Hajela 1992).

Traditional Reliability-Based Design of Shallow Foundation

The traditional reliability-based design of square shallow foundation is first presented herein to provide a reference. The spread foundation example is shown in Figure 3.1 and statistics of uncertain parameters are assumed with a fixed value (that is, taking only mean values of these statistics in Tables 3.3, 3.4, and 3.5). The probability of SLS and ULS failure for each design for a combination of vertical permanent load component of G and variable load of Q is determined using FORM. This analysis is repeated for all possible designs in the design space. For illustration purpose, the results (i.e., failure probabilities) are plotted only for designs with D = 1.0 m, 1.5 m and 2.0 m, as shown in Figure 3.5.

It can be seen from Figure 3.5 that the probabilities of both ULS failure and SLS failure decrease with the increase of B and D. The probability of failure for ULS and SLS is quite similar. As the ULS failure probability requirement is more stringent than the SLS failure probability requirement, in this case, the former controls the design of shallow foundations, which is consistent with previous investigations (Wang and Kulhawy 2008; Wang 2011).

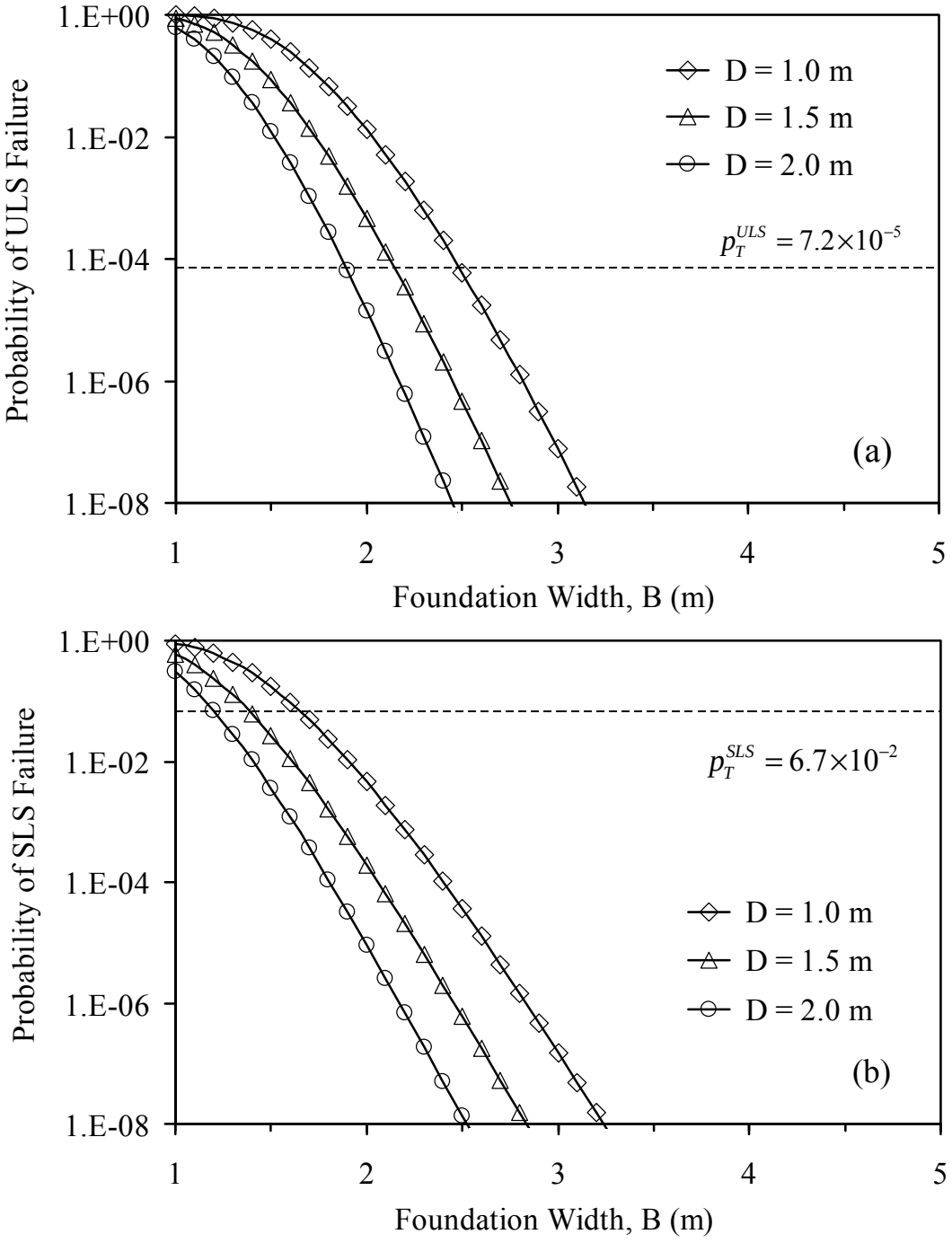

Figure 3.5: Probabilities of failure of selected designs with fixed mean and standard deviation of noise factors: (a) ULS failure; (b) SLS failure

In a traditional reliability-based design, the reliability is used as a constraint to screen for acceptable designs, and then the best design is attained by selecting the least-cost design (Zhang et al. 2011). In this chapter, the procedure for cost estimation by Wang and Kulhawy (2008), described previously, is adopted. It should be noted that cost estimation is not the focus of this chapter, and that the proposed RGD approach is not dependent on any particular cost estimation method. In fact, any reasonable cost estimation methods can be used.

In the example discussed herein (Figure 3.1), the reliability requirements defined in Eurocode 7 for foundation design, specifically, the target ULS reliability index $\beta_T^{ULS} = 3.8$ (corresponding to $p_T^{ULS} = 7.2\times10^{-5}$) and the target SLS reliability index $\beta_T^{SLS} = 1.5$ (corresponding to $p_T^{SLS} = 6.7\times10^{-2}$), are adopted (Wang 2011). If the minimum cost is the only criteria for selecting the "best" design after screening with reliability requirements, then the design with B = 1.9 m and D = 2.0 m will be selected.

The traditional reliability-based design is predicated on the accuracy of the estimated statistics of soil parameters and model factors. To demonstrate the effect of the uncertainty of these estimated statistics on the reliability-based design, a series of analyses is performed. For demonstration purposes, the mean of each noise factor (soil parameters or model factor) is set at its sample mean and the standard deviation of each noise factor is assumed to vary in the range of 95% confidence interval.

Although not shown here, the uncertainty in the statistics of SLS model factor has little effect on the final design, which is consistent with previous finding that the ULS failure controls the design. Thus, only the variation in standard deviation of ϕ', denoted

as σ_S, and the variation in standard deviation of BF_Q, denoted as σ_{BF}, are considered. For illustration purposes, both σ_S and σ_{BF} are assumed three different levels, namely, low, medium, and high variation. These three levels of variation are arbitrarily assigned to be at the lower bound of the 95% confidence interval, the mean value, and the upper bound of the 95% confidence interval.

Table 3.6 shows the least cost designs that satisfy the target failure probability requirement ($p_f^{ULS} < p_T^{ULS} = 7.2\times10^{-5}$) at various levels of σ_S and σ_{BF}. The results show that the least cost designs are sensitive to the assumed σ_S and σ_{BF}. Under the lowest level of σ_S and σ_{BF} (among all cases in Table 3.6), the least cost design costs 769.4 USD, while it costs 1404.0 USD under the highest level of variation. Thus, in a traditional reliability-based design that uses target failure probability as a constraint, the selection of "best" design based solely on least cost is meaningful only if the statistics of noise factors (soil parameters and model factors) can be ascertained.

Table 3.6: Least-cost designs under various standard deviation levels in noise factors

σ_S (^{o})	σ_{BF}	B (m)	D (m)	Cost (USD)
1.12	0.148	1.6	2.0	769.4
1.12	0.203	1.8	1.8	910.8
1.12	0.260	1.9	2.0	1026.0
1.84	0.148	1.8	2.0	936.5
1.84	0.203	1.9	2.0	1026.0
1.84	0.260	2.1	1.9	1200.1
2.43	0.148	2.0	1.9	1104.0
2.43	0.203	2.1	2.0	1216.9
2.43	0.260	2.3	1.9	1404.0

Table 3.7: ULS failure probability of a given design (B = 1.9 m, D = 2.0 m) under different uncertainty levels in noise factors

σ_S (°)	σ_{BF}	B (m)	D (m)	ULS failure probability, p_f^{ULS}
1.12	0.148	1.9	2.0	2.01E-08
1.12	0.203	1.9	2.0	1.95E-06
1.12	0.260	1.9	2.0	4.68E-05
1.84	0.148	1.9	2.0	6.83E-06
1.84	0.203	1.9	2.0	6.36E-05
1.84	0.260	1.9	2.0	3.83E-04
2.43	0.148	1.9	2.0	1.30E-04
2.43	0.203	1.9	2.0	4.77E-04
2.43	0.260	1.9	2.0	1.50E-03

If the standard deviation of noise factors is underestimated by a certain margin, then it is likely that an acceptable design (a design that meets ULS target failure probability) will no longer be satisfactory. For example, the design (B = 1.9 m and D = 2.0 m) was acceptable (meeting the target failure probability) at the uncertainty level of $\sigma_S = 1.84^\circ$ and $\sigma_{BF} = 0.203$. This design is re-analyzed with various levels of uncertainty. The results are shown in Table 3.7, which indicate that in many instances (where the uncertainty levels are higher than the level that was assumed in the previous design), the target ULS failure probability ($p_T^{ULS} = 7.2\times10^{-5}$) is no longer satisfied.

Reliability-Based Robust Geotechnical Design

One way to reduce the effect of the uncertainty of the statistical characterization of soil parameters and model factors in a reliability-based design is considering robustness *explicitly* in the design. In this section, the reliability-based RGD methodology

outlined previously is applied to the same shallow foundation design (see Figure 3.1). For this demonstration exercise, the statistics of the noise factors listed in Tables 3.3, 3.4, and 3.5 are included in the analysis.

As per the flowchart of the RGD procedure shown in Figure 3.4, the mean and standard deviation of the ULS failure probability, denoted as μ_p^{ULS} and σ_p^{ULS}, respectively, can be obtained for all possible designs in the design space using PEM. Since ULS controls the design in this case, only the ULS failure probability is of concern here.

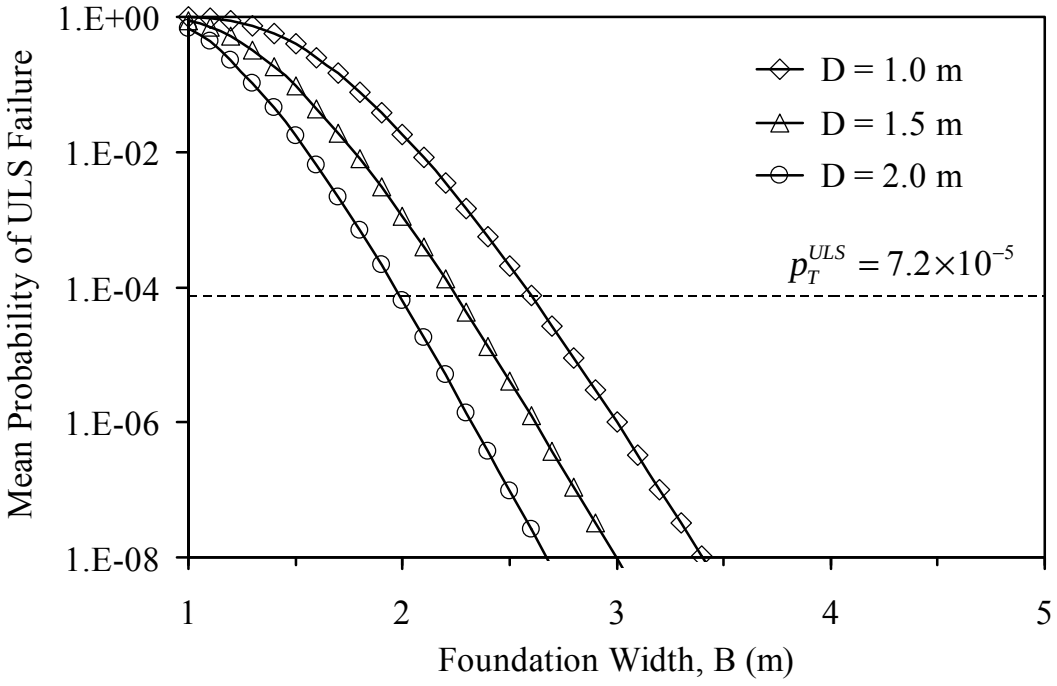

Figure 3.6: Mean ULS failure probabilities of selected designs considering variation in statistics of noise factors

As an example, Figure 3.6 shows the mean ULS failure probability (μ_p^{ULS}) for selected designs with D = 1.0 m, 1.5 m and 2.0 m. Similarly, Figure 3.7 shows the standard deviation of the ULS failure probability (σ_p^{ULS}) of selected acceptable designs with D = 1.0 m, 1.5 m and 2.0 m.

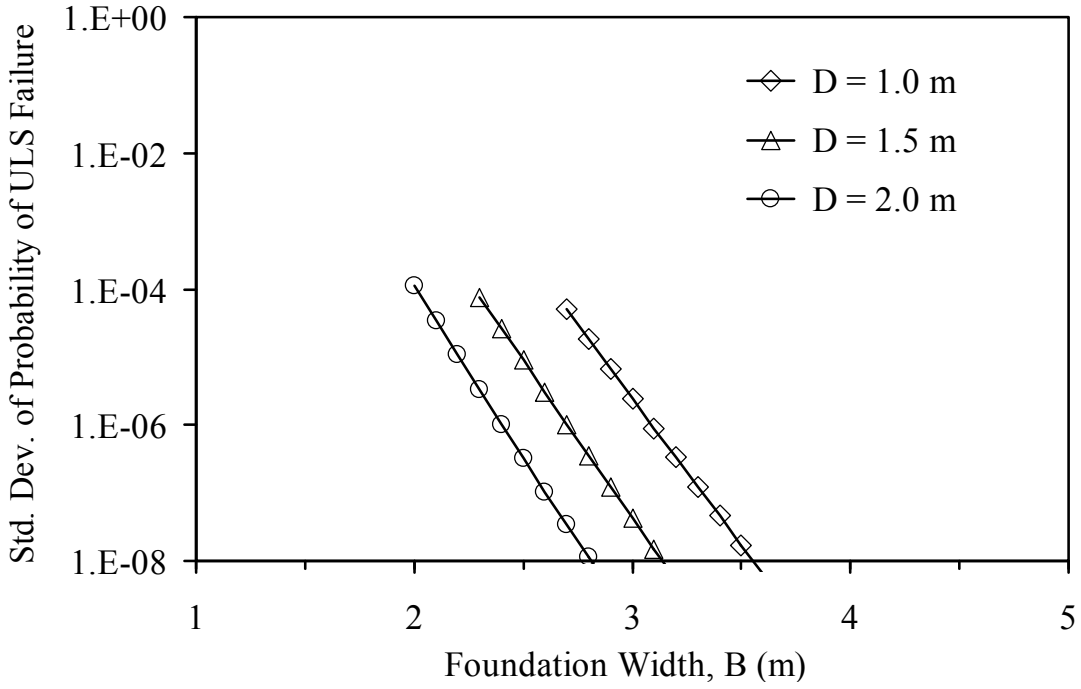

Figure 3.7: Standard deviation of ULS failure probabilities of selected acceptable designs considering variation in statistics of noise factors

Because many designs that meet the safety requirement of $p_f^{ULS} < p_T^{ULS} = 7.2\times10^{-5}$ are associated with different levels of robustness (in terms of σ_p^{ULS}) and cost (which can be calculated using Eq. 3.6), a multi-objective optimization is needed.

NSGA-II algorithm to obtain Pareto Front

As noted previously, the NSGA-II algorithm (Deb et al. 2002) is employed to search for the Pareto Front in the design space. The NSGA-II algorithm is summarized in the following (with reference to Figure 9). First, a random "parent population" P_0 from the design space is created with a size of n. The term "parent population" is widely used in Genetic Algorithm (GA); here, it can be thought of as the first trial set of "optimal" designs. A series of genetic algorithm (GA) operations such as mutation and crossover are performed on "parent population" P_0 to generate the "offspring population" Q_0 with the same size of N. Then, an iterative process is adopted to refine the parent population (Lin and Hajela 1992). In the GA, each step in the iteration is termed as a "generation".

In the t^{th} generation, the parent population P_t and the offspring population Q_t are combined to form an intermediate population $R_t = P_t \cup Q_t$ with a size of $2n$. Non-dominated sorting is next performed on R_t, which groups the points in R_t into different levels of non-dominated fronts. For example, the best class is labeled F_1, and the second best class is labeled F_2, and so on. The best n points are selected into parent population of the next generation, P_{t+1}. Using the scenario illustrated in Figure 3.8 as an example, if the number of points in F_1 and F_2 is less than n, they will all be selected into P_{t+1}. Then, if the number of points in F_1 and F_2 and F_3 exceeds the population size n, the points in F_3 are sorted using the "crowding distance" sorting technique (Deb et al. 2002), which aims to maintain the diversity in the selected points. Thus, the best points in F_3 are selected to fill all remaining slots in the next population P_{t+1}. After obtaining P_{t+1} in the t^{th} generation,

P_{t+1} is then treated as the parent population in the next generation and the process is repeated until P_{t+1} is converged. The final, converged P_{t+1} is the Pareto Front.

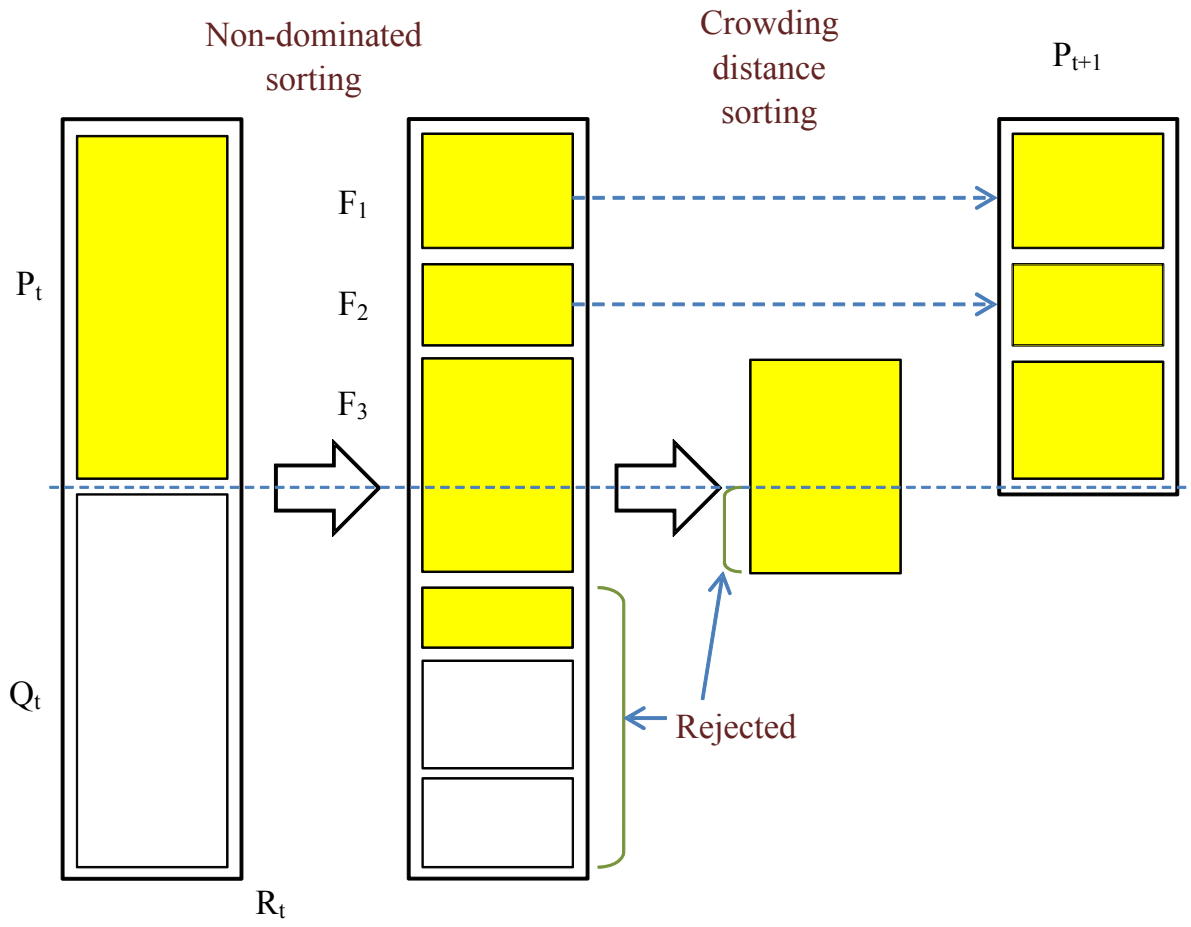

Figure 3.8: An Illustration of NSGA-II algorithm (modified after Deb et al. 2002)

In the shallow foundation design example, this optimization with NSGA-II may be achieved by using target failure probability as a constraint and robustness and cost as objectives. Symbolically, this optimization can be set up as follows:

Find $\mathbf{d} = [B, D]$

Subject to: $B \in \{1.0\text{m}, 1.1\text{m}, 1.2\text{m}, \ldots, 5.0\text{m}\}$ and $D \in \{1.0\text{m}, 1.1\text{m}, 1.2\text{m}, \ldots, 2.0\text{m}\}$

$$\mu_p^{ULS} < p_T^{ULS} = 7.2 \times 10^{-5}$$

Objectives: Minimizing the standard deviation of ULS failure probability (σ_p)

Minimizing the cost for shallow foundation.

As with any Genetic Algorithm (GA) process, the design parameters (*B* and *D* in this case) are generated in the discrete space. The population size of 100 with 100 generations is used in the NSGA-II optimization (Deb et al. 2002). Although not shown here, the points on the Pareto Front (a set of optimum designs) are initially very scattered, but gradually converge. For this shallow foundation design (Figure 3.1), converged results are obtained at 20th generation. At convergence, 62 "unique" designs are selected into the Pareto Front, as shown in Figure 3.9. It can easily be observed that there is an obvious trade-off relationship between cost and robustness. The obtained Pareto Front can be used as a design aid for the decision maker to select the "best" design based on the desired target cost or robustness level.

Selection of best design based on feasibility robustness

The Pareto Front shown in Figure 3.9 uses the standard deviation of the failure probability directly as a measure of robustness. While this Pareto Front provides a trade-off relationship that can aid in making informed design decisions, it may be desirable to

use a relative measure of robustness, a more user-friendly index. Thus, the results shown in Figure 3.9 are further refined.

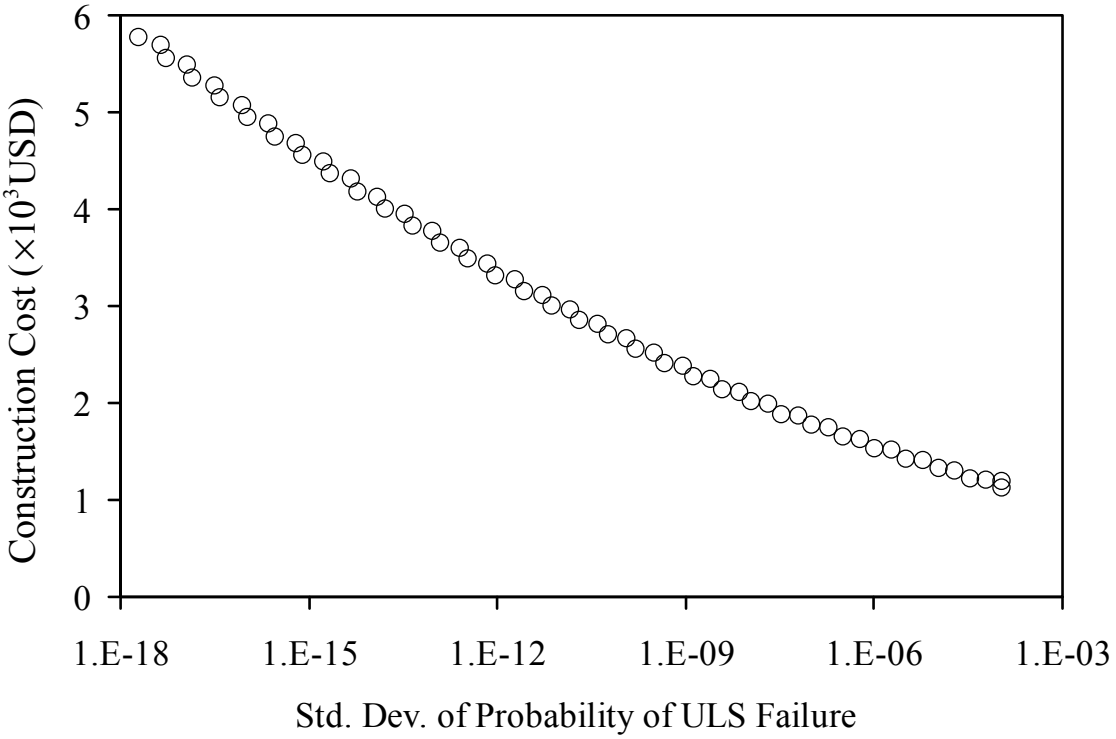

Figure 3.9: Converged Pareto Front for shallow foundation design obtained by NSGA-II based on two-objective (cost and robustness)

"Feasibility robustness," as defined by Parkinson et al. (1993), is the design that can maintain feasible (or safe) status relative to the nominal constraint for a definable probability as it undergoes variations. For the design example of shallow foundation, the ultimate limit state (ULS) requirement controls the design. In the safety constraint that requires the ULS failure probability to be less than the target probability, $p_f^{ULS} \le p_T^{ULS} = 7.2\times10^{-5}$, the failure probability (p_f^{ULS}) at a given state is a random variable

that depends on the uncertainty in statistics of noise factors, and the target probability is a fixed value. Symbolically, feasibility robustness can be formulated as follows:

$$\Pr[(p_f^{ULS} - p_T^{ULS}) < 0] \geq P_0 \tag{3.8}$$

where $\Pr[(p_f^{ULS} - p_T^{ULS}) < 0]$ is the probability that the ULS safety constraint is satisfied, and P_0 is an acceptable probability pre-defined by the designer. Thus, an index may be created for assessing the feasibility robustness.

Determination of the probability $\Pr[(p_f^{ULS} - p_T^{ULS}) < 0]$ requires the knowledge of the distribution of p_f^{ULS}, which is generally difficult to ascertain. Based on the previous studies by Most and Knabe (2010) and Luo et al. (2012b), the resulting histogram of the reliability index such as β^{ULS} (corresponding to p_f^{ULS}) caused by variance in sample statistics can be approximated with a normal distribution. Thus, an equivalent counterpart in the form of $\Pr[(\beta^{ULS} - \beta_T^{ULS}) > 0]$, where $\beta_T^{ULS} = 3.8$ (corresponding to $p_T^{ULS} = 7.2 \times 10^{-5}$), may be used to assess the level of feasibility robustness.

The mean and standard deviation of β^{ULS}, denoted as μ_β and σ_β respectively, can be obtained using FORM integrated with PEM. Then, Eq. (3.8) can be replaced by:

$$\Pr[(\beta^{ULS} - 3.8) > 0] = \Phi(\beta_\beta) \geq P_0 \tag{3.9}$$

where Φ is the cumulative standard normal distribution function, and β_β is defined as:

$$\beta_\beta = \frac{\mu_\beta - 3.8}{\sigma_\beta} \tag{3.10}$$

The term β_β may also be used as an index of feasibility robustness. The relationship between β_β and the cost for the 62 designs on the Pareto Front is shown in Figure 3.10. As expected, the results show that a design with higher feasibility robustness (higher β_β) requires a higher cost. Thus, a trade-off between cost and robustness is obvious. It is noted that in the lower cost range, the curve is relatively flat, indicating that a small increase in cost can result in a large increase in feasibility robustness, which is cost-efficient. In the higher cost range, however, the slope is relatively sharp, indicating that it costs a lot more to raise robustness, which is not cost-efficient.

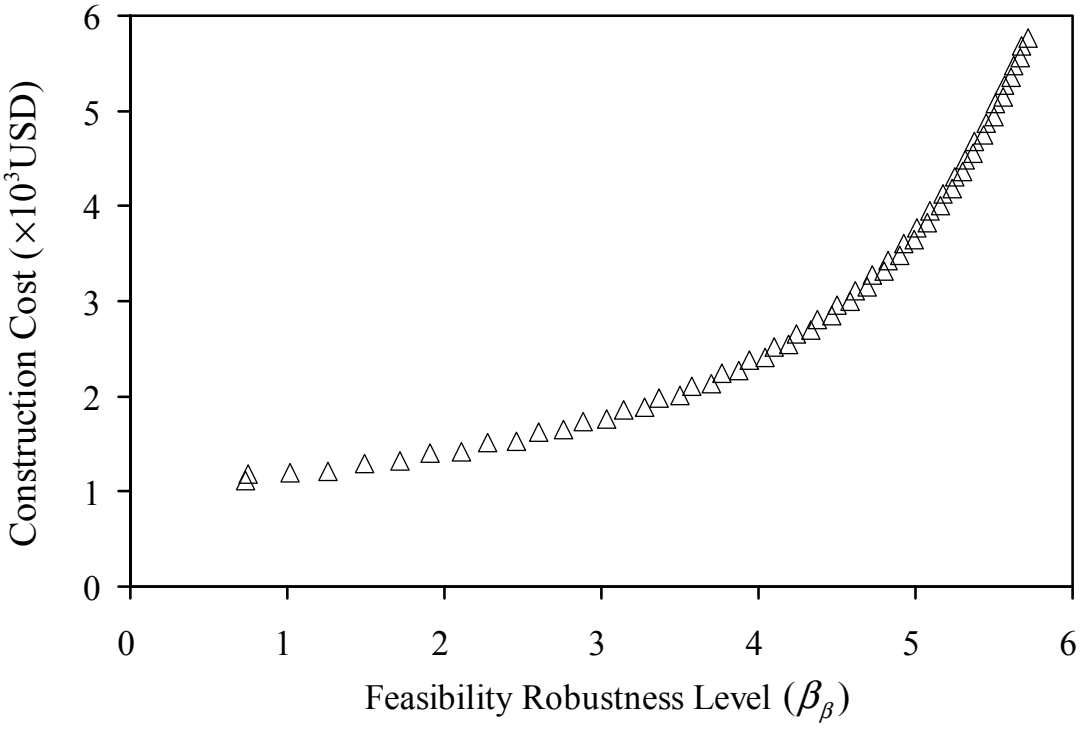

Figure 3.10: Cost versus feasibility robustness for all designs on Pareto Front

By selecting a target feasibility robustness level (β_β^T), the least-cost design among those on the Pareto Front can readily be identified. For example, when the target feasibility robustness is set at $\beta_\beta^T = 2$, which corresponds to an acceptance probability of $P_0 = 97.72\%$, the least-cost design is $B = 2.3$ m and $D = 2.0$ m, which costs 1423.7 USD. The least cost designs of the shallow foundation corresponding to different target feasibility robustness levels are listed in Table 3.8. The feasibility robustness offers an easy-to-use quantitative measure for making an informed design decision considering cost and robustness after satisfying the safety requirements.

Table 3.8: Selected final designs at various feasibility robustness levels

β_β	P_0	B (m)	D (m)	Cost (USD)
1	84.13%	2.1	1.9	1200.1
2	97.72%	2.3	2.0	1423.7
3	99.87%	2.6	2.0	1763.7
4	99.997%	3.1	2.0	2409.8

Additional Discussion: Effect of Spatial Variability

Recent studies (e.g., Schweiger and Peschl 2005; Griffiths et al. 2009; Luo et al. 2011; Luo et al. 2012) have shown that the traditional reliability analysis without considering spatial variability may yield an overestimation of the failure probability in many geotechnical problems. Thus, it would be of interest to examine the effect of spatial variability of soil parameters on the reliability-based robust design of shallow foundations. To demonstrate the procedure to consider the effect of spatial variability, the

ten effective friction angles ϕ' (for dry sand, $c' = 0$) listed in Table 3.2 are assumed to have been obtained from triaxial tests conducted on samples taken at an equal interval of 1 m in this homogeneous sand.

To characterize the soil spatial variability, it is essential to determine a fundamental statistical indicator of spatial variability, namely, *scale of fluctuation* θ, which is defined as the distance within which the soil properties show relatively strong correlation from point to point (Vanmarcke 1977 & 1983). Determination of scale of fluctuation θ generally requires a large amount of in-situ or experimental data taken over a wide range at site of concern, and many approaches have been proposed to determine θ (e.g., DeGroot and Baecher 1993; Baecher and Christian 2003; Fenton and Griffiths 2008). However, in this example, as the sample size of effective friction angles ϕ' is quite small, it is difficult to determine the scale of fluctuation of ϕ'. Nevertheless, according to Vanmarcke (1977), the vertical scale of fluctuation of ϕ' of a site may be approximately estimated as: $\theta = 0.8\left(\overline{d}\right)$ where $\overline{d}$ is the average distance between intersections of fluctuating property and its trend function. Based on the limited data in Table 3.2, $\overline{d}$ is estimated to be about 2 m, and thus $\theta \approx$ 1.6 m, which is within the typical range of vertical scale of fluctuation, θ = 0.5 m to 2.0 m, reported by Cherubini (2000). In the absence of sufficient data, for demonstration purpose, the vertical scale of fluctuation θ of ϕ' is assumed to be a lognormally distributed random variable with a mean of 1.6 m and a COV of 0.3 (Luo et al. 2012). On the other hand, the horizontal scale of fluctuation is generally much larger than the foundation dimension, typically in

the range of 10 m to 30 m; thus, the effect of the horizontal spatial variability may be neglected for the design of shallow foundations (Cherubini 2000).

One way to consider the effect of spatial variability is through a variance reduction technique. Vanmarcke (1983) pointed out that the averaged variability of soil properties over a large domain can be approximated with an equivalent variance. The averaged variance of soil parameter considering the spatial average effect can be obtained as:

$$\sigma_{\Gamma}^2 = \Gamma^2 \cdot \sigma^2 \tag{3.11}$$

where σ= the standard deviation of soil parameter of concern (ϕ' in this study); σ_{Γ} = the reduced standard deviation of soil parameter considering the spatial average effect; and Γ is the reduction factor defined as (assuming an exponential autocorrelation structure):

$$\Gamma^2 = \frac{1}{2}\left(\frac{\theta}{L}\right)^2 \left\{\frac{2L}{\theta} - 1 + \exp\left[-\frac{2L}{\theta}\right]\right\} \tag{3.12}$$

where L is the characteristic length, which is generally problem-dependent. For a shallow foundation, the characteristic length may be approximately estimated as the sum of the embedment depth and the foundation width, $L = D + B$ (Cherubini 2000).

To consider the effect of spatial variability in the reliability-based robust design, the scale of fluctuation θ may be treated as an additional noise factor, and accordingly the statistical characterization of the uncertainty of this noise factor is included in the RGD approach (Figure 3.4). The procedure to derive the Pareto Front is the same as presented previously. It is noted, however, that the standard deviation of ϕ' used in

reliability analysis is automatically reduced to account for the spatial averaging effect through Eq. (3.11).

Figure 3.11 shows the feasibility robustness index β_β for all designs on the derived Pareto Front that considers the effect of spatial variability. As a reference, the data from Figure 3.10 (in which the effect of spatial variability is not considered) are also plotted in Figure 3.11.

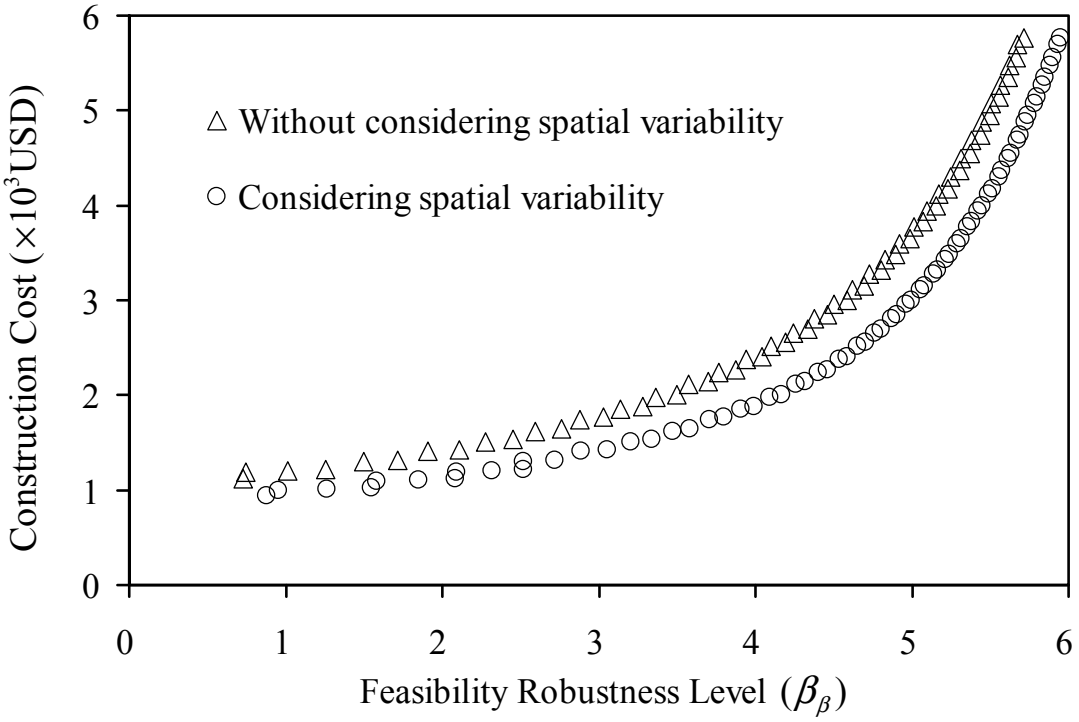

Figure 3.11: Comparison of cost versus feasibility robustness for all designs on Pareto Fronts derived with and without considering spatial variability

It can be observed from Figure 3.11 that for the same design (associated with a "unique" cost), the feasibility robustness index (β_β) considering spatial variability is

higher than that without considering spatial variability. At a given cost, the percent difference in feasibility robustness caused by the effect of spatial variability is more profound in the lower cost range. As the cost increases, the effect of spatial variability becomes less significant, especially at the higher cost range.

Table 3.9: Selected final designs at various feasibility robustness levels considering spatial variability

β_β	P_0	B (m)	D (m)	Cost (USD)
1	84.13%	1.9	1.9	1011.9
2	97.72%	2.0	2.0	1119.4
3	99.87%	2.3	1.9	1404.0
4	99.997%	2.7	2.0	1885.0

The least cost designs of this shallow foundation at different feasibility robustness levels considering spatial variability effect are listed in Table 3.9. Compared to the results shown in Table 3.8, at the same feasibility robustness level the design considering spatial variability costs less than that without considering spatial variability. Thus, for the example shallow foundation studied, the design that achieves the same target feasibility robustness tends to be slightly over-designed (at a slightly higher cost) if spatial variability is not considered. At the same cost level (which implies the same design, as each point in Figure 3.11 represent a unique design), the computed feasibility robustness is slightly lower if spatial variability is not considered. The implication is that the design that does not consider spatial variability is biased toward conservative (or safer) side in the shallow foundation design presented this chapter.

Summary

In this chapter, the concept of robustness is incorporated into the reliability-based design of shallow foundations to deal with the uncertainty in the estimated sample statistics of noise factors (including both key soil parameters and model factors), which is often a major problem in a reliability-based design. The bootstrapping technique is used to quantify the uncertainty in the sample statistics of both soil parameters and model factors, and the PEM integrated with FORM analysis is used to derive the resulting variation in the system response. The significance of design robustness has been demonstrated with a reliability-based design of shallow foundations. As demonstrated in this study, there often exists no single best design when multiple design objectives are imposed. Thus, an optimal set of designs, called Pareto Front, in which no design is inferior to others with respect to all objectives, is the best of what an engineer can obtain under such a scenario. The Pareto Front specifies a trade-off relationship between cost and robustness, after satisfying all safety requirements. This trade-off relationship enables the engineer to make a more informed design decision. Finally, it has been demonstrated through the example design of shallow foundations that NSGA-II is an effective and efficient tool for performing multi-objective optimization for establishing a Pareto Front.

CHAPTER FOUR

ROBUST GEOTECHNICAL DESIGN OF BRACED EXCAVATIONS IN CLAYS*

Introduction

Designing a braced excavation system (i.e., soil-wall-support system) in an urban environment in the face of uncertainty is a risky geotechnical operation, in that the "failure" of such a system (defined as the collapse of the excavation system or exceeding the allowable wall and ground settlement) can have detrimental effects on adjacent structures, with accompanying adverse social and economic effects. One recent excavation failure occurred in Singapore (Committee of Inquiry 2005) in which a stretch of the Nicoll Highway collapsed after the retaining wall that supported the excavation for a Mass Rapid Transit (MRT) tunnel failed. In this collapse, four lives were lost, damages ran into the millions and the project was delayed for approximately a year.

The deterministic design approach is commonly employed in the traditional design of braced excavations. There are two types of design requirements: the stability of the excavation system itself (known as the *stability* requirement) and the protection of adjacent structures against excavation-induced damage (known as the *serviceability* requirement). Two failure modes must be evaluated when ensuring stability: the basal heave failure and the push-in failure (Ou 2006). For the serviceability requirement, the

---

*A similar form of this chapter has been accepted at the time of writing: Juang CH, Wang L, Hsieh HS, Atamturktur S. (2013). Robust Geotechnical Design of braced excavations in clays. Structural Safety, doi:10.1016/j.strusafe. 2013.05.003.

wall and/or ground deformations caused by the excavation must be evaluated and controlled to prevent damage to the adjacent structures. Thus, the owner or regulatory agency often establishes the limiting factors of safety for stability requirements and the limiting maximum wall and/or ground settlement as a means of preventing damage to adjacent infrastructures, respectively (e.g., JSA 1988; PSCG 2000; TGS 2001; Ou 2006). The uncertainties in the soil parameters, however often makes it difficult to determine with certainty if both stability and serviceability requirements in a braced excavation are satisfied. As such, the engineer often faces conflicting goals in either overdesigning a structure for greater liability control or under-designing the structure to cut costs. To address this dilemma, the authors present a Robust Geotechnical Design (RGD) framework for purposes of designing braced excavations in clays.

Originally proposed by Taguchi (Taguchi 1986) for product quality control in manufacturing engineering, the concept of robust design has been used in mechanical and aeronautical designs (Chen et al. 1996; Seepersad et al. 2006; Marano et al. 2008; Paiva 2010). Any successful robust design concept must encompass both easy-to-control parameters, such as the dimension of a diaphragm wall and layout of struts for braced excavations, and hard-to-control factors such as uncertain soil parameters, which are referred to herein as noise factors. In that the uncertainty of these noise factors cannot be fully eliminated, the design objective becomes one of reducing the effects of the uncertainty of these noise factors on the response of the system. Therefore, the purpose of the robust design method is to derive a design that is robust against the effects of the uncertainty of these noise factors, thereby reducing the variability of the system response.

In this chapter, we describe our implementation of a robust geotechnical design (RGD) of braced excavations in a multi-objective optimization framework, within which all possible designs were first screened for safety requirements (including, in this chapter, stability and serviceability requirements). For the designs that satisfy the safety requirements, the cost and robustness were evaluated, and those designs were then optimized with the two objectives of minimizing the cost and maximizing the robustness. Because the two objectives are often conflicting, as is shown later, the result of the optimization is not a single best design, but rather a set of non-dominated designs (Deb et al. 2002), the collection of which is known as the Pareto Front (Cheng and Li 1997). The Pareto Front yields a trade-off relationship between the cost of the braced excavation and the robustness of that excavation design, which may be used to select the most preferred design.

Deterministic Model for Excavation-Induced Wall Deflection

The maximum wall deflection caused by a braced excavation is often used as a basis for field control to prevent damage to the adjacent infrastructures for two reasons. First, it is generally easier to achieve a greater accuracy in predicting the maximum wall deflection, as opposed to predicting ground settlement (Hashash and Whittle 1996; Kung et al. 2007), during the design. Second, it is easier to measure accurately the wall deflection than to measure ground settlement during the construction. Also because the maximum wall deflection is known to correlate with the maximum ground settlement

(Mana and Clough 1981; Kung et al. 2007), we selected the maximum wall deflection as the system response of concern for the robust design of the braced excavation system.

In this study, a computer code TORSA (Taiwan Originated Retaining Structure Analysis) created by Trinity Foundation Engineering Consultants (TFEC) Co. and based upon on the beam-on-elastic foundation theory, was adopted as the deterministic model for predicting the maximum wall deflection. This commercially available code has been validated and widely used by engineers in the design of braced excavations in Taiwan (Sino-Geotechnics 2010). In the beam-on-elastic foundation approach to simulating soil-structure interaction, the Winkler model is often applied, in which the retaining wall is simulated as a continuous beam of unit width, with the soils treated as springs (Ou 2006; Sino-Geotechnics 2010). In TORSA, the Winkler model is solved with the finite element method (FEM). The selection of TORSA as our deterministic model in this study is mainly motivated by its proven accuracy in predicting the maximum wall deflection, its execution speed, and the ease with which it is implemented into our robust design framework (to be elucidated later).

For a braced excavation in clay, the system response (i.e., maximum wall deflection) was determined to be the most sensitive to the normalized undrained strength (s_u / σ_v') and the normalized modulus of horizontal subgrade reaction (k_h / σ_v') (Hsiao et al. 2008; Ou 2006). These two parameters are usually quite uncertain due to soil variability and measurement error. Thus, they are treated as "noise factors" in the context of the robust design.

Methodology for Robust Design of Braced Excavations

Robust design concept and parameters setting

In a typical braced excavation design, the geometric dimensions (length, width, and depth) of the excavation are determined by either the structural engineer or the architect. For a braced excavation in clay using a diaphragm wall, the length of the wall (L), the thickness of the wall (t), the vertical spacing of the struts (S), and the strut stiffness (EA) are the design parameters. In the context of robust design, these are known as "easy to control" parameters because they are specified by a designer. The soil-related input parameters that exhibit a dominant effect on the maximum wall deflection in a braced excavation are the normalized undrained shear strength (s_u / σ'_v) and the normalized modulus of horizontal subgrade reaction (k_h / σ'_v), as noted previously. Besides, the surcharge behind the diaphragm wall (q_s) was also considered as a noise factor. They are treated as noise factors that exhibit significant variability and are "hard to control" (meaning that it is almost impossible for the designer to remove entirely the uncertainty in these parameters).

The purpose of a robust design, particularly in the case of a braced excavation, is to desensitize the system response of a "satisfactory" design to noise factors. Let us assume a braced excavation design scenario where the system response of concern is the maximum wall deflection (δ_{hm}). The noise factors are s_u / σ'_v, k_h / σ'_v and q_s, and the design parameters are L, t, S and EA. A design is considered "satisfactory" if it satisfies all the stability requirements (e.g., the computed factor of safety FS_j greater than the specified minimum FS_j) and the serviceability requirement (the computed δ_{hm} value less

than the specified allowable value). Within our Robust Geotechnical Design, the goal is to derive a satisfactory design by selecting a proper set of design parameters (*L*, *t*, *S*, *EA*) so that the system response, in the form of the maximum wall deflection (δ_{hm}), is sufficiently robust to withstand the *variation* in noise factors ($s_u / \sigma'_v, k_h / \sigma'_v, q_s$).

Developing a general robust geotechnical design (RGD) procedure

The objective of the proposed RGD approach, an example of which is illustrated with a flowchart as shown in Figure 4.1 for a braced excavation, was to identify the most optimal design (or a set of optimal designs) that was not only "satisfactory" (i.e., meeting the safety requirements) but also "robust" and "cost-efficient." The RGD framework is summarized as follows:

In Step 1, we defined the problem of concern and classify the design parameters and the noise factors for all input parameters of the braced excavation system, as described in the previous section.

In Step 2, we then characterized the uncertainty of noise factors and specified the design domain. For a braced excavation in clay, the noise factors in the context of robust design in this study include s_u / σ'_v, k_h / σ'_v and q_s. The uncertainty in these noise factors is often quantified using the available data from site investigation and experiences with similar projects.

For the design parameters, the design domain should be defined based upon their typical ranges, augmented with the local experiences. These design parameters should be

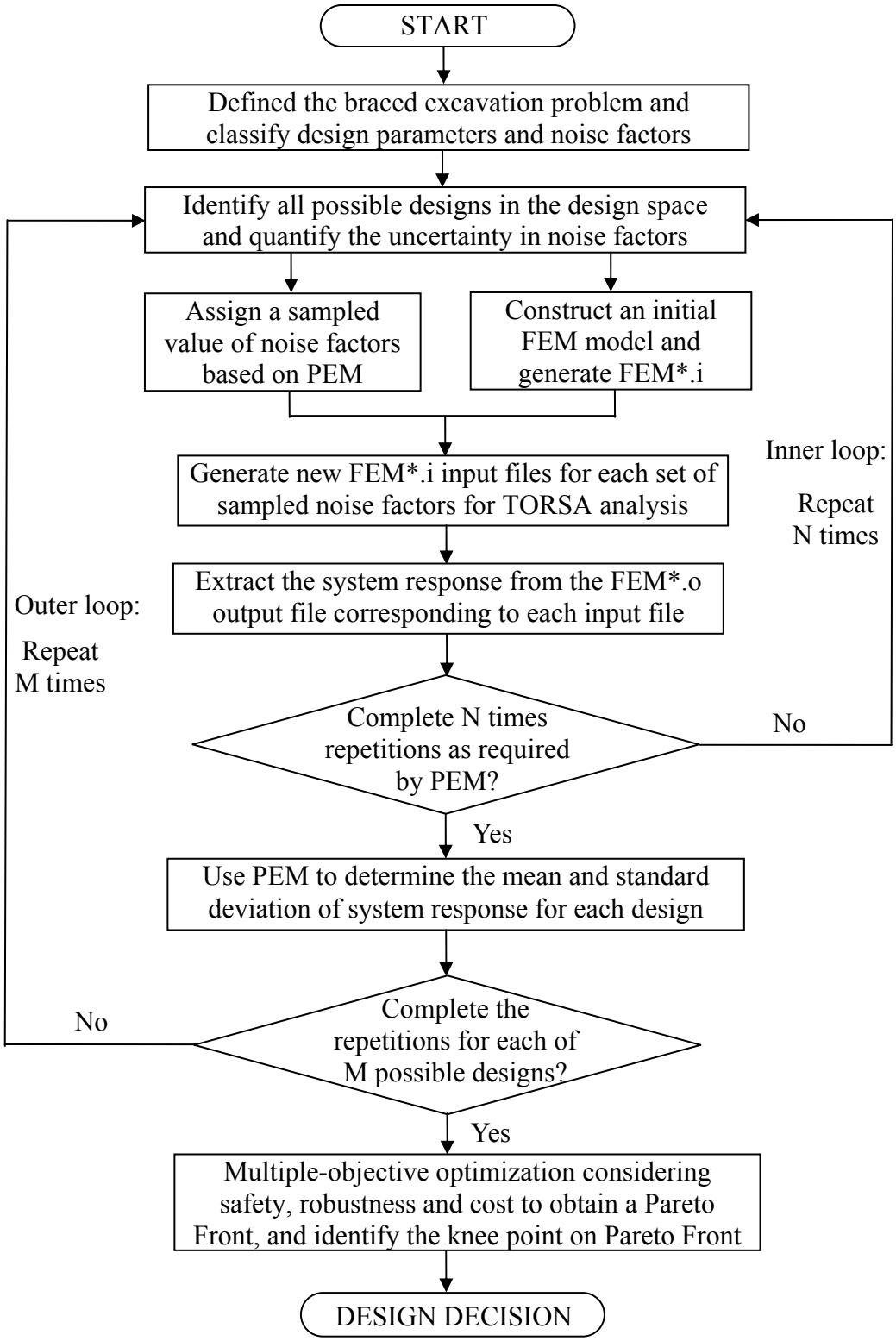

Figure 4.1: Flowchart of the proposed robust geotechnical design of braced excavations

specified in discrete numbers for convenience in construction. Thus, the design domain will consist of a finite number (M) of designs.

In Step 3, we then derived the mean and variance of the system response for robustness evaluation. Recall that a smaller *variation* (in terms of standard deviation) in the system response indicates a greater robustness. Thus, to assess the robustness of a design, the mean and standard deviation of the system response should be evaluated. In this chapter, the Point Estimate Method (PEM; Harr 1987 and Luo et al. 2013) is used to derive the mean and standard deviation of the system response in conjunction with TORSA.

Deriving this mean and variance was most challenging in the context of solving a braced excavation problem, as the "performance function" for the excavation-induced response is a finite element model without an *explicit* function. It involved coupling of the PEM-based reliability analysis (implemented through a Matlab program) and the deterministic FEM code (TORSA), as shown in the inner loop in Figure 4.1. For a given set of design parameters, the *initial* FEM model (the baseline model that is evaluated with only the mean values of the noise factors) is used, and the model file is written and saved as **FEM*.i** (input file name), which contains all necessary data for a FEM analysis with TORSA. In this chapter, the PEM approach was used to evaluate both mean and standard deviation of the system response. The PEM required evaluating the system response at each of the N sets of the sampling points of the noise factors ($N= 2^n$, where n is the number of input noise factors). In each repetition, the values of noise factors for each set of the PEM sampling points were assigned. The corresponding new **FEM*.i** input file for

each of the *N* set of sampling points was generated by modifying the initial **FEM*.i** input file. The system response for each of the *N* set of sampling points was obtained by automatically running TORSA (the FEM code) in the Matlab environment with the corresponding **FEM*.i** input file. The post-processing was undertaken upon completion of the TORSA solution process, and the system response was extracted from the corresponding **FEM*.o** output file generated from the input file. The resulting *N* system responses were then used to evaluate the mean and standard deviation of system response based upon the PEM formulation.

In Step 4, we repeated our analysis in Step 3 for each of *M* designs in the design space. Here, the design parameters in the **FEM*.i** input file were modified automatically in each of the repetitions of Step 3 and the mean and standard deviation of the system response for each design in the design space were determined. This step is represented by the outer loop shown in Figure 4.1.

In Step 5, we performed the multi-objective optimization considering the design objectives and design constraints to seek for robust design solutions. The objectives of this robust design scheme involve two distinct criteria: one involves enhancing the robustness, which is accomplished by minimizing the variation in the system response (maximum wall deflection), and the other involves enhancing the economic efficiency by minimizing the cost. The safety requirements, which include the stability and serviceability requirements, are implemented as the design constraints, which can be specified either deterministically or probabilistically.

Note that a unique optimal solution at which all objectives are optimized is highly unlikely for an optimization problem with multiple, and often conflicting, objectives. Rather, a Pareto Front composed of non-dominated solutions is usually obtained. A non-dominated solution is the one in which the improvement of the design in any one objective can only be achieved at expense of the others (Deb et al. 2002). As noted in previous chapter, Figure 2.3 depicts a possible optimization outcome in a bi-objective space where the Pareto Front lies on the boundary of the feasible region. Thus, the optimal solutions on the Pareto Front are the "best compromise solutions" that are optimal to both objectives (Cheng and Li 1997). In this chapter, the authors used a Non-dominated Sorting Genetic Algorithm version-II (NSGA-II) to obtain these optimal solutions, the procedures of which are detailed in Deb et al. (2002). Using the NSGA-II procedure, a Pareto Front (a set of optimal designs) can be established, which defines a "sacrifice-gain" trade-off relationship between cost and robustness.

If the desired cost/robustness level is specified, the Pareto Front is readily applicable to select the most preferred design. Should there be no available information about the desired level of cost/robustness, a knee point concept (described later) may be used to select the single most preferred design based on the "sacrifice-gain" relationship displayed by the Pareto Front.

Estimation of the Cost in a Braced Excavation

Cost-efficiency must be considered in the design of any geotechnical system (Wang et al. 2008; Zhang et al. 2011). The total cost of braced excavation includes the

costs of the diaphragm wall, costs of the bracing system, costs of excavation/disposal of the dirt, costs of dewatering of the site, and costs of placement of the requisite instrumentation. Because the site dimension and excavation depth is fixed for any such project, the costs for the last three terms are equal and the major optimization item for the cost of the braced excavation is the cost of the supporting system (including both the diaphragm wall and bracing system). Thus, the total cost for the supporting system Z is the summation of the cost of the diaphragm wall and the bracing system, which is expressed as:

$$Z = Z_w + Z_b \tag{4.1}$$

The cost of the diaphragm wall is proportional to the volume of the wall. As the perimeter length of a specific site is a fixed number, the cost of the diaphragm wall is determined by the length and thickness of wall, which is expressed as:

$$Z_w = c_w \times D \times L \times t \tag{4.2}$$

where Z_w is the cost of the diaphragm wall; c_w is the unit cost of diaphragm wall per m^3; D is the perimeter length of the excavation (m); L is the length of the wall (m); and t is the thickness of the wall (m). The unit cost of diaphragm wall c_w (including both material and labor costs) is approximately NT \$10, 000/m^3 in local practice (i.e., braced excavation in clays in Taipei), which corresponds to approximately 330 USD/m^3 (assuming that the currency exchange rate between the US Dollar and the New Taiwan Dollar is 1:30, i.e., NT \$1, 000 ≈ USD \$33).

The cost of the bracing system (e.g. struts consisting of H-section steels) is proportional to the total weight of the bracings. The total weight of the bracing, in turn, is

proportional to the number of vertical levels of the struts and the area of the excavation, which is expressed as:

$$Z_b = c_b \times A \times k \times n \tag{4.3}$$

where Z_b is the cost of the bracing system; c_b is the unit cost of the bracing system per m^2 per level; A is the area of the excavation site (m^2); k is the number of struts per level; n is the number of vertical levels of struts in that bracing system. The unit cost of the bracing system c_b (including both material and labor costs) is approximately NT \$1, 000/m^3 in local practice, which corresponds to approximately 33 USD/m^3. Thus, in sum, the total cost for the supporting system Z is a function of all design parameters. Five strut alterations per level were considered in our design example (presented later) for purposes of determining the strut stiffness: H300, H350, H400, 2@H350 and 2@H400 (note: 2@H350 means two H350 struts used per level). The cost difference between H300, H350 and H400 was generally negligible since the main cost incurred was that for the installation of the struts themselves, the cost of which is related to the number of struts per level. This expense, in turn, corresponded to the design parameter of the strut stiffness per level.

The cost in a braced excavation for purposes of robust design optimization described previously is based on the extensive experience of TFEC, a specialty design-built engineering firm, for braced excavations in Taiwan using the diaphragm walls. This is used as an example to illustrate the RGD methodology; other suitable cost schemes can be used in conjunction with the proposed RGD methodology.

Robust Geotechnical Design of Braced Excavation – Case Study

Brief summary of the example of braced excavation

To illustrate the proposed RGD method, we used a case study of braced excavation design in clays, with the soil profile at the excavation site a homogenous clay layer with the ground water table set at 2 m below the ground surface. The clay is assigned a deterministic unit weight of 1.9 ton/m^3. The excavation site, the dimensions of which are pre-defined by architectural and structural requirements, is rectangular in shape with a length of 40 m and a width of 25 m. The final excavation depth is 10 m and the diaphragm wall with multiple struts was employed as the retaining structure. There are three uncertain noise factors in the design. The normalized undrained strength (s_u / σ'_v) is assumed to have a mean of 0.32 and a COV of 0.2, and the normalized modulus of horizontal subgrade reaction (k_h / σ'_v), is assumed to have a mean of 48 and a COV of 0.5. These two soil parameters are assumed to be positively correlated with a correlation coefficient of 0.7. The surcharge behind the wall is assumed to have a mean of 1 ton/m and a COV of 0.2. These statistics are estimated based on local experience (Ou 2013, personal communication) and published literatures (Phoon et al. 1995; Hsiao et al. 2008; Luo et al. 2013).

As noted previously, the length (L) and the thickness of the wall (t), the vertical spacing of the struts (S), and the strut stiffness (EA) are the design parameters. In this particular example of braced excavation in a uniform clay layer, the length of the wall L typically ranges from 20 m to 30 m with increments of 0.5 m, and the thickness of wall t ranges from 0.5 m to 1.3 m with increments of 0.1 m. The strut stiffness EA typically has

five strut alternations per level: H300, H350, H400, 2@H350 and 2@H400. As a design routine, the preload of the strut is a fixed number depending upon the type of strut. For example, as in a previous design case in which H300 was assigned a preload of 50 tons, H350 was assigned a preload of 75 tons, and H400 was assigned a preload of 100 tons (Sino-Geotechnics 2010). For a typical excavation project undertaken in clay soil, the first level of strut is typically set at 1 m below the ground surface, and the last level at 3 m above the bottom of the excavation, with the location of all struts set at approximately 1 m above the excavation depth at that stage, except for the last stage (Kung et al. 2007; Sino-Geotechnics 2010). Thus, there are four practical choices in the vertical spacing of the struts *S:* 1.5 m, 2 m, 3 m and 6 m, which corresponds to the number of struts 5, 4, 3 and 2 as shown in the layout of struts in Figure 4.2. Based upon the combination of the design parameters (L, t, S, EA), there are totally 3780 possible discrete designs in the design space.

Optimization of braced excavation to obtain Pareto Front

For each of all the designs in the design space, PEM is used in evaluating both the mean and standard deviation of the maximum wall deflection given the noise factors, and the cost estimation method described previously is used in computing the cost of the supporting system of each design. With all these data, a thorough multi-objective optimization, using NSGA-II, which considers safety, robustness and cost, is then undertaken.

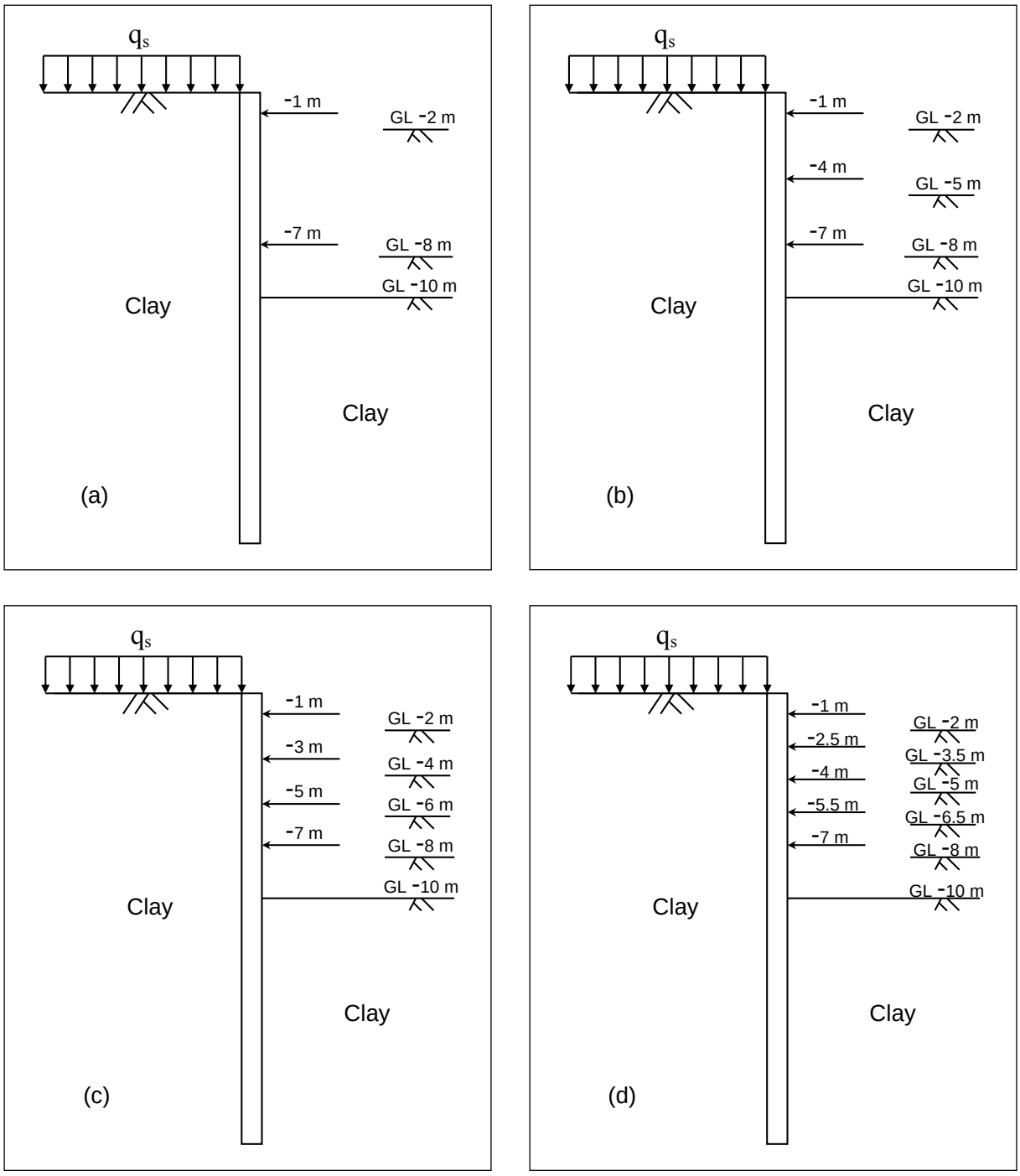

Figure 4.2: Four different strut layouts for design of braced excavations: (a) 6 m spacing; (b) 3 m spacing; (c) 2 m spacing; (d) 1.5 m spacing

In this configuration, the stability and serviceability constraints are enforced to ensure the safety of the braced excavation, and then the standard deviation of wall deflection is minimized to ensure robustness, and the cost-efficiency is achieved by minimizing the costs for the supporting system of the braced excavation. A formulation for the robust design of this braced excavation using NSGA-II is illustrated in Figure 4.3.

The population size of 100 with 100 generations (note: these are the limits chosen for optimization) is adopted in the NSGA-II optimization. It is noted that the points on the Pareto Front were initially very scattered, but they gradually converged to the final Pareto Front. The converged results were obtained at 20^{th} generation (or iterations) for this braced excavation design example, which yielded 25 "unique" non-dominated optimal designs. The parameters of these designs are listed in Table 4.1, which collectively constitute the Pareto Front shown in Figure 4.4.

The Pareto Front shown in Figure 4.4 offers a trade-off relationship between robustness (measured in terms of standard deviation of wall deflection) and cost of the excavation system (or more precisely, the supporting system). Reducing the standard deviation of the wall deflection (and enhancing the robustness) requires an increase in the cost of the supporting system. It should be noted that all designs on Pareto Front are satisfactory with respect to the deterministic safety constraints.

Given: L_E = 40 m (length of excavation)

B_E = 25 m (width of excavation)

H_f = 10 m (final excavation depth)

Find the value of Design Parameters:

t (wall thickness), L (wall length), S (strut spacing), EA (strut stiffness)

Subject to Constraints:

$t \in$ {0.5 m, 0.6 m, 0.7 m, 0.8 m, …, 1.3 m}

$L \in$ {20 m, 20.5 m, 21 m, 21.5 m, …, 30 m}

$S \in$ {1.5 m, 2 m, 3 m, 6 m}

$EA \in$ {H300, H350, H400, 2@H350, 2@H400}

Mean factor of safety for the push-in and basal heave ≥ 1.5

Mean maximum wall deflection ≤ 7 cm ($0.7\%H_f$)

Objective:

Minimizing the standard deviation of the maximum wall deflection (cm)

Minimizing the cost for the supporting system (USD)

Figure 4.3: Formulation of the robust geotechnical design of braced excavations with NSGA-II

Table 4.1: List of the designs on the Pareto Front with a deterministic constraint

No.	t (m)	L (m)	S (m)	EA	Robustness (cm)	Cost ($\times 10^6$USD)
1	0.5	20	3	H350	3.11	0.53
2	0.5	21	3	H350	3.09	0.55
3	0.5	20	2	H350	2.59	0.56
4	0.5	21	2	H350	2.58	0.58
5	0.5	20	1.5	H400	1.29	0.59
6	0.6	20	2	H400	1.07	0.65
7	0.6	20	1.5	H400	1.02	0.68
8	0.8	20.5	3	H400	1.01	0.80
9	0.8	20	2	H400	0.97	0.82
10	0.8	20	1.5	H400	0.96	0.85
11	1	20.5	6	2@H350	0.84	1.01
12	1	21	6	2@H350	0.83	1.03
13	1.1	20	3	2@H350	0.80	1.14
14	1.1	20.5	3	2@H350	0.79	1.17
15	1.2	20.5	6	2@H350	0.77	1.19
16	1.2	21	6	2@H350	0.75	1.21
17	1.2	20.5	3	2@H350	0.72	1.25
18	1.2	21	3	2@H350	0.71	1.28
19	1.2	21.5	3	2@H350	0.70	1.30
20	1.2	21	2	2@H350	0.69	1.35
21	1.2	21.5	2	2@H350	0.68	1.37
22	1.2	22	2	2@H350	0.67	1.40
23	1.2	21.5	1.5	2@H350	0.66	1.44
24	1.2	22.5	1.5	2@H350	0.65	1.49
25	1.2	24	1.5	2@H350	0.64	1.57

Note: Robustness is evaluated in terms of the standard deviation of the maximum wall deflection; a smaller standard deviation indicates a greater robustness.

By definition, the Pareto-Front includes two groups of designs: (1) of those with an identical level of robustness, the most inexpensive design is selected; (2) of those with an identical level of cost, the most robust design is selected. The decision maker (designer) can then choose a design from this Pareto Front, as any design point is "non-

dominated" with respect to these two objectives. Once the designer specifies a cost level, selecting the design with least standard deviation of the wall deflection within the cost level on Pareto Front will provide the most robust design. For example, if the limiting budget for a supporting system is 1×10^6 USD, the design with parameters t = 0.8 m, L = 20 m, S = 1.5 m and EA = H400 is the most robust design (No. 10 design in Table 4.1) within that cost level. Similarly, the most preferred design may also be selected based on a desired level of robustness. Further discussion of the most preferred design is presented in the section that follows.

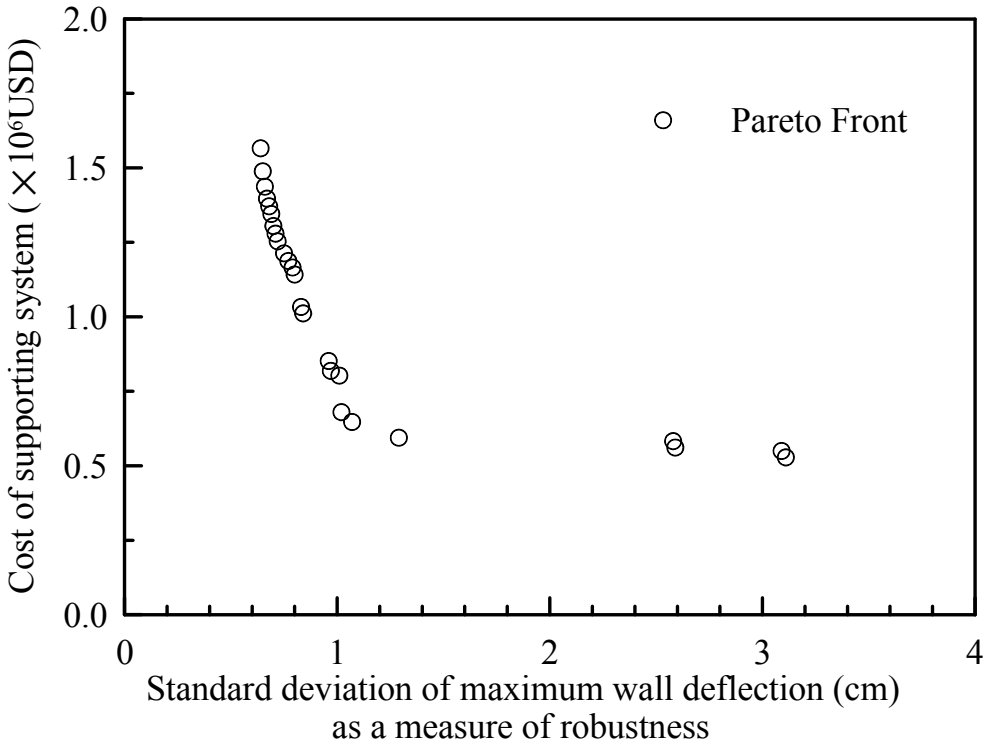

Figure 4.4: The Pareto Front optimized for both cost and robustness using deterministic constraints

Selection of the most preferred design based on concept of knee point

Although the trade-off relationship in terms of a Pareto Front provides valuable information to the designer with which they may make an informed decision by *explicitly* considering cost and robustness, the designer may prefer to locate a single most optimal design rather than a set of designs. Consequently, additional steps may be necessary to refine this decision-making based upon the Pareto Front for the most preferred solution.

In many cases, in a Pareto Front generated from a bi-objective optimization, there exists a most preferred point, known as the knee point (Deb and Gupta 2011). Any design (i.e., any point on the Pareto Front) apart from the knee point requires a large sacrifice in one objective to achieve a small gain in the other objective. Thus, the knee point may be defined as the point on the Pareto Front that has the maximum reflex angle computed from its neighboring points, as shown in Figure 4.5(a). The reflex angle denotes the bend of the point on the Pareto Front from its left to right side, which provides a measure of the gain-sacrifice in the trade-off relationship. The reflex angle is measured from its two neighboring points, however, which is only a local property and may not extend to the entire front. To mitigate this locality issue, Deb and Gupta (2011) used the normal boundary intersection method as illustrated in Figure 4.5(b) to further define the knee point. On the Pareto Front in Figure 4.5(b), two boundary points, A and B, are used to construct a straight boundary line. For any point on the boundary line z, a corresponding point (P_z) on the Pareto Front along the normal ($\hat{n}$) course of the boundary line can be located. The knee point is the point (P_{z^*}) on the Pareto Front that has the maximum distance from its corresponding point z^* on the boundary line (Deb and Gupta 2011).

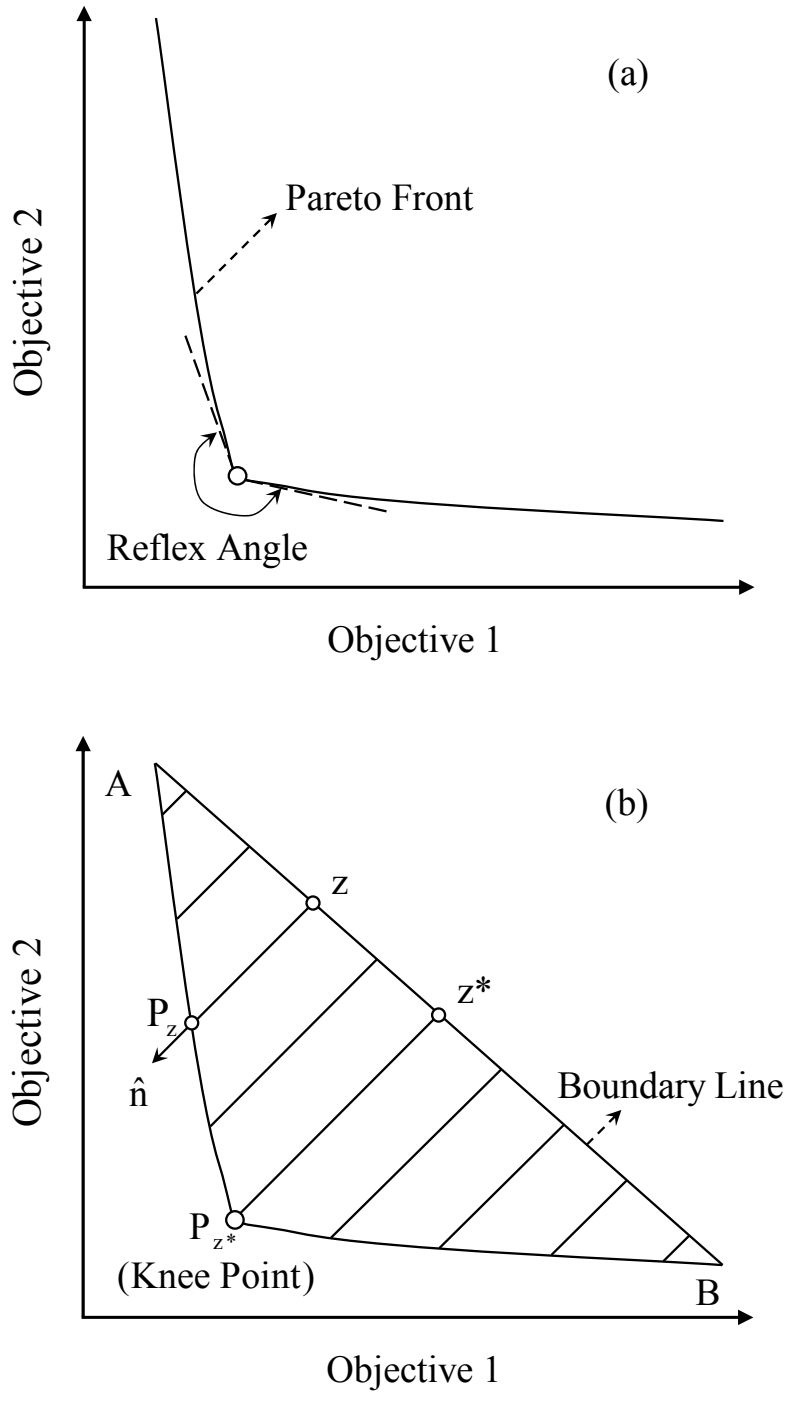

Figure 4.5: Illustration of the reflex angle and the knee point identification (modified after Deb and Gupta 2011)

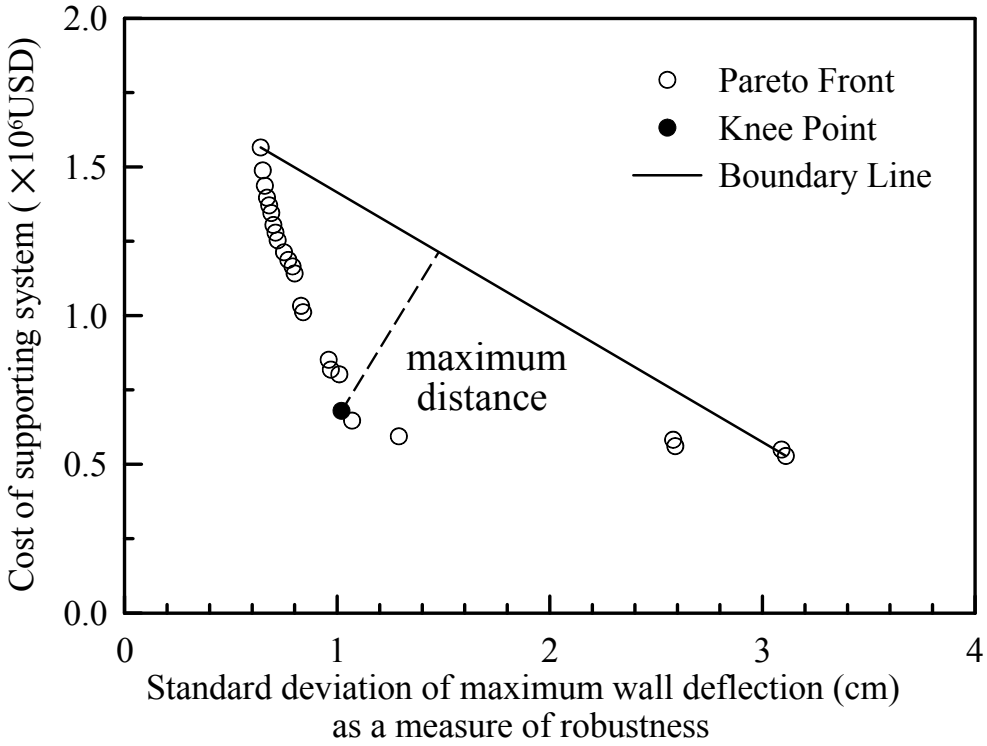

Figure 4.6: Example of the knee point identification based upon the obtained Pareto Front (for robustness, a smaller standard deviation indicates a greater robustness)

Based upon the definition of the knee point from the concept of the normal boundary intersection method (Deb and Gupta 2011), the knee point of the Pareto Front in Figure 4.4 is determined by searching for the point farthest from the boundary line. The knee point in Figure 4.6 has the following parameters: t = 0.6 m, L = 20 m, S = 1.5 m and EA = H400 (No. 7 design in Table 4.1), with a cost of 0.68×10^6 USD. As shown in Figure 4.6, below this cost level, a slight cost increase can significantly improve the robustness (reducing the standard deviation of the wall deflection). Above this cost level (e.g., the cost of the design is further increased sharply), however, the effect of enhancing

the robustness (reducing the standard deviation of the wall deflection) becomes markedly inefficient and ineffective.

Further Discussions

In our analysis described in the previous section, the serviceability requirement of any braced excavation was enforced using a deterministic limiting value. Rather than using a deterministic constraint, the client may prefer to adopt the reliability constraint in terms of the probability of exceedance of a specific limiting value (Goh et al. 2005; Hsiao et al. 2008). For braced excavation, the serviceability limit state may be defined as:

$$y() = \delta_{hm} - \delta_{lim} \tag{4.4}$$

where δ_{hm} is the predicted maximum wall deflection (a random variable) and δ_{lim} is the specified limiting maximum wall deflection (usually as a fixed value in the codes).

In practice, however, the target probability of exceedance of the specific limiting wall deflection value is not defined *explicitly* in the design codes and published literatures. Thus, in this section, we describe how to establish Pareto Front using various target levels of probability of exceedance (P_E) as constraints during the optimization process. Through the adoption of various exceedance levels, we can incorporate a degree of flexibility in the robust design process to allow for consideration of allowable risk (i.e., the consequence of the serviceability failure).

For demonstration purposes, the robust design optimization is performed with various reliability constraints, implemented with three levels of probability of exceedance

(P_E < 10%, 20%, and 40%). The resulting Pareto Fronts under these constraints are illustrated in Figure 4.7, with the detailed design parameters for each design this figure listed in Table 4.2. It is noted that the Pareto Front for the case of P_E < 20% is almost identical to that for case of P_E < 10% except that one additional point is identified (No. 2 design in Table 4.2). Similarly, the Pareto Front for the case of P_E < 40% happens to generate also one additional point (No. 1 design in Table 4.2).

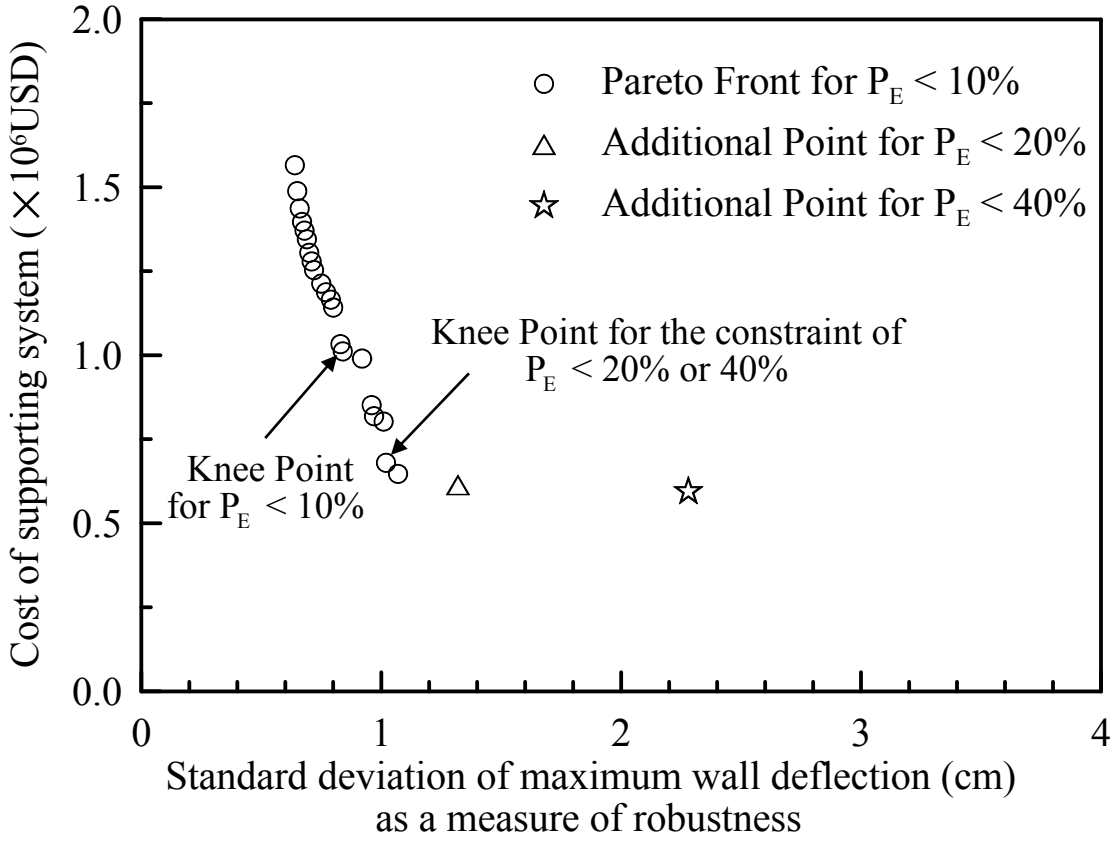

Figure 4.7: The optimized Pareto Fronts at various constraint levels of probability of exceedance (for robustness, a smaller standard deviation indicates a greater robustness)

Table 4.2: List of the designs on the Pareto Front with a reliability constraint ($P_E < 40\%$)

No.	t (m)	L (m)	S (m)	EA	Robustness (cm)	Cost ($\times 10^6$USD)
1	0.5	20	1.5	H350	2.28	0.59
2	0.6	20	3	H400	1.32	0.61
3	0.6	20	2	H400	1.07	0.65
4	0.6	20	1.5	H400	1.02	0.68
5	0.8	20.5	3	H400	1.01	0.80
6	0.8	20	2	H400	0.97	0.82
7	0.8	20	1.5	H400	0.96	0.85
8	1	20	6	2@H350	0.92	0.99
9	1	20.5	6	2@H350	0.84	1.01
10	1	21	6	2@H350	0.83	1.03
11	1.1	20	3	2@H350	0.80	1.14
12	1.1	20.5	3	2@H350	0.79	1.17
13	1.2	20.5	6	2@H350	0.77	1.19
14	1.2	21	6	2@H350	0.75	1.21
15	1.2	20.5	3	2@H350	0.72	1.25
16	1.2	21	3	2@H350	0.71	1.28
17	1.2	21.5	3	2@H350	0.70	1.30
18	1.2	21	2	2@H350	0.69	1.35
19	1.2	21.5	2	2@H350	0.68	1.37
20	1.2	22	2	2@H350	0.67	1.40
21	1.2	21.5	1.5	2@H350	0.66	1.44
22	1.2	22.5	1.5	2@H350	0.65	1.49
23	1.2	24	1.5	2@H350	0.64	1.57

Note: For the constraint of $P_E < 20\%$, all but design No. 1 are on the Pareto Front; for the constraint of $P_E < 10\%$, all but designs No. 1 and No. 2 are on the Pareto Front.

Based on the procedure described previously, the knee points obtained for the Pareto Fronts with the constraints of $P_E < 20\%$ and $P_E < 40\%$ are identical. This knee point is a design represented by the following design parameters: t = 0.6 m, L = 20 m, S = 1.5 m and EA = H400 (No. 4 design in Table 4.2), which costs 0.68×10^6 USD. It is interesting to note that this knee point is identical to the knee point obtained previously

using the deterministic constraint. If the constrain of $P_E < 10\%$ is adopted, a different knee point is obtained, which has the following design parameters: $t = 1.0$ m, $L = 20.5$ m, $S = 6$ m and $EA = 2@H350$ (No. 9 design in Table 4.2) with a cost of 1.01×10^6 USD.

Finally, it should be noted that the above analysis is based on a limiting wall deflection specified in a Chinese code (PSCG 2000) for a Level III protection of adjacent infrastructures. However, the entire robust geotechnical design (RGD) methodology is easily adaptable for other desired limiting wall deflection requirements.

Summary

This chapter described a robust geotechnical design (RGD) methodology for addressing the design uncertainties inherent in braced excavations (particularly the uncertainties of geotechnical parameters and surcharges). In the robust design system, the purpose is to minimize the effects of these uncertainties through the careful adjustment of the design parameters. Within the RGD framework, a multi-objective optimization procedure is used to select designs that are optimal in terms of both cost and robustness, while satisfying all requisite safety requirements. These safety requirements can either be enforced deterministically or probabilistically. As a result, a set of optimal, non-dominated designs, collectively known as Pareto Front, can be obtained. In this regard, the established Pareto Front, along with its corresponding knee point is shown as a valuable design tool for robust design of braced excavations.

CHAPTER FIVE

CONCLUSIONS AND RECOMMENDATIONS

Conclusions

The following conclusions are drawn from the results of the study on the robust geotechnical design of drilled shafts presented in Chapter II:

(1) The determination of least cost design in a traditional reliability-based design is meaningful only if the statistics of soil parameters can be accurately estimated. If the COV and correlation coefficient values are underestimated or overestimated by a certain margin, then there is a significant chance that an acceptable design (a design that satisfies ULS and SLS constraints based on fixed statistics values) will no longer be satisfactory. Thus, it is necessary to consider the robustness against the variation in the estimated statistics of soil parameters.

(2) Robustness as one of the design objectives has been illustrated. In fact, the concept of robustness is incorporated into the reliability-based design to deal with the uncertainty in the estimated sample statistics of soil parameters. In the context of robust geotechnical design of drilled shafts for axial load in sand, B (diameter) and D (depth or length) are considered as the design parameters (denoted as $\mathbf{d}$), and the soil parameters ϕ' and K_0 are considered as the noise factors (denoted as $\mathbf{z}$). In the reliability-based design, the safety and serviceability requirements are satisfied by meeting the constraint,

$p_f^{SLS}(\mathbf{d},\mathbf{z}) \le p_T^{SLS} = 0.0047$. It is noted that probability of the SLS failure $p_f^{SLS}(\mathbf{d},\mathbf{z})$ is a random variable, the value of which depends on both design parameters **d** and noise factors **z**. The essence of robustness design is to minimize the variation of $p_f^{SLS}(\mathbf{d},\mathbf{z})$ caused by the uncertainty in the estimated sample statistics of soil parameters by adjusting the design parameters.

(3) To consider the robustness of the design against the uncertainty in the estimated sample statistics of soil parameters, the standard deviation of the SLS failure probability $p_f^{SLS}(\mathbf{d},\mathbf{z})$ is adopted as a measure of robustness. The uncertainty of the estimated COV of a given noise factor may be estimated from a range of COV published in the literature. The variation in the failure probability can be computed using the PEM integrated with FORM analysis.

(4) The robustness is considered along with cost as the design objectives, and as a result, a Pareto Front is established through non-dominated sorting. This Pareto Front gives a trade-off relationship between cost and robustness. To improve the decision making process further, the concept of feasibility robustness is adopted. Through an implementation of feasibility robustness, the best design can be selected from the Pareto Front based on the designer's objectives.

The following conclusions are drawn from the results of the study on the robust geotechnical design of shallow foundations presented in Chapter III:

(1) Quantification of uncertainties in soil parameters and geotechnical models is a prerequisite for a reliability-based design. Due to inexactness of geotechnical models and lack of soil parameters data, uncertainties exist in the derived statistics of model factors and soil parameters, which compromises the effectiveness of the reliability-based design. The reliability-based robust geotechnical design (RGD) methodology can reduce the effect of these unavoidable uncertainties (including uncertainties in both soil parameters and model factors) by achieving a certain level of design *robustness*, in addition to meeting safety and cost requirements.

(2) This study demonstrates that the bootstrapping technique is an effective tool for characterizing the uncertainty in the sample statistics derived from a small sample. Through the analysis, it can be found that the variation of sample mean is quite negligible, while the variation of sample standard deviation is large. This suggests that the standard deviation of soil parameters estimated from a small sample is usually not precise. With the gained information through bootstrapping analysis, the variation in the resulting failure probability of a given design caused by uncertainties in the sample statistics can be evaluated.

(3) When multiple design requirements (including safety, cost, and robustness) are imposed, a single best design often does not exist. In fact, an optimization with multiple design objectives usually leads to a Pareto Front, which is a set of optimal designs that are superior to all other designs in the design space,

but within the set, no design is dominated by any other designs. By applying the RGD methodology implemented in a multi-objective genetic algorithm framework, a Pareto Front is derived, which describes a trade-off relationship between cost and robustness at a given safety (reliability) level. The derived Pareto Front and the associated feasibility robustness index enable the engineer to make an informed design decision.

(4) The effect of soil spatial variability can also be considered in the RGD methodology by treating the scale of fluctuation as an additional noise factor. The results show that at the same feasibility robustness level, the design considering spatial variability costs less than that without considering spatial variability. The implication is that the design that does not consider spatial variability is biased toward conservative (or safer) side in the shallow foundation design presented this chapter.

The following conclusions are drawn from the results of the study on the robust geotechnical design of braced excavations presented in Chapter IV:

(1) In the design of braced excavation, the maximum wall deflection is often measured and used as a field control, as an excessive wall deflection not only causes a serviceability problem but also signals an increasingly higher chance of failure of the wall and bracing system. Thus, the maximum wall deflection is used as the system response of concern for robust design of braced excavations. In this chapter, RGD methodology is further refined by treating

the variation of maximum wall deflection caused by uncertainties in soil parameters and surcharges as a robustness measure.

(2) The RGD methodology is demonstrated as an effective tool through an illustrative example using industrial-strength finite element code (TORSA) for design of braced excavations. By enforcing design robustness in the face of uncertainties, which is not considered in any traditional design methods, the variation of the system response (in terms of maximum wall deflection) caused by the input parameter uncertainties is controlled by the designer through a tradeoff consideration of cost efficiency and robustness, while safety is guaranteed. The safety requirements can either be enforced deterministically or probabilistically.

(3) It is interesting to note that robust design allows for reduction in the variation of the system response of concern without having to eliminate the sources of the uncertainties in the designed system. In the braced excavation design, such robustness is achieved by carefully adjusting the design parameters of both the diaphragm wall and the bracing system in a given set of design settings (i.e., excavation geometry and excavation depth). As in many engineering problems, inevitably, higher cost is involved when the design robustness is sought. Thus, a tradeoff consideration based upon the Pareto front obtained through multi-objective optimization is required. Together with use of a knee point concept, a single most preferred design may be obtained. The established Pareto Front, along with its corresponding knee point, has proven as an effective tool for

selection of the most preferred design in the design of braced excavation system.

Recommendations

To further expand the work presented in this dissertation, a number of research topics may be undertaken, which include the following:

(1) It should be of interest to further investigate the applicability of the developed robust design framework in the design of other geotechnical systems such as subway tunnels, embankments, reinforced soil structures, geothermal piles and off-shore structure foundations.

(2) The design robustness in this dissertation study is measured with the standard deviation of the system response caused by the uncertainty in the noise factors. Other measures such as signal-to-noise ratio (Phadke 1989), vulnerability function (Ait Brik et al. 2007) and reliability sensitivity (Zhang et al. 2005) should be investigated for their suitability for use in the developed geotechnical robust design framework.

(3) It should be of interest to further investigate the robust design of braced excavations using the tied-back and soil-nailed shoring systems. Alternative finite element codes for predicting the excavation-induced wall and ground responses may be adopted and possible implementation of the robust geotechnical design framework in a spreadsheet may be explored.

(4) It should be of interest to further extend the developed robust design framework into a robust maintenance framework for geotechnical systems. Possible integration of life-cycle performance assessment within the robust maintenance optimization framework may be explored.

REFERENCES

Ait Brik, B., Ghanmi, S., Bouhaddi N., and Cogan S. (2007). "Robust design in structural mechanics." International Journal for Computational Methods in Engineering Science and Mechanics, 8(1), 39-49.

Akbas, S.O. (2007). "Deterministic and probabilistic assessment of settlements of shallow foundations in cohesionless soils." Ph.D. thesis, Cornell University, Ithaca.

Akbas, S.O., and Kulhawy, F.H. (2009a). "Axial compression of footings in cohesionless soils. I: load–settlement behavior." Journal of Geotechnical and Geoenvironmental Engineering, 135(11), 1562-1574.

Akbas, S.O., and Kulhawy, F.H. (2009b). "Axial compression of footings in cohesionless soils. II: bearing capacity." Journal of Geotechnical and Geoenvironmental Engineering, 135(11), 1575-1582.

Akbas, S.O., and Kulhawy, F.H. (2011). "Reliability based design of shallow foundations in cohesionless soil under compression loading: serviceability limit state." Proceedings of Georisk 2011: Getotechnical risk assessment & management, GSP224, Atlanta, 616-623.

Amoroso, L. (1938). "Vilfredo Pareto." Econometrica, 6(1), 1-21.

Amundaray, J. I. (1994). "Modeling geotechnical uncertainty by bootstrap resampling." Ph.D. thesis, Purdue University, West Lafayette, IN.

Ang, A.H.-S., and Tang, W.H. (1984). Probability concepts in engineering planning and design, vol.2: Decision, risk, and reliability, Wiley, New York.

Baecher, G.B., and Christian, J.T. (2003). Reliability and statistics in geotechnical engineering, Wiley, New York.

Bourdeau, P.L., and Amundaray, J.I. (2005). "Non-parametric simulation of geotechnical variability." Géotechnique, 55(1), 95-108.

Casagrande, A. (1965). "The role of the "calculated risk" in earthwork and foundation engineering." Journal of the Soil Mechanics and Foundations Division, 91(4):1-40.

Chalermyanont, T., and Benson, C. (2004). "Reliability-based design for internal stability of mechanically stabilized earth walls." Journal of Geotechnical and Geoenvironmental Engineering, 130(2), 163-173.

Chen, W., Allen, J.K., Mistree, F., and Tsui, K.-L. (1996). "A procedure for robust design: minimizing variations caused by noise factors and control factors." Journal of Mechanical Design, 118(4), 478-485.

Chen, W., and Lewis, K. (1999). A robust design approach for achieving flexibility in multidisciplinary design. AIAA Journal, 37(8), 982-990.

Cheng, F.Y., and Li, D. (1997). "Multi-objective optimization design with Pareto genetic algorithm." Journal of Structural Engineering, 123(9), 1252-1261.

Cherubini, C. (2000). "Reliability evaluation of shallow foundation bearing capacity on c', φ' soils." Canadian Geotechnical Journal, 37(1), 264-269.

Christian, J.T., Ladd, C.C., and Baecher, G.B. (1994). "Reliability applied to slope stability analysis." Journal of Geotechnical Engineering, 120 (12), 2180-2207.

Coduto, D.P. (2010). Foundation design: principles and practices, 2nd edn, Prentice Hall, New Jersey.

Committee of Inquiry. (2005). Report of the Committee of Inquiry into the Incident at the MRT Circle Line Worksite that led to the Collapse of the Nicoll Highway on 20 April 2004. Ministry of Manpower, Singapore.

Deb, K., Pratap, A., Agarwal, S., and Meyarivan, T. (2002). "A fast and elitist multiobjective genetic algorithm: NSGA-II." IEEE Transactions on Evolutionary Computation, 6(2), 182-197.

Deb, K., and Gupta S. (2011). "Understanding knee points in bicriteria problems and their implications as preferred solution principles." Engineering Optimization, 43 (11), 1175-1204.

DeGroot, D.J., and Baecher, G.B. (1993). "Estimating autocovariance of in-situ soil properties." Journal of Geotechnical Engineering, 119(1), 147-166.

Dithinde, M., Phoon, K.K., De Wet, M., and Retief, J. V. (2011). "Characterisation of model uncertainty in the static pile design formula." Journal of Geotechnical and Geoenvironmental Engineering, 137(1), 70-85.

Doltsinis, I., and Kang, Z. (2005). "Robust design of non-linear structures using optimisation methods." Computer Methods in Applied Mechanics and Engineering, 194(12–16), 1779-1795.

Doltsinis, I., and Kang, Z. (2006). "Perturbation-based stochastic FE analysis and robust design of inelastic deformation processes." Computer Methods in Applied Mechanics and Engineering, 195(19-22), 2231-2251.

Duncan, J.M. (2000). “Factors of safety and reliability in geotechnical engineering.” Journal of Geotechnical and Geoenvironmental Engineering, 126 (4), 307-316.

Duncan, J.M. (2001). “Closure to factors of safety and reliability in geotechnical engineering.” Journal of Geotechnical and Geoenvironmental Engineering, 126 (8), 717-721.

Fenton, G.A., Griffiths, D.V., and Williams, M.B. (2005). “Reliability of traditional retaining wall design.” Géotechnique, 55(1), 55-62.

Fenton, G.A., and Griffiths, D.V. (2008). Risk assessment in geotechnical engineering, Wiley, New York.

Frangopol, D.M., and Maute, K. (2003). “Life-cycle reliability-based optimization of civil and aerospace structures.” Computers and Structures, 81, 397-410.

Gencturk, B., and Elnashai, A. S. (2011). “Multi-objective optimal seismic design of buildings using advanced engineering materials,” Mid-America Earthquake (MAE) Center, Research Report 11-01, Department of Civil and Environmental Engineering, University of Illinois at Urbana-Champaign, IL.

Ghosh, A., and Dehuri, S. (2004). “Evolutionary algorithms for multi-criterion optimization: a survey.” International Journal of Computing and Information Sciences, 2(1), 38-57.

Gilbert, R.B., and Tang, W.H. (1995). “Model uncertainty in offshore geotechnical reliability.” Proc. 27th Offshore Technology Conference, Houston, Texas, pp. 557-567.

Goh, A.T.C., and Kulhawy, F.H. (2005). “Reliability assessment of serviceability performance of braced retaining walls using a neural network approach.” International Journal for Numerical and Analytical Methods in Geomechanics, 29(6), 627-642.

Griffiths, D.V., Fenton, G.A. and Manoharan, N. (2002). “Bearing capacity of a rough rigid strip footing on cohesive soil: A probabilistic study.” Journal of Geotechnical and Geoenvironmental Engineering, 128(9), 743-755.

Griffiths, D.V., Huang, J., and Fenton, G.A. (2009). “Influence of Spatial Variability on Slope Reliability Using 2-D Random Fields.” Journal of Geotechnical and Geoenvironmental Engineering, 135(10), 1367-1378.

Harr, M.E. (1987). Reliability-based design in civil engineering. McGraw-Hill, New York.

Hashash, Y.M.A., and Whittle, A.J. (1996). "Ground movement prediction for deep excavations in soft clay." Journal of Geotechnical Engineering, 122(6), 474-486.

Hsiao, E.C.L., Schuster, M., Juang, C.H., and Kung, T.C. (2008). "Reliability analysis of excavation induced ground settlement for building serviceability evaluation." Journal of Geotechnical and Geoenvironmental Engineering, 134(10), 1448-1458.

Jamali, A., Hajiloo, A., and Nariman-Zadeh, N. (2010). "Reliability based robust Pareto design of linear state feedback controllers using a multi-objective uniform-diversity genetic algorithm (MUGA)." Expert Systems with Applications, 37(1), 401-413.

JSA. (1988). Guidelines of Design and Construction of Deep Excavations. Japanese Society of Architecture. Tokyo, Japan.

Juang, C.H., Yang, S.H., Yuan, H., and Khor, E.H. (2004). "Characterization of the uncertainty of the Robertson and Wride model for liquefaction potential evaluation." Soil Dynamics and Earthquake Engineering, 24(9), 771-780.

Juang, C.H., Fang, S.Y., Tang, W.H., Khor, E.H., Kung, G.T.C., and Zhang, J. (2009). "Evaluating model uncertainty of an SPT-based simplified method for reliability analysis for probability of liquefaction." Soils and Foundations, 49(12), 135-152.

Juang, C.H., Schuster, M., Ou, C.Y., and Phoon, K.K. (2011). "Fully-probabilistic framework for evaluating excavation-induced damage potential of adjacent buildings," Journal of Geotechnical and Geoenvironmental Engineering, 137(2), 130-139.

Kang, Z. (2005). Robust design optimization of structures under uncertainties. Shaker Verlag, Aachen, Germany.

Kulhawy, F. H. (1991). "Drilled shaft foundations." Foundation engineering handbook, 2nd Ed., H. Y. Fang, ed.,Van Nostrand Reinhold, New York, 537-552.

Kulhawy, F.H., Trautmann, C.H., Beech, J.F., O'Rourke, T.D., McGuire, W., Wood, W.A., and Capano, C. (1983). "Transmission line structure foundations for uplift—compression loading." Rep. No.EL-2870, Electric Power Research Institute, Palo Alto, Calif.

Kumar, A., Nair, P.B., Keane, A.J., and Shahpar, S. (2008). "Robust design using Bayesian Monte Carlo." International Journal for Numerical Methods in Engineering, 73, 1497-1517.

Kung, G.T.C., Juang, C.H., Hsiao, E.C.L., and Hashash, Y.M.A. (2007). "A simplified model for wall deflection and ground surface settlement caused by braced

excavation in clays." Journal of Geotechnical and Geoenvironmental Engineering, 133(6), 731-747.

Lacasse, S., and Nadim, F. (1994). "Reliability issues and future challenges in geotechnical engineering for offshore structures." Proc., 7th International Conference on Behaviour of Offshore Structures, Cambridge, Massachusetts, pp. 9-38.

Lacasse, S., and Nadim, F. (1996). "Uncertainties in characterizing soil properties." In ASCE Uncertainties'96 Conference Proceedings, C.H. Benson, Ed., Madison, WI, pp.49-75.

Lagaros, N.D., and Fragiadakis, M. (2007). "Robust performance based design optimization of steel moment resisting frames." Journal of Earthquake Engineering, 11(5), 752-772.

Lagaros, N.D., and Papadrakakis, M. (2007). "Robust seismic design optimization of steel structures." Structural and Multidisciplinary Optimization, 33(6), 457-469.

Lagaros, N.D., Plevris, V., and Papadrakakis, M. (2010). "Neurocomputing strategies for solving reliability-robust design optimization problems." Engineering Computations, 27(7), 819-840.

Lee, K.H., and Park, G.J. (2001). "Robust optimization considering tolerances of design variables." Computers and Structures 79(1): 77-86.

Lee, M.C.W., Mikulik, Z., Kelly, D.W., Thomson, R.S., and Degenhardt, R. (2010). "Robust design-a concept for imperfection insensitive composite structures." Composite Structures, 92(6), 1469-1477.

Lee, Y.F., Chi, Y. Y., Juang, C. H. and Lee, D.H. (2012). "Reliability analysis of rock wedge stability- a Knowledge-based Clustered Partitioning (KCP) approach." Journal of Geotechnical and Geoenvironmental Engineering, 138(6), 700-708.

Lin, C.Y., and Hajela, P. (1992). "Genetic algorithm in optimization with discrete and integer design variables." Engineering Optimization, 19(4), 309-327.

Luo, Z., Atamturktur, H.S., Juang, C.H., Huang, H., and Lin, P.S. (2011). "Probability of serviceability failure in a braced excavation in a spatially random field: Fuzzy finite element approach," Computers and Geotechnics, 38(8), 1031-1040.

Luo, Z., Atamturktur, S., Cai, Y., and Juang, C.H. (2012). "Simplified approach for reliability-based design against basal-heave failure in braced excavations considering spatial effect." Journal of Geotechnical and Geoenvironmental Engineering, 138(4), 441-450.

Luo, Z., Atamturktur, S., and Juang, C.H. (2013). "Bootstrapping for characterizing the effect of uncertainty in sample statistics for braced excavations." Journal of Geotechnical and Geoenvironmental Engineering, 139(1), 13-23.

Mana, A.I., and Clough, G.W. (1981). "Prediction of movements for braced cuts in clay." Journal of the Geotechnical Engineering Division, 107(6), 759-777.

Marano, G.C., Sgobba, S., Greco, R., and Mezzina, M. (2008). "Robust optimum design of tuned mass dampers devices in random vibrations mitigation." Journal of Sound and Vibration, 313(3-5): 472-492.

Mathur, V.K. (1991). "How well do we know Pareto optimality?" Journal of Economic Education, 22 (2), 172-178.

Mayne, P.W., and Kulhawy, F.H. (1982). "Ko-OCR relationships in soil." Journal of the Geotechnical Engineering Division, 108(6), 851-872.

Most, T., and Knabe, T. (2010). "Reliability analysis of bearing failure problem considering uncertain stochastic parameters." Computers and Geotechnics, 37(3), 299-310.

Najjar, S.S., and Gilbert, R.B. (2009). "Importance of lower-bound capacities in the design of deep foundations." Journal of Geotechnical and Geoenvironmental Engineering, 135(7), 890-900.

Orr, T. L. L., and Farrell, E. R. (1999). Geotechnical design to Eurocode 7, Springer, Berlin.

Ou, C.Y. (2006). Deep excavation-theory and practice. Taylor and Francis, England.

Paiva, R.M. (2010). "A robust and reliability-based optimization framework for conceptual aircraft wing design." Ph.D. thesis. University of Victoria, Canada.

Papadopoulos, V., and Lagaros, N.D. (2009). "Vulnerability-based robust design optimization of imperfect shell structures." Structural Safety, 31(6), 475-482.

Park, G.J., Lee, T.H., Lee, K., and Hwang, K.H. (2006). "Robust design: an overview." AIAA Journal, 44 (1), 181-191.

Parkinson, A., Sorensen, C., and Pourhassan, N. (1993). "A general approach for robust optimal design." Journal of Mechanical Design, 115(1), 74-80.

Phadke, M.S. (1989). Quality engineering using robust design. Prentice Hall, Englewood Cliffs.

Phoon, K. K. (2004). "General non-Gaussian probability models for first order reliability method (FORM): A state-of-the-art report." ICG Rep. No. 2004-2-4 (NGI Rep. No. 20031091-4), International Center for Geohazards, Oslo, Norway.

Phoon K. K., and Kulhawy, F. H. (1999). "Characterization of geotechnical variability." Canadian Geotechnical Journal, 36(4), 612-624.

Phoon, K.K., and Kulhawy, F.H. (2005). "Characterization of model uncertainties for laterally loaded rigid drilled shafts." Géotechnique, 55(1), 45-54.

Phoon, K. K., Kulhawy, F. H., and Grigoriu, M. D. (1995). "Reliability based design of foundations for transmission line structures." Rep. TR-105000, Electric Power Research Institute, Palo Alto, California.

Phoon, K.K., Kulhawy, F.H., and Grigoriu, M.D. (2003a). "Development of a reliability-based design framework for transmission line structure foundations." Journal of Geotechnical and Geoenvironmental Engineering, 129(9), 798-806.

Phoon, K.K., Kulhawy, F.H., and Grigoriu, M.D. (2003b). "Multiple resistance factor design for shallow transmission line structure foundations." Journal of Geotechnical and Geoenvironmental Engineering, 129(9), 807-818.

Parkinson, A., Sorensen, C., and Pourhassan, N. (1993). "A general approach for robust optimal design." Journal of Mechanical Design, 115(1), 74-80.

PSCG. (2000). Specification for Excavation in Shanghai Metro Construction, Professional Standards Compilation Group, Shanghai, China.

R. S. Means Co. (2007). R. S. Means building construction cost data, Kingston, Mass.

Sandgren, E., and Cameron, T.M. (2002). "Robust design optimization of structures through consideration of variation." Computers and Structures, 80 (20-21), 1605-1613.

Schuster, M.J., Juang, C.H., Roth, M.J.S., and Rosowsky, D.V. (2008). "Reliability analysis of building serviceability problems caused by excavation." Géotechnique, 58(9), 743-749.

Schweiger, H.F., and Peschl, G.M. (2005). "Reliability analysis in geotechnics with the random set finite element method." Computers and Geotechnics, 32(6), 422-435.

Seepersad, C.C., Allen, J.K., McDowell, D.L., and Mistree, F. (2006). "Robust design of cellular materials with topological and dimensional imperfections." Journal of Mechanical Design, 128 (6), 1285-1297.

Sino-Geotechnics. (2010). User Manual of Taiwan Originated Retaining Structure Analysis for Deep Excavation. Sino-Geotechnics Research and Development Foundation, Taipei, Taiwan.

Taguchi, G. (1986). Introduction to quality engineering: Designing quality into products and processes, Quality Resources, White Plains, New York.

Tang, W.H. and Gilbert, R.B. (1993). Case study of offshore pile system reliability. Proc., 25th Offshore Technology Conference, Society of Petroleum Engineers, Houston, Texas, pp. 677-686.

TGS. (2001). Design Specifications for the Foundation of Buildings. Taiwan Geotechnical Society, Taipei, Taiwan.

Tsui, K.-L. (1992). "An overview of Taguchi method and newly developed statistical methods on robust design." IIE Transactions, 24 (5), 44-57.

Tsui, K.-L. (1999). "Robust design optimization for multiple characteristic problems." International Journal of Production Research, 37(2), 433-445.

Vanmarcke, E.H. (1977). "Probabilistic modeling of soil profiles." Journal of the Geotechnical Engineering Division, 103(11), 1227-1246.

Vanmarcke, E.H. (1983). Random Fields - Analysis and Synthesis, MIT-Press, Cambridge, Massachusetts.

Vesić, A. S. (1975). "Bearing capacity of shallow foundations." Foundation engineering handbook, H. F. Winterkorn and H. Y. Fang, eds., Van Nostrand Reinhold, New York, 121-147.

Wang, Y. (2011). "Reliability-based design of spread foundations by Monte Carlo Simulations." Géotechnique, 61(8), 677-685.

Wang, Y., and Kulhawy, F.H. (2008). "Economic design optimization of foundations." Journal of Geotechnical and Geoenvironmental Engineering, 134(8), 1097-1105.

Wang, Y., Au, S. K., and Kulhawy, F. H. (2011a). "Expanded reliability-based design approach for drilled shafts." Journal of Geotechnical and Geoenvironmental Engineering, 137(2), 140-149.

Wang, Y., Cao, Z., and Kulhawy, F.H. (2011b). "A comparative study of drilled shaft design using LRFD and Expanded RBD." Proceedings of Georisk 2011: Geotechnical Risk assessment & management, GSP No. 224, Atlanta, 648-655.

Whitman, R.V. (1984). "Evaluating calculated risk in geotechnical engineering." Journal of Geotechnical Engineering, 110(2), 143-188.

Whitman, R.V. (2000). "Organizing and evaluating uncertainty in geotechnical engineering." Journal of Geotechnical and Geoenvironmental Engineering, 126(7), 583-593.

Wu, T.H., Tang, W.H., Sangrey, D.A., and Baecher, G.B. (1989). "Reliability of offshore foundations — State-of-the-art." Journal of Geotechnical Engineering, 115(2), 157-178.

Zhang, J., Tang, W.H., Zhang, L.M., and Huang, H.W. (2012). "Characterising geotechnical model uncertainty by hybrid Markov Chain Monte Carlo simulation." Computers and Geotechnics, 43, 26-36.

Zhang, J., Zhang, L.M., and Tang, W.H. (2009). "Bayesian framework for characterizing geotechnical model uncertainty." Journal of Geotechnical and Geoenvironmental Engineering, 135(7), 932-940.

Zhang, J., Zhang, L.M., and Tang, W.H. (2011). "Reliability-based optimization of geotechnical systems." Journal of Geotechnical and Geoenvironmental Engineering, 137, (12), 1211-1221.

Zhao, Y. G., and Ono, T. (2000). "New point estimates for probability moments." Journal of Engineering Mechanics, 126(4), 433-436.

Zhang, Y., He, X., Liu, Q., and Wen, B. (2005). "Robust reliability design of Banjo flange with arbitrary distribution parameters." Journal of Pressure Vessel Technology, 127(4), 408-413.